1-1-2018

Optimal Operation of Integrated Microgrids

Abdullah Albaker
University of Denver

OPTIMAL OPERATION OF INTEGRATED MICROGRIDS

_____

A Dissertation

Presented to

the Faculty of the Daniel Felix Ritchie School of Engineering and Computer Science

University of Denver

_____

In Partial Fulfillment

of the Requirements for the Degree

Doctor of Philosophy

_____

by

Abdullah Albaker

November 2018

Advisor: Dr. Amin Khodaei

Author: Abdullah Albaker
Title: OPTIMAL OPERATION OF INTEGRATED MICROGRIDS
Advisor: Dr. Amin Khodaei
Degree Date: November 2018

ABSTRACT

Microgrids' deployments are increasing and projected to increase even more in future due to the significant advantages that are provided by this technology for end-use customers. However, microgrids can be connected to each other to create integrated microgrids system, which can further promote the anticipated and desired benefits. An integrated operation of microgrids can potentially improve the local power system reliability and resilience, increase the individual microgrids' economic benefits, and promote further utilization of renewable energy resources. Integrating microgrids, to achieve a microgrid network or cluster, is expected be an essential application towards smarter power grids and a key operational feature in emerging modern distribution grids. Consequently, finding the optimal schedule of the integrated microgrids during the grid-connected and islanded operation modes is necessary to achieve the most possible economic and environmental benefits.

In this dissertation, the integrated microgrids systems' operation is investigated, researched and studied. The impact of elevating prosumers to provisional microgrids (to form an integrated microgrids system) is discussed and examined, and further independent and integrated microgrid optimal scheduling models are developed and mathematically simulated, to identify its merits and importance in the distribution grid. In addition, the value/quantity of the unused capacities in the microgrids is discussed and investigated, and a communicative optimal scheduling model for integrated microgrids

systems is developed and proposed, in which the local power exchange between the integrated microgrids is determined through an iterative exchange of relevant information based on unused capacity and unmet power in the microgrids. Moreover, the microgrids' privacy is taken into consideration by a developed optimal scheduling model based on the Lagrange Relaxation (LR) method, where the optimal scheduling problem is decomposed into individual optimal scheduling problems using the LR to take prevailing privacy issues into account. Furthermore, an optimal scheduling model for integrated microgrids systems in holonic distribution grids is developed, where the proposed model is capable of determining the optimal network topology, i.e., optimal connections among the integrated microgrids, to ensure minimum microgrid-specific and system-wide operation cost as well as maximum reliability of the entire integrated system.

It should be mentioned that all proposed models are mathematically formulated using mixed-integer programming, and studied through numerical simulations to show their performance and effectiveness.

ACKNOWLEDGMENTS

I was privileged to be advised by Dr. Amin Khodaei during my doctoral studies. I am forever grateful for his support and guidance. He helped me tremendously to learn how to pursue research independently. His rigor in tackling challenging problems has always been inspiring. His professional emphasis on developing my writing skills greatly improved my experience during my Ph.D. I really do appreciate all his significant efforts and endless supports and wish him all the best.

I would like to thank all my colleagues in the lab for their support and collaboration throughout my Ph.D. journey; we worked as a single team and smartly shared the knowledge. They are really fabulous team members.

I am deeply indebted to my family for everything, especially to my parents; without their gaudiness and support over the years, I will never achieve this level of education. Also, I am deeply grateful to my wife who supports me throughout my study in the U.S.; and really appreciate her patience and understanding while I spent countless hours preparing this dissertation.

Finally, I would like to thank “University of Hail” who granted me this significant chance to pursue my higher education in the leading country of education and knowledge, and hope to be able to transfer the acquired knowledge to the next promising generation.

TABLE OF CONTENTS

LIST OF FIGURES

LIST OF TABLES

NOMENCLATURE

Abbreviations

CMG	Coupled Microgrid
DER	Distributed Energy Resource
DES	Distributed Energy Storage
DG	Distributed Generation
LR	Lagrange Relaxation
PMG	Provisional Microgrid
VOLL	Value of Lost Load

Indices

ch	Superscript for energy storage charging mode
d	Index for loads
dch	Superscript for energy storage discharging mode
h	Index for day
i	Index for DERs
k	Index for intra-hour time periods
s	Index for scenarios
t	Index for inter-hour time period
m,n	Index for microgrids

Sets

A	Set of all DERs
D_A	Set of adjustable loads
G	Set of dispatchable units
M	Set of all microgrids
M_C	Set of coupled microgrids
M_P	Set of provisional microgrids

N	Set of scenarios
S	Set of energy storage systems
T	Set time periods
T_K	Set of intra-hour time periods
T_T	Set of inter-hour time periods
W	Set of nondispatchable units

Parameters

F(.)	Generation cost for dispatchable units
DR	Ramp down rate
DT	Minimum down time
E	Load total required energy
MC	Minimum charging time
MD	Minimum discharging time
MU	Minimum operating time
U	Islanding state (0 when islanded, 1 otherwise)
UR	Ramp up rate
UT	Minimum up time
α,β	Specified start and end times of adjustable loads
γ	Step size for Lagrangian multiplier update
κ	Coefficient of present-worth value
λ	Local power exchange price
η	Energy storage efficiency
ρ	Market price
μ	Penalty coefficient
υ	Value of lost load
Ψ	Probability of islanding scenarios

Variables

C	Energy storage available (stored) energy
D	Load demand
D^{PM}	PMG Load demand
I	Commitment state of dispatchable units
LS	Load curtailment
P	DER output power
P^{G}	Local power exchange
$P^{\max}$	Installed dispatchable unit capacity
P^{M}	Utility grid power exchange
R	Unused capacity in islanded mode
SD	Shut down cost
SU	Start up cost
T^{ch}	Number of successive charging hours
T^{dch}	Number of successive discharging hours
T^{on}	Number of successive ON hours
T^{off}	Number of successive OFF hours
u	Energy storage discharging state (1 when discharging, 0 otherwise)
v	Energy storage charging state (1 when charging, 0 otherwise)
w	Local power exchange state (1 when transfer power, 0 otherwise)
z	Adjustable load state
τ	Time period

Chapter One: Introduction

Microgrids are introduced to address challenges related to the wide deployment of distributed energy resources (DERs) in distribution networks by offering an intelligent, localized, and reliable control of local generation and load resources. Based on the U.S. Department of Energy definition [1], DER installations comprising three distinct characteristics could be deliberated as microgrids: (i) defined electrical boundaries; (ii) employment of a local controller to operate the system as a single controllable entity; and (iii) the islanding capability. The deployments of microgrids are increasing and projected to increase even more due to vital advantages that this technology can provide [2]-[4]. Microgrids, however, are costly installation and the economic viability of the microgrid deployment cannot be justified for all consumers. Thus many have chosen to only use local DERs to partially offset local electricity usage, commonly called prosumers. Microgrids offer significant advantages for both local consumers and the utility grid, from improving load-point reliability and power quality to enhancing energy efficiency and helping postpone the upstream network upgrades, many of which are enabled through microgrid's noteworthy capability in islanding in response to grid disturbances [4]-[6]. Microgrids improve security and resiliency of the electricity supply and delivery, while helping improve system economics and environmental impacts. Microgrids are small-scale power systems that consist of various types of DERs installed locally close to loads. DERs consist of distributed generators (DGs) and distributed energy storages

(DESs), where numerous technologies are developed such as combined heat and power, fuel cell, micro-turbine, and renewable energy resources [6]-[9]. The microgrid is capable of operation in two modes: grid-connected and islanded. The decision to operate in the islanded or the grid-connected mode is made by the microgrid master controller based on security and economic considerations [10]-[13]. The master controller is the main entity responsible for the decisions that related to the optimal operation of local DERs, power exchange with the utility power grid, and switching the microgrid between grid-connected and islanded modes.

The microgrid operates in the grid-connected mode for economic and reliability purposes, where sufficient power can be exchanged with the utility grid. However, the microgrid may supply its local need of power by the locally installed DGs rather than purchasing power from the utility grid to achieve the economic objectives [14]-[16]. In addition, it may also import more than its need of power from the utility grid to be stored in the DES when real-time market prices at low levels, and sell them back to the utility at peak hours, i.e. when real-time market prices at highest levels. Microgrids infrequently operate in the islanded mode and rely on local DERs for electricity supply.

Islanding is the microgrid's most prominent feature, in which, it is defined as the microgrid ability to be disconnected from the utility grid and operate on its own. Microgrids operate in the islanded mode by relying on generated power by local DGs and the stored energy in the DES [17]-[20]. Islanding happens mostly in case of upstream disturbances and/or utility grid voltage fluctuations. Significant advantages are provided by the islanding operation as it increases the load-point reliability during major power failures and enhances social cost savings, which makes the islanded design crucial in the

microgrid planning decisions [20]-[22]. The microgrid is switched into the islanded mode using upstream switches that are located at a specified point in the network, called the point of common coupling (PCC), between the microgrid and the utility grid. This feature, however, results in some drawbacks, which are being identified as microgrids penetration increases worldwide:

- Microgrid islanding requirement dictates the deployment of a high percentage of dispatchable generation, primarily in form of gas-fired turbines or micro-turbines. Thus, the deployment of variable generation resources, primarily renewables which could not be efficiently dispatched for islanding purposes, would be relatively low in microgrids;
- The capital-intensive DER installations will be underutilized as microgrids commonly purchase low-price power from the utility grid which benefits from economies-of-scale in generation and utilizes less costly nuclear, coal, and gas units. Therefore, microgrid DERs would only be employed in infrequent islanded hours for the mere purpose of improving reliability.

These issues could increase the return on investment, significantly impact the microgrid economic benefits, and lower the anticipated environmental merits [23]-[24]. Therefore, proper solutions should be found to make benefit from this unused capacity. There has been limited discussion in the literature that how this unused capacity can be efficiently leveraged. Provisional Microgrids (PMGs), as elevated prosumers without the islanding capability, are proposed and designed based on the microgrid's unused capacity in [24] as a potential solution to this problem. PMG consists of a cluster of loads and renewable DGs that act as a single entity with clearly defined electrical boundaries to

boost the desired economic benefits and promote the use of renewable energy resources. Even though master controllers exist in the PMGs, they do not have the capability to fully island the PMG from the utility grid during major outages as the PMG lacks adequate dispatchable generation. Therefore, it is electrically connected to neighboring microgrids, called coupled microgrids (CMGs), to enhance its ability to be islanded in case of upstream disturbances [24]-[28]. In [24] an uncertainty-constrained optimal scheduling model is developed based on a decomposed two-level model. The study in [25] further investigates the provisional microgrids optimal planning problem and considers the anticipated interactions among the provisional microgrid and the coupled microgrid in both grid-connected and islanded operation modes. Robust optimization method is used to capture uncertainties in the problem. Elevating prosumers to provisional microgrids is investigated in [26] to show its impact on reducing the undesired load curtailments during the islanded operation, which mainly rely on the unused capacity of the coupled microgrid to enhance the reliability and ensure seamless islanding. In [27], the design and operation of the PMGs is investigated. The rationale, relevance, and features of the PMG along with its operation modes are further discussed. The study in [28] proposes a communicative scheduling model for the integrated microgrids, where the information of the unmet power in the PMG and unused capacity prices in the CMG are exchanged iteratively among the integrated microgrids until the optimal solution is reached.

Microgrids can be connected to each other to form integrated microgrids, which also called interconnected microgrids, networked microgrids, multi-microgrid (MMG), or microgrid clusters. Integrating the microgrids can provide several advantages as it can enhance the reliability, resiliency, and the operation of the power systems [29]-[31]. In

addition, it can boost the utilization of the renewable energy resources, make a full use of the installed DESs in the microgrids, and increase microgrids' economic benefits [32]-[34]. The integrated microgrids concept is widely discussed in the literature. The study in [29] proposes a cyber-network communication system for multiple microgrids, where a self-healing microgrid system is formed to increase the resiliency of the integrated microgrids. The study in [30] presents a multi-microgrid state estimation and fuzzy state estimation that objects to investigate the increase penetration of the microgeneration in the distribution networks through exploiting and extending the microgrid technology, involving the development of new tools for multi-microgrid management and operation. The proposed algorithm is robust and can be efficiently used for local state estimation. In [35], a coalition formation game is formulated between these DERs and an algorithm is proposed for forming the coalitions. The proposed algorithm allows the DERs to make distributed decisions on whether to form or break coalitions, while minimizing their operation costs. In [36], the price competition among integrated microgrids is analyzed using a game theory framework. The system is modeled by assuming that in each time slot, a microgrid may either have one unit of excess power, or one unit of deficit power, or neither excess nor deficit power, each associated with a probability. Consequently, microgrids can compete to sell their excess power to those with deficit power. By defining energy cost saving as the total energy cost reduction with the proposed microgrid energy cooperation over the traditional case of no cooperation, the study in [37] solves an off-line optimization problem and proposes a distributed algorithm for the optimal off-line energy management solution of integrated microgrids. A method of joint optimization and distributed control of integrated microgrids is proposed in [38]. The

generation plan of controllable DERs is determined via an optimization framework, which minimizes the aggregated operation cost of the integrated microgrids. The study [39] proposes a distributed optimization method based on the alternating direction method of multipliers (ADMM) for the generation scheduling of integrated microgrids. The study in [40] develops a modeling framework for evaluating the power exchange capability between the interconnected microgrids and the distribution network. The proposed modeling framework includes prediction and correction models that respectively predict and determine the interchange capability. In [41], two microgrids are integrated and tested using the HOMER software. In [42], the interactions between distribution network operation and integrated microgrids are characterized. In addition to cybersecurity and resilience, state estimation is implemented in integrated microgrids in [43]. In [44], an optimization problem is investigated and studied based on model predictive control (MPC) for a network of microgrids. This work provides valuable insights on how power generation of integrated microgrids could be effectively distributed in the network in order to minimize the cost of power purchased by microgrids. In [45], a technique based on recurrent neural network (RNN) is proposed to achieve the optimal operation of microgrids connected to the utility grid. The proposed RNN allows optimizing the power supply, minimizing the power supplied by the utility grid, and maximizing the power supplied by renewable energy sources. Control problems of the integrated microgrids are investigated and studied in [31], [46]-[51]. The study in [31] assesses the merits and drawbacks of the integrated microgrids using multi-criterion decision aids. The economic, technical, and environmental impacts of such trading mechanism are further investigated. The study in [46] presents an advanced control

functionality to manage the high penetration of the DERs and active loads in the distribution networks. In [47], a method for tertiary control level for load sharing is described. The proposed method works with distributed secondary control system to benefit from its communication structure in propagating voltage set points. The study in [48] develops a real-time tertiary control algorithm for DC microgrid clusters. The developed algorithm solves a set of load flow equations to improve the efficiency and the voltage stability of the distribution network, and periodically forecasts the net available energy at each microgrid in the cluster to improve the short-term planning. The study in [49] presents a strategy for designing a communication and control infrastructure based on the virtual microgrid concept in a distribution system. A new decentralized control scheme based on the self-organization approach for managing integrated microgrids is proposed in [50]. The proposed decentralized control scheme improves the scalability and flexibility, and achieves comparable performance in terms of system reliability when compared to a centralized scheme. The study in [51] presents a distributed control schemes for integrated low-voltage DC microgrids. In order to provide proper references for power flow control, a systems-on-chip of batteries inside the microgrids is proposed, making microgrids tend to have equal systems-on-chip despite different loads. Studies focus on the compromise between cost and reliability in the integrated system are discussed in [32]-[34], [52]-[54]. A probabilistic Monte Carlo based iterative methodology is applied in [32] for the optimal planning of integrated microgrids, where this study is implemented to a six-microgrid system operating in the islanded mode. The numerical simulations suggest that three interconnection lines should be installed to ensure that each microgrid will satisfy the given reliability constraints while satisfying

the limited capital cost. The study in [33] presents an optimal economic dispatch strategy for an integrated system involves two microgrids and a single DES. An economic operation model based on the price difference of microgrids and time sequential weight is proposed in [34]. The numerical simulations show the impact of the DES on the integrated microgrids in terms of minimizing the operation cost. The study in [52] discusses the concept of integrated microgrids, and further investigates the possibility of smart distribution systems using the integrated systems. The study in [53] addresses the small signal modeling and stability issues in the integrated DC microgrids. In [54], modular-architecture microgrids are discussed to assure expansibility, reliability, and controlled cost in integrated systems. It is shown that through a coordinated optimization and management, the reliability and functionality may be improved within a limited cost. Many studies are made in the literature on the optimization of integrated microgrids. In [55], an algorithm for multi-objective optimal power flow is used, and decentralized power dispatch model is described in [56]. The study in [57] deals with potential benefits from individual and integrated microgrids in terms of economy, loss avoidance, and emissions reduction, using electricity market prices, with different renewable generation penetration levels. The study in [58] presents an integrated energy exchange scheduling for a multi-microgrid system under a pricing strategy using adjusted prices, and further proposed a decentralized optimal scheduling strategy for the microgrid central controller to minimize the microgrids operation cost and satisfy the consumers' needs. The study in [59] develops a joint energy trading and scheduling strategy for integrated autonomous microgrids. In addition, it designs an incentive mechanism using Nash bargaining theory and investigated the possible interaction among the integrated microgrids. In [60], a

distributed mechanism for energy trading between the integrated microgrids is proposed in a competitive market based on a game-theoretic analysis, where the proposed game-theoretic strategy provides incentives for energy trading between the integrated microgrids. The study in [61] proposes a stochastic and probabilistic modeling framework to minimize the operation cost of each microgrid in a multi-microgrid system, and utilized the particle swarm optimization algorithm to solve the optimization problem. In [62], an energy management framework for the integrated microgrids is presented, where the scenario-based two-stage stochastic optimization approach is proposed to capture the uncertainties related to the load demand and the generation of renewable energy resources. The study in [63] designs a bargaining-based energy trading market for the energy trading among the integrated microgrids and proposed a decentralized algorithm to solve the bargaining problem. The study in [64] proposes a system of systems framework for optimizing the operation of active distribution grids based on a decentralized optimization approach to maximize the benefit of each independent system.

High penetration of DERs creates new dynamics that current distribution networks are inadequate to handle [65]-[67]. Current distribution networks do not provide enough intelligence to encourage and manage optimal cooperation among the recently emerged systems such as microgrids. Therefore, it is necessary to develop smarter distribution networks to achieve the envisioned smart grids. A new generation of distribution grids, called the holonic distribution grids, is recently discussed and predicted to be extensively implemented in the future due to their capability in boosting the connectivity among autonomous entities [67]-[68]. The holonic paradigm was first proposed in [69]. Holonic system approach is based on the hierarchy concept, where each

holon represents a self-contained and autonomous system. However, in holonic distribution grids a holon, e.g., a microgrid, could be a whole and at the same time part of a whole. Hence, the holonic approach can be described as a hybrid between the distributed and centralized approaches, where autonomous subsystems adapt within the holonic system and managed by a supervisory controller [67]-[69]. The holons can be dynamically reconfigured and reorganized to adapt themselves in a dynamic environment. Through the aggregation mechanism provided by the holonic distribution grids, holons can form scalable architectures that support achieving local and global benefits. The study in [65] presents a goal-based holonic multi-agent system to support the power distribution systems in operating as cyber-physical systems, and further provides details on its design and operation. In addition, it demonstrates the role of the holonic multi-agent system for two applications in power distribution systems including the control of the reactive power at solar PV installations and the system state estimation provided by residential smart meters. The study in [70] proposes a holonic control architecture to address the smart grids control challenges for attaining global and local objectives at the macro- and micro-levels, respectively. A proof-of-concept implementation is exemplified to investigate the use of the proposed holonic architecture by integrating basic control solutions. In [71], a holonic multi-agent system architecture is presented to control power distribution systems in an adaptive manner. The islanded operation of the distribution system in case of emergencies is further taken into consideration. In [72], a fractal model for power systems based on a holonic structure is presented enabling multiple aggregation layers while maintaining sufficient autonomy of systems. The study in [73] proposes an intelligent control strategy for renewable energy

systems based on the holonic structure. In addition, a multi-criteria decision aid method is applied and identified in this study to control the system's components. In [74], a generic architecture of smart grids is proposed based on the holarchy concept. The suggested architecture of the system involves various independent prosumers with a bottom-up organization in a recursive manner to form various aggregation layers that contribute to a dynamic system reconfiguration. In [75], an optimal scheduling model of integrated microgrids in holonic distribution grids is proposed, enabling dynamic reconfiguration by determining the optimal connections among the microgrids aiming at enhancing the local and global benefits.

The rest of the dissertation is organized as follows. Elevating prosumers to the status of PMGs is investigated in Chapter Two, and the potential benefits of this elevation on the integrated microgrids are further investigated. Chapter Three discusses operation of the PMGs and further evaluates the microgrid unused capacity, where a microgrid optimal scheduling model is developed for the purpose of assessment. Chapter Four proposes a communicative scheduling model for the integrated microgrids, where the local power exchange price and the unmet power quantity are iteratively exchanged among the integrated microgrids. Chapter Five proposes a privacy-preserving optimal scheduling model for the integrated microgrids Based on the Lagrangian relaxation method. Chapter Six proposes an optimal scheduling model for the integrated microgrids in the holonic distribution grids. Finally, the conclusion and the future directions are provided in Chapter Seven. All proposed models are examined on a test system to investigate their merits and effectiveness.

Chapter Two: Elevating Prosumers to Provisional Microgrids

Prosumers are rapidly increasing in the U.S. and around the world due to the economic benefits associated with utilizing local DERs [22]-[25]. Prosumers usually utilize renewable energy resources, which produce variable generation that is difficult to be controlled and are further associated with high forecast errors. Consequently, prosumers can potentially face similar load curtailments as consumers during utility grid disturbances. To address these challenges while making sure that the investment is not as costly as a microgrid, a new type of microgrid, called PMG, is recently introduced [24]-[26]. In this chapter, the advantages of elevating prosumers to PMGs are investigated. The optimal scheduling models of the PMG and the CMG are developed, along with an integrated scheduling model [26]. It is further discussed how this elevation can benefit both microgrids during the islanded operation mode.

2.1 Model Outline

Figure 2.1 illustrates the structure of the proposed model. In grid-connected mode, the PMG and the CMG would individually exchange power with the main power grid with the objective of maximizing the economic benefits (i.e., minimizing the operation cost). The CMG would optimally schedule local dispatchable generators, energy storage, and the exchange power with the utility grid to minimize its operation cost, while the PMG would utilize its local generated power (which is commonly variable generation) to supply local loads and purchase the additional power requirements from the utility grid to

maintain load-supply balance. However, in case of upstream network disturbances, the PMG and the CMG would both be disconnected from the utility grid and switch to the islanded operation. In the islanded mode, the PMG would connect to the CMG and the two microgrids would start exchanging power, taking into consideration the connecting line capacity limit and the available generation capacity in the CMG. The integrated microgrids would be optimally scheduled to minimize their own operation costs, which in the optimal case, would be equivalent to the minimum of the total operation cost of the integrated system. In this case, the PMG would benefit from power transferred from the CMG to meet its local demand, hence increase its reliability, and the CMG would increase its economic benefits by selling its excess generation to the PMG. In case of insufficient power, PMG loads will be partially curtailed based on their relative criticality and adjustability, i.e. less important loads would be curtailed first. Load curtailments are implemented, as a last resort, to remove power mismatch and achieve supply-demand balance.

A 24-hour scheduling horizon is used to solve the proposed problem, and one hour time period is considered to obtain schedules based on hourly operation. Shorter time periods can be performed to follow fast changes in the system in an accurate manner without loss of generality.

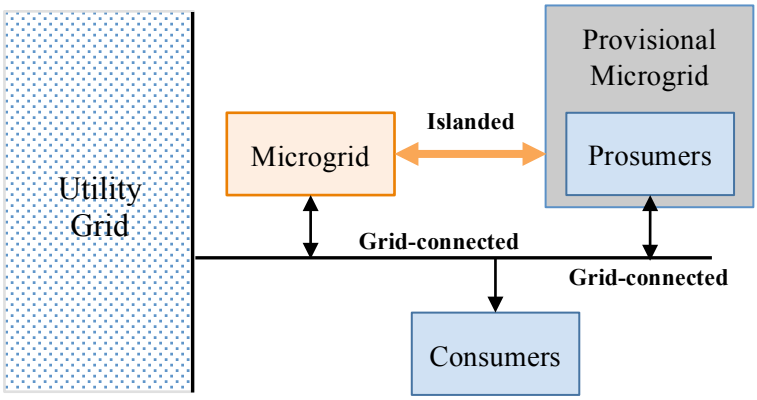

Figure 2.1 Illustration of the proposed model during the grid-connected and the islanded operation.

2.2 Problem Formulation

2.2.1 CMG Optimal Scheduling

The objective of the microgrid optimal scheduling problem is to minimize the microgrid total operation cost, as in (2.1):

$$\min \sum_{t} \sum_{i \in G} F_i(P_{it0}) I_{it} + \sum_{t} \sum_{s} \rho_t P_{ts}^{M} + \sum_{t} \sum_{s} \lambda_t P_{ts}^{G} \qquad (2.1)$$

The first term in the objective represents the operation cost of dispatchable generators in the CMG, which comprises generation, startup and shutdown costs throughout the selected horizon. The second term represents the cost of power exchange with the utility grid, which could be cost or revenue depending on the flow direction. The last term denotes the cost/revenue associated with local power exchange with the integrated microgrids, here PMG, which also depends on the flow direction. These cost terms are calculated for defined scenarios in the CMG optimal scheduling which determine the operation mode (i.e., grid-connected or islanded) in each time period. The grid-connected and islanded operation modes are distinguished in the objective and in the

constraints as well, using scenario index s, where s=0 implies the grid-connected mode and any value of s more than zero implies the islanded mode.

The objective of the CMG optimal scheduling is subject to operational constraints, which include constraints for dispatchable generators and energy storage, as follows:

$$\sum_i P_{its} + P_{ts}^M + P_{ts}^G = \sum_d D_{dts} \qquad \forall t, \forall s \tag{2.2}$$

$$-P^{M,\max} U_{ts} \le P_{ts}^M \le P^{M,\max} U_{ts} \qquad \forall t, \forall s \tag{2.3}$$

$$P_i^{\min} I_{it} \le P_{its} \le P_i^{\max} I_{it} \qquad \forall i \in \mathrm{G}, \forall t, \forall s \tag{2.4}$$

$$P_{its} - P_{i(t-1)s} \le UR_i \qquad \forall i \in \mathrm{G}, \forall t, \forall s \tag{2.5}$$

$$P_{i(t-1)s} - P_{its} \le DR_i \qquad \forall i \in \mathrm{G}, \forall t, \forall s \tag{2.6}$$

$$T_i^{\mathrm{on}} \ge UT_i (I_{it} - I_{i(t-1)}) \qquad \forall i \in \mathrm{G}, \forall t, s = 0 \tag{2.7}$$

$$T_i^{\mathrm{off}} \ge DT_i (I_{i(t-1)} - I_{it}) \qquad \forall i \in \mathrm{G}, \forall t, s = 0 \tag{2.8}$$

$$P_{its} \le P_{it}^{\mathrm{dch},\max} u_{it} - P_{it}^{\mathrm{ch},\min} v_{it} \qquad \forall i \in \mathrm{S}, \forall t, \forall s \tag{2.9}$$

$$P_{its} \ge P_{it}^{\mathrm{dch},\min} u_{it} - P_{it}^{\mathrm{ch},\max} v_{it} \qquad \forall i \in \mathrm{S}, \forall t, \forall s \tag{2.10}$$

$$C_{its} = C_{i(t-1)s} - P_{its} u_{it} \tau / \eta_i - P_{its} v_{it} \tau \qquad \forall i \in \mathrm{S}, \forall t, \forall s \tag{2.11}$$

$$C_i^{\min} \le C_{its} \le C_i^{\max} \qquad \forall i \in \mathrm{S}, \forall t, \forall s \tag{2.12}$$

$$T_i^{\mathrm{ch}} \ge MC_i (u_{it} - u_{i(t-1)}) \qquad \forall i \in \mathrm{S}, \forall t, s = 0 \tag{2.13}$$

$$T_i^{\mathrm{dch}} \ge MD_i (v_{it} - v_{i(t-1)}) \qquad \forall i \in \mathrm{S}, \forall t, s = 0 \tag{2.14}$$

$$u_{its} + v_{its} \le 1 \qquad \forall i \in \mathrm{S}, \forall t, s = 0 \tag{2.15}$$

The power balance constraint (2.2) guarantees that the total produced power by local DERs plus any exchanged power from/to the utility grid or from/to the PMG, matches the microgrid local hourly load. The flow of the line connecting the CMG to the utility grid is limited by minimum and maximum flow limits (2.3), and further imposed to zero during the islanded operation using a binary islanding indicator. Generated power by dispatchable units is limited by maximum and minimum capacity limits and is further associated with the commitment state (2.4). Ramp up and down rate limits are also considered in (2.5)-(2.6), respectively. Constraints (2.7)-(2.8) represent minimum up and down time limits of dispatchable units. Dispatchable units could be further limited by emission and fuel limits, which are however neglected here. The energy storage power is limited to maximum and minimum limits for both charging and discharging modes (2.9)-(2.10). Available stored energy is computed based on charged/discharged power and the storage efficiency (2.11), and constrained by minimum and maximum capacity limits (2.12). The energy storage is further subject to minimum charging/discharging time limits (2.13)-(2.14). Finally, (2.15) ensures that the energy storage is operating at one mode, either charging or discharging, at each time period.

2.2.2 PMG Optimal Scheduling

The objective of the PMG optimal scheduling problem is to minimize the total operation cost during grid-connected operation, and decrease the chance of load curtailment, i.e. increase the system reliability, during the islanded operation.

$$\min \sum_{t}\sum_{s} \rho_t P_{ts}^{M} + \sum_{t}\sum_{s} \lambda_t P_{ts}^{G} + \sum_{t}\sum_{s} \upsilon_t LS_{ts} \tag{2.16}$$

The first term in the objective is the cost of power exchange with the utility grid, which could be either a cost or revenue, depends on the flow direction, and the second term is cost of power exchange with the CMG during the islanded operation. Nondispatchable generations are forecasted values that are obtained based on the generators characteristics and historical data, therefore handled as constants in the problem formulation. It is assumed that the PMG has adjustable loads that can be deferred or curtailed; hence the objective function will be subject to the following operation constraints:

$$P_{ts}^{M} + P_{ts}^{G} + LS_{ts} = \sum_{d} D_{dts} \qquad \forall t, \forall s \tag{2.17}$$

$$D_{dt}^{\min} z_{dt} \le D_{dts} \le D_{dt}^{\max} z_{dt} \qquad \forall d \in \mathrm{D_A}, \forall t, \forall s \tag{2.18}$$

$$\sum_{t \in [\alpha_d, \beta_d]} D_{dts} = E_d \qquad \forall d \in \mathrm{D_A}, \forall s \tag{2.19}$$

$$T_{d}^{\mathrm{on}} \ge MU_{d}(z_{dt} - z_{d(t-1)}) \qquad \forall d \in \mathrm{D_A}, \forall t, s = 0 \tag{2.20}$$

Power balance equation (2.17) ensures that the power exchange with the utility grid and the CMG matches the PMG hourly demand. The load curtailment is further added to the power balance equation to obtain a feasible solution in the islanded operation. Adjustable loads are restricted to maximum and minimum rated power limits (2.18), required energy to accomplish the operating cycle when switched on (2.19), and the minimum operating time (2.20).

2.2.3 Integrated Microgrids Optimal Scheduling

The objective in the grid-connected operation is to minimize the total operation cost of the integrated microgrids, while the objective in the islanded operation is to

improve the entire system reliability by decreasing the amount of load curtailments. The objective is defined as

$$\begin{aligned}&\min \sum_t \sum_{i\in \mathrm{G}} F_i(P_{it0}) I_{it} + \sum_t \sum_s \rho_t^1 P_{ts}^{M,1} + \sum_t \sum_s \lambda_t P_{ts}^{G,1} \\ &+ \sum_t \sum_s \rho_t^2 P_{ts}^{M,2} + \sum_t \sum_s \lambda_t P_{ts}^{G,2} + \sum_t \sum_s \upsilon_t LS_{ts}\end{aligned} \tag{2.21}$$

This objective represents the costs associated with dispatchable generators in the CMG, the cost of power exchange with the utility grid for both CMG and PMG, the cost of local power exchange, and the possible cost of unserved energy in PMG. Superscripts 1 and 2 are used for the CMG and the PMG, respectively, to differentiate the utility power exchange, local exchange, and the utility price at the point of connection to the grid. The cost of unserved energy occurs only during the islanded operation while it is zero when grid-connected. The objective of the integrated microgrids is further subject to developed operational constraints for both microgrids, i.e., (2.2)-(2.15) and (2.17)-(2.20), as well as the following coupling constraint:

$$P_{ts}^{G,1} + P_{ts}^{G,2} = 0 \qquad \forall t, \forall s \tag{2.22}$$

$$-P^{G,\max} \le P_{ts}^{G,1} \le P^{G,\max} \qquad \forall t, \forall s \tag{2.23}$$

$$-P^{G,\max} \le P_{ts}^{G,2} \le P^{G,\max} \qquad \forall t, \forall s \tag{2.24}$$

Constraint (2.22) denotes that the PMG local power exchange plus the CMG local power exchange equals zero, i.e., it ensures that the amount of power offered by the CMG is entirely provided to the PMG. Of course the power losses in the line connecting PMG to CMG is assumed to be negligible, conceivably due to their proximity. Accordingly the objective terms associated with local power exchange will cancel out each other as they are equal in value but opposite in sign. The local power exchange is

further subject to associated line flow limits as in (2.23) and (2.24). It should be noted that in practice the integrated problem cannot be formulated and solved as there is no single entity that has the load and DER information from both the PMG and the CMG. In this regard, a distributed model is required to solve the problem in a localized and iterative manner. The solution of the distributed problem, however, would be similar to the solution of the integrated problem, which would provide insights on the significance of elevating prosumers to PMGs.

2.3 Numerical Simulations

A PMG with five adjustable loads and three nondispatchable generators is utilized to investigate and analyze the proposed PMG optimal scheduling model, with characteristics as in Tables 2.1-2.3, respectively. A CMG that consists of four dispatchable generators, two nondispatchable generators, and one DES is further utilized, with characteristics as in Tables 2.4-2.7. The line capacity limit for the power transfer with the utility grid is assumed to be 10 MW for both the PMG and the CMG. The forecasted market prices over a 24-hour horizon are given in Table 2.8. A total of 25 scenarios are considered in the proposed optimal scheduling model, where one scenario denotes the grid-connected operation and the rest present the islanded operation scenarios. The PMG and the CMG would exchange power during islanded operation, up to 4 MW. The price of local power exchange, i.e. λ, is assumed to be \$100/MWh. The problems are modeled and solved using CPLEX 11.0 [76]. The following cases are studied:

Table 2.1 Aggregated Generation of Nondispatchable Units in PMG

Time (h)	1	2	3	4	5	6
Power (MW)	0	0	0	0	2.52	3.20
Time (h)	7	8	9	10	11	12
Power (MW)	2.48	2.84	2.72	2.40	2.48	4.44
Time (h)	13	14	15	16	17	18
Power (MW)	4.84	6.27	4.93	5.12	4.21	3.28
Time (h)	19	20	21	22	23	24
Power (MW)	2.84	3.68	2.29	2.40	0	0

Table 2.2 PMG Hourly Fixed Loads

Time (h)	1	2	3	4	5	6
Load (MW)	1.86	1.82	1.81	1.92	1.88	1.88
Time (h)	7	8	9	10	11	12
Load (MW)	2.16	2.33	2.39	2.51	2.58	2.59
Time (h)	13	14	15	16	17	18
Load (MW)	2.97	3.26	3.28	3.35	3.44	3.44
Time (h)	19	20	21	22	23	24
Load (MW)	3.32	3.31	2.99	2.78	2.10	2.02

Table 2.3 Adjustable Loads (S: Shiftable, C: Curtailable)

Load	Type	Min.-Max Capacity (MW)	Required Energy (MWh)	Required Start-End Time (h)	Min Up Time (h)
L1	S	0 - 0.4	1.6	11 - 15	1
L2	S	0 - 0.4	1.6	15 - 19	1
L3	S	0.02 - 0.8	2.4	16 - 18	1
L4	S	0.02 - 0.8	2.4	14 - 22	1
L5	C	1.8 - 2	47	1 - 24	24

Table 2.4 Dispatchable Units

Unit	Cost Coefficient ($/MWh)	Min.-Max. Capacity (MW)	Min. Up/Down Time (h)	Ramp Up/ Down Rate (MW/h)
G1	27.7	1 – 5	3	2.5
G2	39.1	1 - 5	3	2.5
G3	61.3	0.8 - 3	1	3
G4	65.6	0.8 - 3	1	3

Table 2.5 DES

Storage	Capacity (MWh)	Min.-Max. Charge/Discharge Power (MW)	Min. Charge/Discharge Time (h)
DES	10	0.4 – 2	5

Table 2.6 CMG Hourly Fixed Loads

Time (h)	1	2	3	4	5	6
Load (MW)	8.73	8.54	8.47	9.03	8.79	8.81
Time (h)	7	8	9	10	11	12
Load (MW)	10.12	10.93	11.19	11.78	12.08	12.13
Time (h)	13	14	15	16	17	18
Load (MW)	13.92	15.27	15.36	15.69	16.13	16.14
Time (h)	19	20	21	22	23	24
Load (MW)	15.56	15.51	14.00	13.03	9.82	9.45

Table 2.7 Aggregated Generation of Nondispatchable Units in CMG

Time (h)	1	2	3	4	5	6
Power (MW)	0	0	0	0	0.63	0.80
Time (h)	7	8	9	10	11	12
Power (MW)	0.62	0.71	0.68	0.35	0.62	1.11
Time (h)	13	14	15	16	17	18
Power (MW)	1.21	1.57	1.23	1.28	1.05	0.82
Time (h)	19	20	21	22	23	24
Power (MW)	0.71	0.92	0.57	0.60	0	0

Table 2.8 Hourly Market Prices

Time (h)	1	2	3	4	5	6
Price ($/MWh)	15.03	10.97	13.51	15.36	18.51	21.80
Time (h)	7	8	9	10	11	12
Price ($/MWh)	17.30	22.83	21.84	27.09	37.06	68.95
Time (h)	13	14	15	16	17	18
Price ($/MWh)	65.79	66.57	65.44	79.79	115.5	110.3
Time (h)	19	20	21	22	23	24
Price ($/MWh)	96.05	90.53	77.38	70.95	59.42	56.68

Case 1: Independent Scheduling: In this case there will be no power exchange between the PMG and the CMG during both grid-connected and islanded operation. In other word, the PMG in this case fell to the level of a prosumer since it relies on its own generation during the islanded operation. The PMG operation cost in this case is $2,637.36, while the CMG operation cost is $8,333.01. The average PMG load curtailment in this case, considering all scenarios, is 1.918 MWh. The commitment results for dispatchable units and the DES in the CMG are shown in Table 2.9.

Table 2.9 DER Schedule

	Hour (1-24)																							
G1	1	1	1	1	1	1	1	1	1	1	1	1	1	1	1	1	1	1	1	1	1	1	1	1
G2	1	1	1	1	1	1	1	1	1	1	1	1	1	1	1	1	1	1	1	1	1	1	1	1
G3	0	0	0	0	0	0	0	0	0	0	0	1	1	1	1	1	1	1	1	1	1	1	0	0
G4	0	0	0	0	0	0	0	0	0	0	0	1	1	1	1	1	1	1	1	1	1	1	0	0
DES	-1	-1	-1	-1	-1	-1	-1	1	1	1	1	1	0	0	0	1	1	1	1	1	0	0	0	0

Case 2: Integrated Scheduling: In this case the power is exchanged between the PMG and the CMG during the utility grid disturbances, i.e. both microgrids will be disconnected from the utility grid while making a local connection to the other microgrid. It should be noted that the local power exchanges for both microgrids would be exactly the same in value but different in sign (i.e., the direction). The CMG operation cost is calculated as $3,811.86 in this case (i.e., a 54.26% reduction compared to Case 1), while the PMG operation cost is $7,415.23 (i.e., a 181.16% increase compared to Case 1). However, the load curtailment in this case is dramatically dropped to an average of 0.0033 MWh, which implies a significant improvement of the reliability level, i.e., 99.83%, at the PMG. The commitment results for dispatchable units and the DES for this case are shown in Table 2.9, where shaded results indicate changes from Case 1. The impact of increasing the line capacity limit between integrated microgrids on the average load curtailment and the operation cost of both microgrids are shown in Figures 2.2 and 2.3, respectively. Power exchange among these two microgrids is shown in Table 2.10.

Table 2.10 Power Exchange Among Integrated Microgrids

Scenario	1	2	3	4	5	6
$P^{G,I}$ (MW)	3.66	3.62	3.61	3.72	1.16	0.48
Scenario	7	8	9	10	11	12
$P^{G,I}$ (MW)	1.48	1.29	1.47	1.91	1.90	0
Scenario	13	14	15	16	17	18
$P^{G,I}$ (MW)	0	0	0.95	0.83	1.83	2.68
Scenario	19	20	21	22	23	24
$P^{G,I}$ (MW)	2.28	1.43	2.50	2.98	4	4

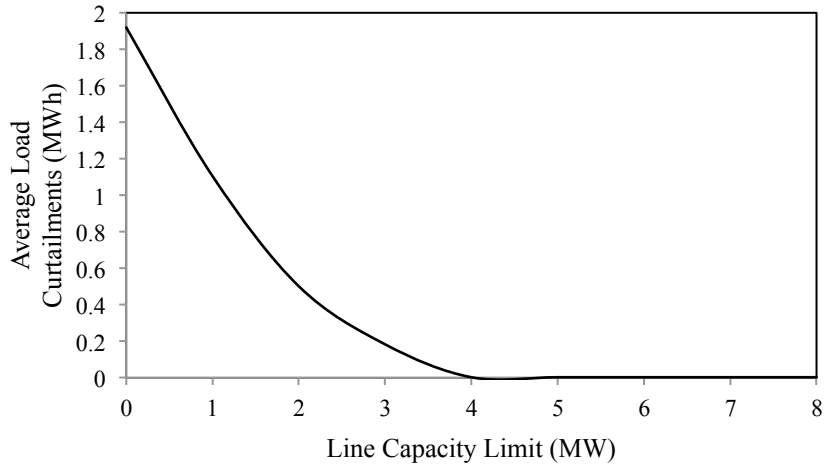

Figure 2.2 Impact of increasing the line capacity limit on load curtailments.

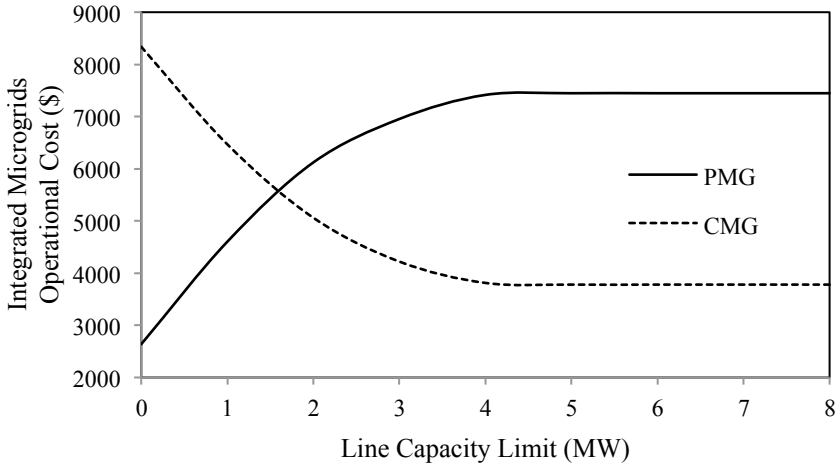

Figure 2.3 Impact of increasing the line capacity limit on total operational cost.

Chapter Three: Operation of Provisional Microgrids

The rapid evolvement of critical civil infrastructure towards more controllable and intelligent systems, under the context of smart cities, has necessitated a comprehensive synergy among various disciplines for addressing ongoing technical and economic challenges and laying the required groundwork for future advancements. This chapter investigates the PMG as an enabling technology for the widespread, low-cost, and viable interactions of end-use customers and provides for a bottom-up approach in creating smarter cities, i.e., starting by transforming customers rather than systems. This chapter discusses how provisional microgrids can be elevated to the status of microgrids, and accordingly increase the supply reliability of local customers in case of utility grid supply interruptions [27]. The rationale, relevance, and features of the provisional microgrid along with its operation modes are further discussed. Furthermore, a valuation of microgrid unused capacity in the islanded operation is discussed in this chapter [23], where a microgrid optimal scheduling model is developed for the purpose of assessment, and accordingly determines price and quantity curves of these unused capacities.

3.1 Provisional Microgrids

The concept of a provisional microgrid is introduced to support the use of renewable generation in the distribution network; it holds similar characteristics of microgrids as it contains interconnected loads and DERs and a master controller that controls and regulates the operation of the provisional microgrid. However, it is not

capable of operation in the islanded mode by itself and must be electrically coupled to at least one existing microgrid. Figure 3.1 depicts the provisional microgrid operation modes (islanded and grid-connected). The provisional microgrid would rely on locally generated power by the renewable energy resources and on the power transfer from the coupled microgrid [24], [26]. The provisional microgrid represents an enabling technology for the widespread low-cost and viable connection of end-use customers and provides for a bottom-up approach in creating smarter cities. The advantages of the provisional microgrid can be demonstrated in increasing liveability in communities (by ensuring a cost-effective operation), workability (by collaborating with existing microgrids and enabling a viable response in emergency operations), and sustainability (by advancing the deployment of emission-free renewable energy resources). The purpose of introducing the provisional microgrid is to accelerate fundamental understanding and stimulate new ideas on dynamic systems that enhance customers' interconnection and interdependency while providing services and innovative applications to enable more connected, workable, liveable, and sustainable communities.

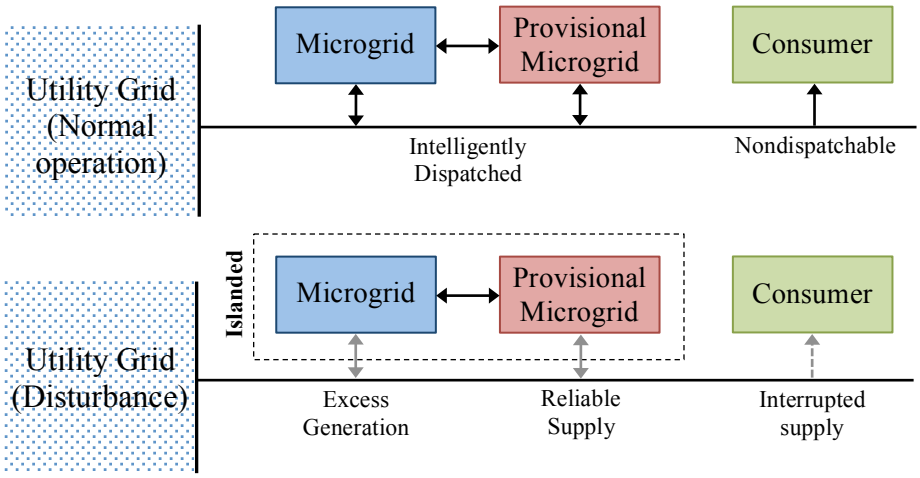

Figure 3.1 Illustration of the operation modes of a provisional microgrid.

Suppose that a provisional microgrid seeks to supply the forecasted load PD_t^{P} at time t. Within the scheduling horizon, the provisional microgrid master controller must ensure the following:

$$P_t^{\mathrm{C}} + P_t^{\mathrm{M}} + P_t^{\mathrm{P}} + LS_t = PD_t^{\mathrm{P}} \qquad \forall t, \tag{3.1}$$

where P_t^{C} is power exchanged by the coupled microgrid, P_t^{M} is power exchanged with the utility grid, P_t^{P} is generated power in the provisional microgrid, and LS_t is the load curtailment. The provisional microgrid is normally connected to the utility grid. However, in case of upstream disturbances, the provisional microgrid would switch to the islanded mode and rely on the generated power by locally installed DERs and the power exchanged with the coupled microgrid to satisfy local loads. Within this context, the provisional microgrid operation can be broken down as follows which is also summarized in Table 3.1:

(a) In the grid-connected operation, the provisional microgrid coordinates the available local generation and the power exchange with the utility grid and the coupled microgrid to maintain supply-demand balance.

(b) In the islanded mode (i.e., upstream network disturbance), the provisional microgrid would be disconnected from the utility grid distribution network and import its further energy requirements from the coupled microgrid to supply the local loads. Based on the available generation at the coupled microgrid side, it is possible that the provisional microgrid loads would be partially curtailed.

Table 3.1 Provisional Microgrid Operational Modes

Operation Mode	Provisional Microgrid	Coupled Microgrid	Utility Grid
Grid-connected	$P_t^{\mathrm{P}} \in [0, \overline{P}^{\mathrm{P}}]$ $LS_t = 0$	$P_t^{\mathrm{C}} \in [-\overline{P}^{\mathrm{C}}, \overline{P}^{\mathrm{C}}]$ (two-way flow)	$P_t^{\mathrm{M}} \in [-\overline{P}^{\mathrm{M}}, \overline{P}^{\mathrm{M}}]$ (two-way flow)
Islanded	$P_t^{\mathrm{P}} \in [0, \overline{P}^{\mathrm{P}}]$ $LS_t \in [0, PD_t^{\mathrm{P}}]$	$P_t^{\mathrm{C}} \in [0, \overline{P}^{\mathrm{C}}]$ (Import)	$P_t^{\mathrm{M}} = 0$ (No transfer)

3.2 Rational, Relevance, and Features

The objective behind proposing the provisional microgrid is that by eliminating the islanding requirement the necessity of deploying a high percentage of dispatchable DERs is further eliminated, which facilitates the deployment of any generation mix. Consequently, a high percentage of renewable DGs (primarily small-scale wind and solar units) without concerning about islanding requirements could be installed. This deployment, however, is only applicable for loads that have low criticality and sensitivity characteristics, since the power exchanged with the coupled microgrid is based on the coupled microgrid's unused capacity, which could be low during an islanded operation. The generation of the renewable DGs in the provisional microgrid would be fully utilized regardless of the electricity rate at the utility grid, which alleviates the underutilization concern of the installed capacity. The provisional microgrid would benefit from the connection to the coupled microgrid to obtain the required flexibility for coordinating the renewable generation, if needed, and import additional power as needed to supply local loads during the islanded mode [24], [26]. Mutual benefits stem from this integration (i.e., connecting the provisional microgrid to the coupled microgrid) as the coupled microgrid would maximize its economic benefits by selling its excess generation to the provisional microgrid, which in turn benefits from this power exchange to supply the

local loads and achieve the required reliability. Though the primary application of the microgrids is to manage and control the increasing penetration of the DERs and addressing the economic and reliability aspects for local consumers, the primary application of the provisional microgrids is to promote the use of the renewable energy resources in the distribution network and provide desired reliability levels for local consumers by leveraging the unused capacity in the already installed microgrids.

The idea behind the provisional microgrids is quite different from the networked microgrids. Networked microgrids, also identified as integrated microgrids or microgrid clusters, comprise two or more interconnected microgrids that exchange the power among themselves to reduce the total power losses, manage local loads, and enhance the reliability and economic objectives, and are able to be islanded individually; while the provisional microgrid, as the name implies, depends on at least one coupled microgrid for islanding capability. The proposed provisional microgrid solution has specific characteristics, including (1) it can operate when connected to the utility grid, but has the capability to synergistically operate with the coupled microgrid for reliability and resilience purposes; (2) it mainly consists of renewable DGs, and if desired, energy storage; (3) it makes smart decisions to connect/disconnect to/from the utility grid and the coupled microgrid to reach desired objectives; (4) it is capable of optimally operating smart appliances such as HVAC systems, which will be carried out by its master controller; and (5) it is interoperable externally and internally using standard protocols that meet control and communication potentials as desired by the utility, and/or the community where it is installed. Provisional microgrid technology is scalable to

significantly higher levels of penetration in distribution grids as it is expected to have minimal interconnection issues with the utility grid.

3.3 Operation Modes

The islanding is implemented to promptly disconnect the provisional and the coupled microgrids from the faulty upstream network, and protect the local DGs and voltage sensitive loads from the disturbances. The dynamic connection to the utility grid and the coupled microgrid is ensured by adding (3.2) and (3.3) to the developed economic and reliable operation model. Let v be the utility grid connection binary variable (1 during normal grid operation and 0 during emergency operation), and w be the coupled microgrid connection binary variable (1 when coupled and 0 when fully islanded); hence:

$$P^{u} v_t \le P_t^{u} \le P^{-u} v_t \qquad \forall t \qquad (3.2)$$

$$P^{m} w_t \le P_t^{m} \le P^{-m} w_t \qquad \forall t \qquad (3.3)$$

Once integrated with the developed operation model, the dynamic connection/disconnection scheme will be determined under the optimization framework and based on the value of the binary connection variables. Possible combinations and the resultant operation modes (OM) are listed as follows:

OM1: $v = 1$, $w = 1$ → Normal operation (grid-connected and microgrid-coupled).

OM2: $v = 1$, $w = 0$ → Normal operation (grid-connected only).

OM3: $v = 0$, $w = 1$ → Emergency operation (microgrid-coupled).

OM4: $v = 0$, $w = 0$ → Emergency operation (fully islanded).

The connection between the provisional and the coupled microgrid is to be sustained during emergency incidents, i.e. OM3 is preferred over OM4. This connection is characterized by providing mutual benefits for both microgrids, i.e. the provisional and the coupled microgrid, where the reliability level in the provisional microgrid would be improved by importing its further need of power from the coupled microgrid, in particular during the islanded operation, while the coupled microgrid would increase its economic benefits by selling its excess generation to the connected provisional microgrid. The provisional microgrid, however, would further benefit from this connection by exploiting the dispatchable DERs in the coupled microgrid to regulate the frequency and control the voltage, if needed.

3.4 Illustrative Study

The robust day-ahead schedule of a test provisional microgrid [26] is determined based on a certain 3 MW transfer limit with the coupled microgrid and an arbitrary 3-hour islanding (hours 17:00, 18:00, and 19:00). The scheduling results are shown in Figures 3.2 and 3.3. Figure 3.2 illustrates the provisional microgrid power exchange between the utility grid and the coupled microgrid. The figure clearly demonstrates that the provisional microgrid will interact with the utility grid in the grid-connected mode and will rely on the generation from the coupled microgrid in the islanded mode. Figure 3.3 shows the provisional microgrid load curtailment during the islanded mode. If adequate generation is not available, as this is the case in hour 18:00, load will be partially curtailed. It is noteworthy that the corresponding prosumer (before being elevated to a provisional microgrid) would encounter a total load curtailment of 7.67 MWh instead of 0.08 MWh in this case. In terms of outage cost, assuming a small value

of lost load (VOLL) of $10/kWh and negotiated price of $0.1/kWh, it represents a saving of $75,900. The coupled microgrid would further benefit from this transaction as it would be paid for the 7.59 MWh energy sold to the provisional microgrid at the negotiated price.

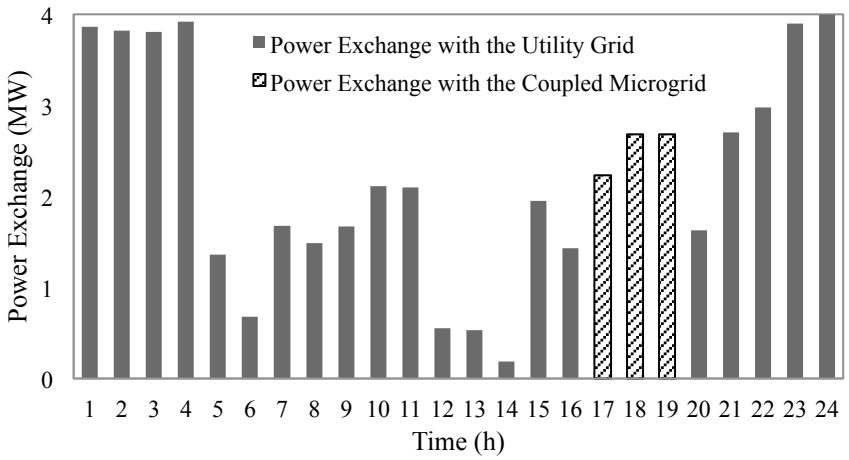

Figure 3.2 Provisional microgrid imported power from the utility grid and the coupled microgrid during the selected scheduling horizon.

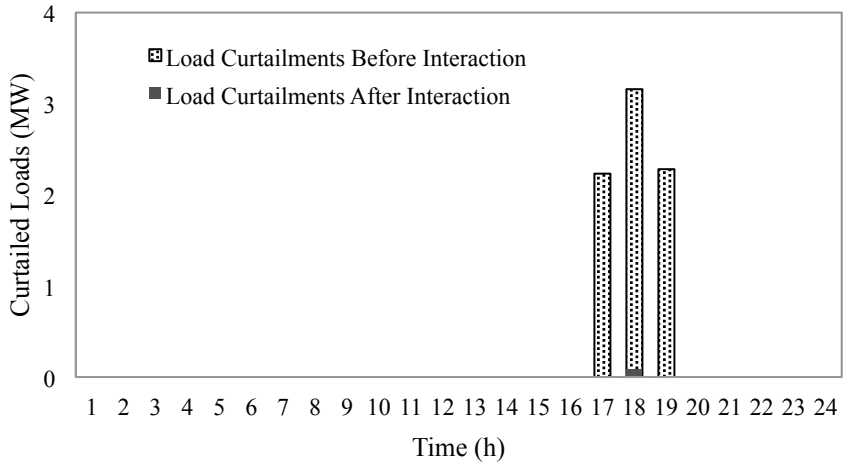

Figure 3.3 Provisional microgrid load curtailments during the islanded mode.

3.5 Valuation of Microgrid Unused Capacity in Islanded Operation

Islanding is the most important characteristics of the microgrid which enables disconnection from the utility grid in case of network disturbances. However, islanded operation requires that the installed dispatchable DGs capacity exceeds the microgrid critical loads, which may cause limitations in the use of renewable energy resources, and dictate the deployment of high percentages of dispatchable DGs. This DG installation, which is targeted to supply the peak critical load during islanding, will result in a large installed capacity which may not be always fully used, i.e., the resources will be underutilized, causing a negative impact on the microgrid anticipated return on investment. One of the proposed solutions for exploiting these underutilized capacities is to export power to other connected microgrids such as PMGs.

The availability of microgrid unused capacity during the islanded mode is investigated and the price and the quantity of unused capacity is accordingly determined, resulting in formation of price/quantity curves that can be used as bids to other connected microgrids and/or provisional microgrids [23]. The investigation is done through a complete optimal scheduling model as developed in this section.

3.5.1 Model Outline

The proposed microgrid optimal scheduling model minimizes the microgrid total operation cost and determines the hourly unused/available capacity in different islanded operation scenarios. The proposed model optimally schedules power exchange with the utility grid, generation of locally installed DGs, and the charging/discharging schedule of the DES. Figure 3.4 shows a microgrid that is operated in two different operation modes; islanded and grid-connected. In the grid-connected mode, the microgrid would exchange

power with the utility grid, exporting or importing power, based on excess generation or deficit of power, respectively, to achieve supply-demand balance. The real-time market prices and the generation cost of the installed dispatchable DGs are taken into consideration in the microgrid optimal operation to maximize the desired economic benefits. The DES is utilized in the grid-connected mode to increase the economic benefits, where it stores power when the real-time market prices are low and discharges back to the grid at peak hours, i.e. when the real-time market prices are high. In the islanded mode, the microgrid is disconnected from the utility grid and would rely on installed dispatchable DGs, potential generation from nondispatchable DGs, and the stored energy in the DES to supply local loads. In this mode, the unused capacity in each hour can be computed, which involves generations by dispatchable DGs, available energy in the DES, and local consumption. The proposed problem is solved using one-hour time intervals in a one-year scheduling horizon.

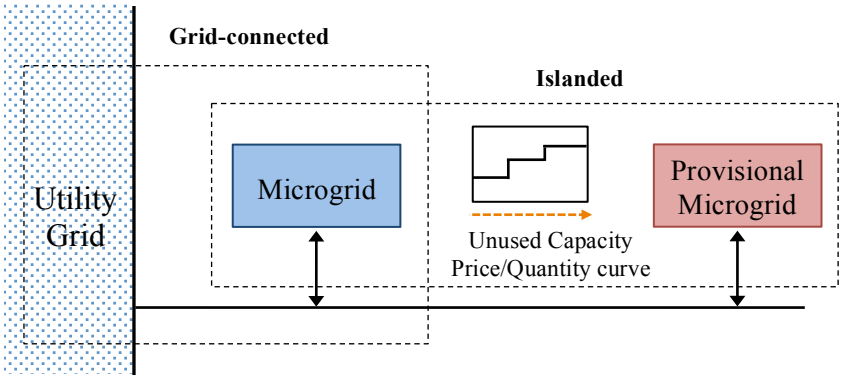

Figure 3.4 Grid-connected and islanded operation modes of the microgrid.

3.5.2 Problem Formulation

The objective of the microgrid optimal scheduling problem is to minimize the microgrid total operation cost and to determine the unused capacity in each hour throughout one-year time horizon in various islanded operation scenarios, as in (3.4):

$$\min \sum_{i\in \mathrm{G}} \sum_{t} \sum_{h} F_i(P_{ith0}) I_{ith} + \sum_{t} \sum_{h} \sum_{s} \rho_t P^M_{ths} + \kappa \sum_{t} \sum_{h} \sum_{s} R_{ths} \tag{3.4}$$

The first term in the objective function represents costs associated with dispatchable DGs generation. This cost is shown as a fuel cost, multiplied by a binary variable representing the commitment state of that particular DG. The second term represents costs/benefits resulting from exchanging power with the utility grid, which depends on the flow direction. This term would result in benefit when the microgrid exporting its excess generation to the utility grid, and cost otherwise. The last term is added to the objective to determine the hourly unused capacity in various islanded operation scenarios. This term is determined through developed constraints as will be further explained. These cost terms are computed based on the microgrid operation mode, i.e. grid-connected or islanded, in each time period. The operation mode is recognized in the objective and in the operational constraints using scenario index s, when s=0 it is assumed that the microgrid operates in the grid-connected mode, and when s>0 it is assumed that microgrid operates in the islanded mode.

This objective is subject to operational constraints associated with dispatchable DGs, DES, and adjustable loads, as follows:

$$\sum_{i} P_{iths} + P^M_{ths} = \sum_{d} D_{dths} \qquad \forall t, \forall h, \forall s \tag{3.5}$$

$$-P^{M,\max}U_{ths} \le P^{M}_{ths} \le P^{M,\max}U_{ths} \qquad \forall t, \forall h, \forall s \tag{3.6}$$

$$P_i^{\min} I_{iht} \le P_{iths} \le P_i^{\max} I_{iht} \qquad \forall i \in \mathrm{G}, \forall t, \forall h, \forall s \tag{3.7}$$

$$P_{iths} - P_{i(t-1)hs} \le UR_i \qquad \forall i \in \mathrm{G}, \forall t, \forall h, \forall s \tag{3.8}$$

$$P_{i(t-1)hs} - P_{iths} \le DR_i \qquad \forall i \in \mathrm{G}, \forall t, \forall h, \forall s \tag{3.9}$$

$$T_i^{\mathrm{on}} \ge UT_i(I_{ith} - I_{ih(t-1)}) \qquad \forall i \in \mathrm{G}, \forall t, \forall h, s = 0 \tag{3.10}$$

$$T_i^{\mathrm{off}} \ge DT_i(I_{ih(t-1)} - I_{iht}) \qquad \forall i \in \mathrm{G}, \forall t, \forall h, s = 0 \tag{3.11}$$

$$P_{iths} \le P_{ith}^{\mathrm{dch},\max} u_{ith} - P_{ith}^{\mathrm{ch},\min} v_{ith} \qquad \forall i \in \mathrm{S}, \forall t, \forall h, \forall s \tag{3.12}$$

$$P_{iths} \ge P_{ith}^{\mathrm{dch},\min} u_{ith} - P_{ith}^{\mathrm{ch},\max} v_{ith} \qquad \forall i \in \mathrm{S}, \forall t, \forall h, \forall s \tag{3.13}$$

$$C_{iths} = C_{i(t-1)hs} - P_{iths} u_{ith} \tau / \eta_i - P_{iths} v_{ith} \tau \qquad \forall i \in \mathrm{S}, \forall t, \forall h, \forall s \tag{3.14}$$

$$C_i^{\min} \le C_{iths} \le C_i^{\max} \qquad \forall i \in \mathrm{S}, \forall t, \forall h, \forall s \tag{3.15}$$

$$T_i^{\mathrm{ch}} \ge MC_i(u_{ith} - u_{i(t-1)h}) \qquad \forall i \in \mathrm{S}, \forall t, \forall h, s = 0 \tag{3.16}$$

$$T_i^{\mathrm{dch}} \ge MD_i(v_{ith} - v_{i(t-1)h}) \qquad \forall i \in \mathrm{S}, \forall t, \forall h, s = 0 \tag{3.17}$$

$$u_{iths} + v_{iths} \le 1 \qquad \forall i \in \mathrm{S}, \forall t, \forall h, s = 0 \tag{3.18}$$

$$D_{dth}^{\min} z_{dth} \le D_{dths} \le D_{dth}^{\max} z_{dth} \qquad \forall d \in \mathrm{D_A}, \forall t, \forall h, \forall s \tag{3.19}$$

$$\sum_{t \in [\alpha_d, \beta_d]} D_{dths} = E_d \qquad \forall d \in \mathrm{D_A}, \forall h, \forall s \tag{3.20}$$

$$T_d^{\mathrm{on}} \ge MU_d(z_{dth} - z_{d(t-1)h}) \qquad \forall d \in \mathrm{D_A}, \forall t, \forall h, s = 0 \tag{3.21}$$

Constraint (3.5) is the power balance equation, which is crucial to prevent undesired fluctuations in frequency and voltage, and involves generated power by local dispatchable units, exchanged power to/from the utility grid, and local hourly load

consumption. Power exchange between the microgrid and the utility grid is subject to line capacity limit, which is indicated by (3.6). However, it is further imposed to zero during islanded operation scenarios using a binary islanding indicator. Constraint (3.7) is the minimum and maximum generation capacity limits for the dispatchable DGs, which is further subject to commitment state. Constraints (3.8) and (3.9) satisfy ramping up and down rate limits for dispatchable DGs, respectively. Constraints (3.10) and (3.11) satisfy limits for the minimum up and down operating time of dispatchable DGs, respectively. Dispatchable DGs could be further constrained by fuel and emission limits, which are however neglected here. Constraints (3.12)-(3.18) are specified for the DES. Charging and discharging power of the DES is constrained by maximum and minimum limits by (3.12)-(3.13). Available stored energy in DES is computed based on charged and discharged power and the storage efficiency in (3.14), and is further subject to maximum and minimum capacity limits (3.15). The DES is also subject to minimum successive operating time limit when it starts charging/discharging (3.16)-(3.17). Finally, (3.18) is added to ensure only one operating mode, i.e. charging or discharging, at each time period. Constraints (3.19)-(3.21) are stated for the adjustable loads in the microgrid. Adjustable loads are constrained by maximum and minimum rated power limits (3.19). The required energy to accomplish an operating cycle for each load in the time intervals identified by consumers is satisfied by (3.20), where start/end operating times are represented by α_d/β_d. Constraint (3.21) is the minimum required successive operating time when loads are switched on.

The objective of the microgrid optimal scheduling problem is further subject to the following constraints in order to determine the hourly unused capacity of the microgrid during each time period in the islanded operation:

$$R_{ths} \le M(1-U_{ths}) \qquad \forall t, \forall h, \forall s \tag{3.22}$$

$$R_{ths} \ge \left(\sum_{i\in \mathrm{G}} P_{iths}^{\max} + \sum_{i\in \mathrm{W}} P_{iths} + \sum_{i\in \mathrm{S}} P_{iths} - \sum_{d} D_{dths}\right) (1-U_{ths}) \qquad \forall t, \forall h, \forall s \tag{3.23}$$

The available capacity is limited by the binary islanding indicator in (3.22) to ensure that the unused capacity is calculated only for the islanded mode. When microgrid operates in the grid-connected mode, i.e., U=1, (3.22) will impose a value of 0 to the unused capacity, otherwise this constraint will be relaxed as M is considered to be a large positive constant. Constraint (3.23) computes the unused capacity in the islanded operation, where it involves the maximum installed capacity of the dispatchable DGs, the forecasted generation of nondispatchable DGs, stored power in the DES, and the microgrid loads consumption, which includes the hourly forecasted fixed loads and the optimized load consumption of the adjustable loads. This term further includes the binary islanding indicator, resulting a value of 0 in the right-hand-side in the grid-connected mode. In the proposed constraint, the maximum capacity is only considered for dispatchable DGs, for the obvious reason that these units can be controlled and can generate desired power.

3.5.3 Numerical Simulations

A microgrid that consists of four dispatchable DGs, two nondispatchable DGs (here solar and wind generators), one DES, and five adjustable loads is utilized to analyze and investigate the proposed optimal scheduling model and determine the quantity and

price of the hourly unused capacity. The characteristics of the microgrid dispatchable DGs, the DES, and the adjustable loads are shown in Tables 3.2-3.4, respectively. The DES efficiency is assumed to be 90% in this study. The hourly average forecasted solar and wind generation for the one-year time period are provided in Tables 3.5-3.6, respectively. The hourly average microgrid fixed loads consumption over the one-year time horizon is shown in Table 3.7. The hourly average market prices as forecasted over a 24-hour are shown in Table 3.8. The line connecting the microgrid to the utility grid is assumed to have a capacity of 10 MW. A total of 25 scenarios are utilized in the proposed optimal scheduling model, where scenario zero implies the grid-connected operation and scenarios 1-24 represent the islanded mode. Islanded scenarios are predetermined, in which in each one an islanding of 1 h in each day is assumed and the scenario is created accordingly. The proposed problem is modeled and solved using CPLEX 11.0 [76].

Table 3.2 Microgrid's Dispatchable Units

Unit	Cost Coefficient ($/MWh)	Min.-Max. Capacity (MW)	Min. Up/Down Time (h)	Ramp Up/ Down Rate (MW/h)
G1	27.7	1 – 5	3	2.5
G2	39.1	1 - 5	3	2.5
G3	61.3	0.8 - 3	1	3
G4	65.6	0.8 - 3	1	3

Table 3.3 DES

Storage	Capacity (MWh)	Min.-Max. Charge/Discharge Power (MW)	Min. Charge/Discharge Time (h)
DES	10	0.4 – 2	5

Table 3.4 Microgrid's Adjustable Loads
(S: Shiftable, C: Curtailable)

Load	Type	Min.-Max Capacity (MW)	Required Energy (MWh)	Required Start-End Time (hour)	Min Up Time (hour)
L1	S	0 - 0.4	1.6	11 - 15	1
L2	S	0 - 0.4	1.6	15 - 19	1
L3	S	0.02 - 0.8	2.4	16 - 18	1
L4	S	0.02 - 0.8	2.4	14 - 22	1
L5	C	1.8 - 2	47	1 - 24	24

Table 3.5 PV Generation
(Hourly Average Over the One-Year Horizon)

Hour	1	2	3	4	5	6
Power (MW)	0	0	0	0	0	0
Hour	7	8	9	10	11	12
Power (MW)	0.005	0.066	0.219	0.409	0.556	0.646
Hour	13	14	15	16	17	18
Power (MW)	0.681	0.661	0.592	0.483	0.340	0.173
Hour	19	20	21	22	23	24
Power (MW)	0.053	0.006	0	0	0	0

Table 3.6 Wind Generation
(Hourly Average Over the One-Year Horizon)

Hour	1	2	3	4	5	6
Power (MW)	0.157	0.167	0.192	0.212	0.235	0.259
Hour	7	8	9	10	11	12
Power (MW)	0.277	0.292	0.308	0.310	0.306	0.303
Hour	13	14	15	16	17	18
Power (MW)	0.292	0.250	0.211	0.181	0.171	0.174
Hour	19	20	21	22	23	24
Power (MW)	0.178	0.183	0.187	0.186	0.176	0.164

Table 3.7 Microgrid's Fixed Load
(Hourly Minimum, Average, and Maximum Over the One-Year Horizon)

Hour	1	2	3	4	5	6
Min (MW)	4.86	4.82	4.79	4.79	4.79	4.79
Average (MW)	7.94	7.86	7.78	7.71	7.67	8.18
Max (MW)	13.76	13.66	13.57	13.44	13.46	13.95
Hour	7	8	9	10	11	12
Min (MW)	4.90	4.82	4.81	4.82	2.81	4.84
Average (MW)	8.76	9.03	9.42	9.76	9.92	10.09
Max (MW)	14.27	14.62	15.23	15.55	15.74	15.72
Hour	13	14	15	16	17	18
Min (MW)	4.88	4.90	4.86	4.94	4.94	4.98
Average (MW)	10.22	10.26	10.23	10.18	10.11	9.87
Max (MW)	15.76	15.87	16	15.91	15.76	15.42
Hour	19	20	21	22	23	24
Min (MW)	4.94	4.92	4.92	4.92	4.90	4.86
Average (MW)	9.19	9.01	8.80	8.65	8.50	8.17
Max (MW)	15.04	14.91	14.61	14.53	14.38	13.81

Table 3.8 Market Prices
(Hourly Average Over the One-Year Horizon)

Hour	1	2	3	4	5	6
Price ($/MWh)	15.13	10.72	13.44	15.42	18.62	21.79
Hour	7	8	9	10	11	12
Price ($/MWh)	17.28	22.86	21.81	27.12	37.30	69.25
Hour	13	14	15	16	17	18
Price ($/MWh)	65.82	66.15	64.86	80.28	116.6	111.9
Hour	19	20	21	22	23	24
Price ($/MWh)	97.39	91.40	77.56	71.73	59.06	56.66

The microgrid operation cost for the one-year horizon is calculated at $2,367,440. The hourly average unused capacity for each month is shown in Figure 3.5. The average unused capacity for each month in the studied one-year horizon is illustrated in Figure 3.6. It can be clearly seen that the lowest unused capacity occurs in July, at an average of 2.1 MW, where the load peaks and is at its highest level during the year. In contrast, the average unused capacity in December is 6.9 MW, which is the highest during the year and represents a significant underutilization of the installed dispatchable capacity.

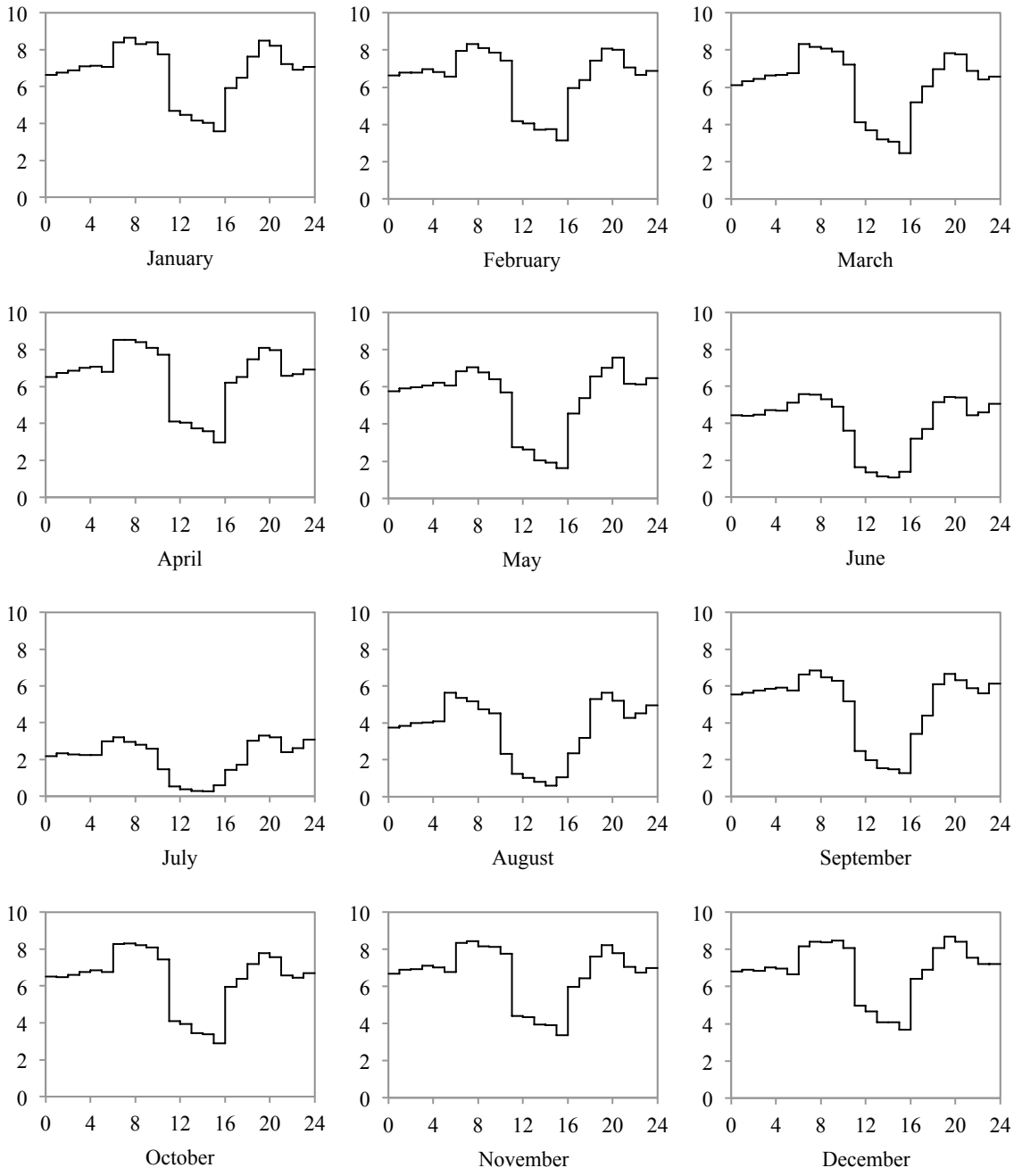

Figure 3.5 Monthly unused capacity, where horizontal axis represents Time (h), and vertical axis represents the Unused Capacity (MW).

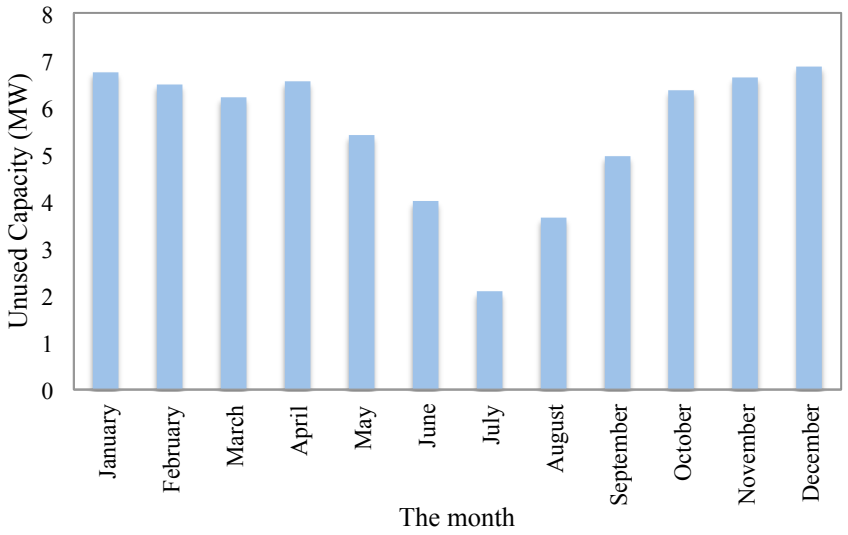

Figure 3.6 Monthly unused capacity in megawatt.

Monthly unused capacity prices are further calculated based on the quantity of the unused capacity and on the cost coefficients of the microgrid dispatchable DGs, which are illustrated in Figure 3.7. It can be noticed that the summer months have one or two price steps (one or two dispatchable DGs have unused capacity), while the other months have three price steps (three dispatchable DGs have unused capacity). Although the quantity of the unused capacity in the summer months is small comparing to the other months of the year, it is only associated with high prices. To clarify that, the optimal scheduling problem utilizes the dispatchable DG with the smallest cost coefficient first and then moves to the next dispatchable DG to minimize the microgrid total operation cost, which results in the classification of the unused capacity prices. For example, in the June, 1.8 MW of the unused capacity can be seen at a price of $61.3 (from G3), while the rest of the unused capacity is at a price of $65.6 (from G4); on the other hand, in the December, three different price levels can be observed as 2.5 MW at $39.1 (from G2), 2.2 MW at $61.3 (from G3), and 2.2 MW at a price of $65.6 (from G4).

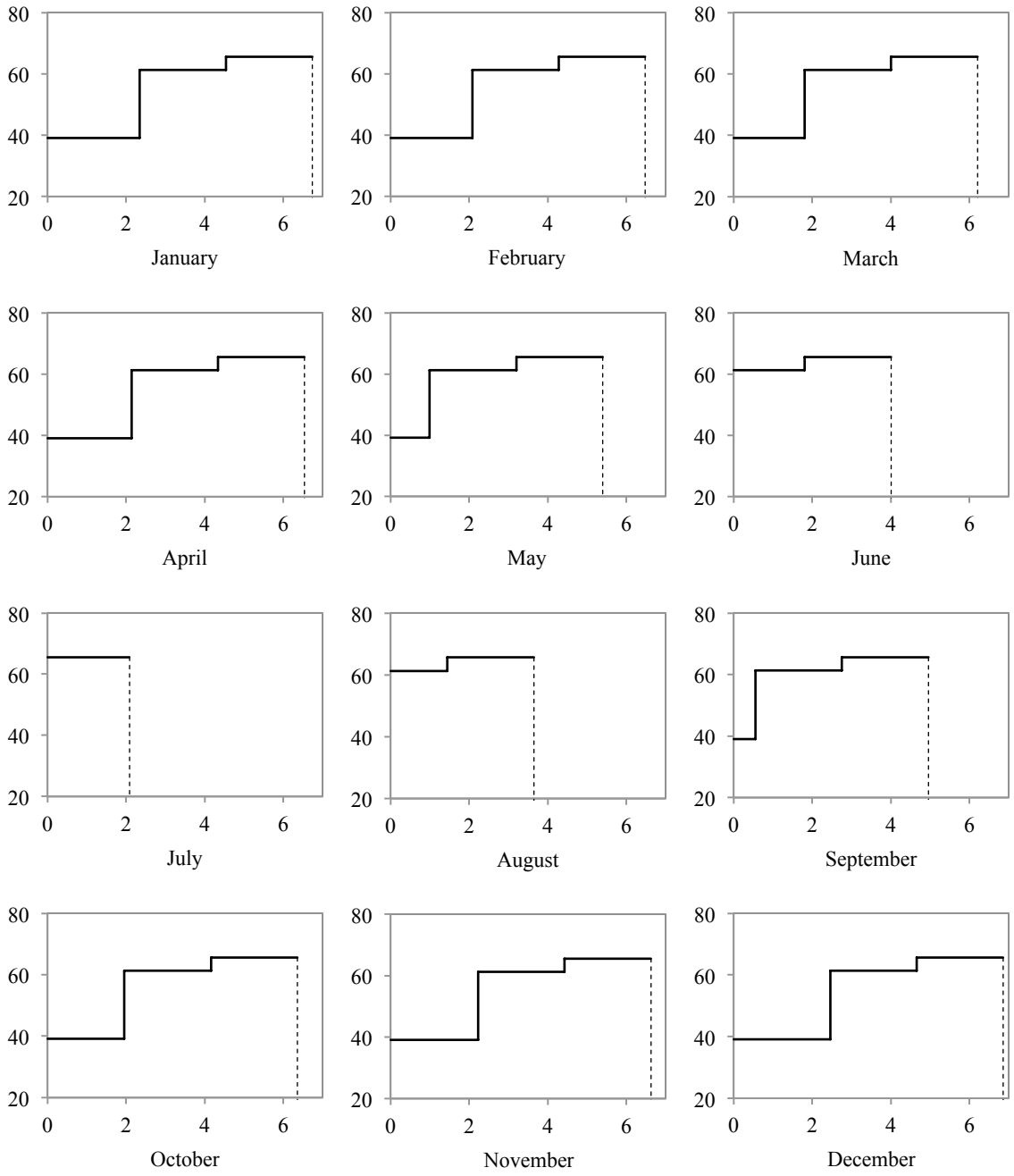

Figure 3.7 Monthly prices of the unused capacities, where horizontal axis represents Quantity (MW), and vertical axis represents Price ($/MWh).

3.6 Discussion

The provisional microgrid concept is investigated in this chapter and an optimal scheduling problem is solved to test the performance of this newly-proposed technology.

Provisional microgrids enhance the penetration of the renewable DGs in the distribution network by removing the islanded capability requirement and obtaining the required flexibility and reliability for local consumers by utilizing the unused capacity of the existing microgrids. Coupled microgrids, in turn, would economically benefit from this connection. The illustrative study indicates a considerable improvement in terms of reliability for the provisional microgrid and an increase in economic benefits for the coupled microgrid. The significance of this technology is further demonstrated for end-use customers while increasing the use of the installed capacity of the DERs within the coupled microgrid.

On the other hand, although the installation of dispatchable DGs in the microgrid is essential to ensure supply-demand balance during the islanded mode and to prevent the undesired load curtailments in case of upstream disturbances, the underutilization of these capital-intensive DGs may impact the anticipated return on the investment. However, this issue is mitigated in this chapter by evaluating the microgrid unused capacity to be further sold to connected provisional microgrids. The provisional microgrid would benefit from exchanging power with the coupled microgrid to improve the reliability and enhance the islanded capability; hence, reducing the load curtailments in the islanded operation. The economic benefits of the microgrid, on the other hand, would be maximized as the excess generation can be sold during islanded mode to obtain the most possible benefit from the locally installed dispatchable DGs capacity.

Chapter Four: Communicative Scheduling of Integrated Microgrids

A communicative optimal scheduling model for managing the interaction between the PMG and the CMG is proposed in this chapter [28]. The proposed model determines the local price of the power exchange along with the optimal power amount to be exchanged between the integrated microgrids. The model is decomposed into associated PMG and CMG problems and solved in an iterative manner.

4.1 Model Outline

The proposed CMG optimal scheduling model aims to minimize the CMG total operation cost and to determine the hourly prices of the unused capacity in the islanded operation mode, which well be used to sell the power to the integrated microgrid, here the PMG. On the other hand, the proposed PMG optimal scheduling model minimizes the PMG total operation cost and shows the additional requirement of power to supply the local demand by calculating the amount of the load shedding in the islanded operation mode.

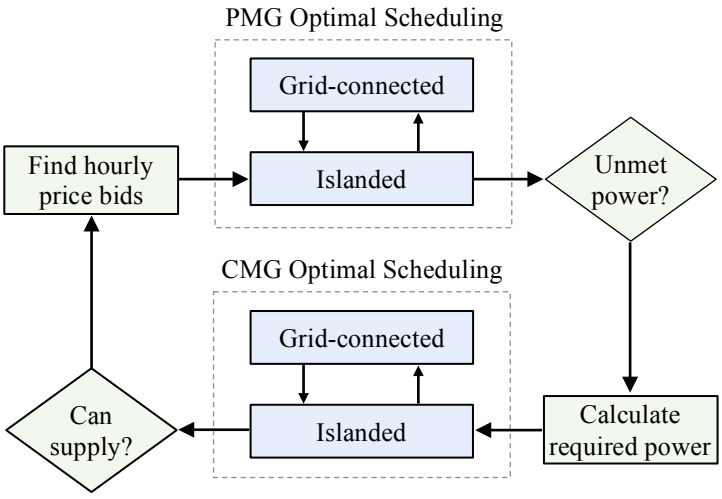

Figure 4.1 Flowchart of the proposed communicative scheduling model.

Figure 4.1 shows the flowchart of the proposed models, where both problems are optimally scheduled. In the grid-connected mode, the CMG and the PMG would independently exchange the power with the utility grid to maintain the load-supply balance. The CMG optimally schedules the generation of the locally installed DGs, the charging/discharging of the installed DES, and the power exchange with the utility grid to achieve the desired economic benefits. The real-time market prices and the generation cost of the installed dispatchable DGs are taken into account in the CMG optimal scheduling. The DES is optimally scheduled in the grid-connected mode to increase the CMG economic benefits, where it is charged/discharged based on the real-time market prices. The PMG would rely on the generation of the locally installed DGs, which are commonly variable generations, and imports its unmet power need from the utility grid. In the islanded operation mode, both of the microgrids would be disconnected from the utility grid and start exchanging power for mutual benefits, taking into account the available generation capacity in the CMG as well as the capacity limit of the tie-line. The CMG would be optimally scheduled and send the hourly price bids of the unused

capacity to the PMG, while the PMG would be optimally scheduled and send its unmet power need to the CMG. This iterative process will continue until the optimal solution for both problems is found. The proposed problems are solved using one-hour time interval in a 24-hour scheduling horizon.

4.2 Problem Formulation

The problem formulation is divided into two separate problems associated with the CMG and the PMG. The two problems will be solved iteratively in the islanded operation mode until the optimal scheduling for both problems achieved. Figure 4.2 shows how the power would be exchanged among the integrated microgrids during the islanded and the grid-connected modes.

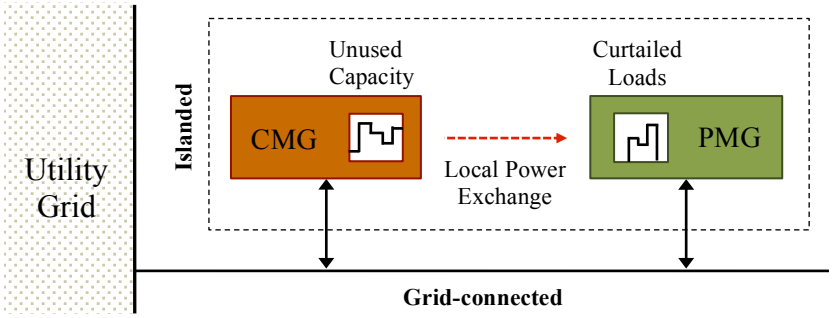

Figure 4.2 Grid-connected and islanded operations of the integrated microgrids.

4.2.1 Coupled Microgrid Problem Formulation

The objective of the CMG optimal scheduling problem is to minimize the CMG total operation cost, as in (4.1):

$$\min \sum_{i \in G} \sum_{t} F_i(P_{it0}) I_{it} + \sum_{t} \sum_{s} \rho_t P_{ts}^{M,1} \tag{4.1}$$

This objective comprises two terms; the first term signifies the dispatchable DGs operation cost, which is represented as a fuel cost multiplied by a binary variable

indicating the commitment state of that individual DG. The second term signifies the power exchange with the utility grid. This term could be either a cost or revenue depending on the power flow direction between the microgrid and the utility grid. The CMG imports its further need of power from the utility grid to supply the local demand when the local generation is insufficient or when the real-time market prices are low (cheaper than the DGs' generation cost), in which this term would be a cost. However, when excess generation is available in the CMG or when the real-time market prices are high, the CMG exports power to the utility grid to maximize its economic benefit, in which this term would be a benefit and appear with a negative sign. These costs terms are calculated for different operation scenarios, which determine the operation mode (i.e. grid-connected or islanded mode). The operation mode in the objective and in the operation constraints is distinguished using index s, where s=0 denotes the grid-connected mode, and s>0 denotes the islanded mode.

The CMG optimal scheduling objective is subject to dispatchable DGs, DES, and lines capacity limits constraints, as follows:

$$\sum_i P_{its} + P_{ts}^{M,1} = \sum_d D_{dts} + D_{ts}^{PM} \Leftrightarrow \lambda_{ts} \qquad \forall t, \forall s \tag{4.2}$$

$$-P^{M,\max} U_{ts} \le P_{ts}^{M,1} \le P^{M,\max} U_{ts} \qquad \forall t, \forall s \tag{4.3}$$

$$P_i^{\min} I_{it} \le P_{its} \le P_i^{\max} I_{it} \qquad \forall i \in \mathrm{G}, \forall t, \forall s \tag{4.4}$$

$$P_{its} - P_{i(t-1)s} \le UR_i \qquad \forall i \in \mathrm{G}, \forall t, \forall s \tag{4.5}$$

$$P_{i(t-1)s} - P_{its} \le DR_i \qquad \forall i \in \mathrm{G}, \forall t, \forall s \tag{4.6}$$

$$T_i^{\mathrm{on}} \ge UT_i (I_{it} - I_{i(t-1)}) \qquad \forall i \in \mathrm{G}, \forall t, s = 0 \tag{4.7}$$

$$T_i^{\text{off}} \geq DT_i(I_{i(t-1)} - I_{it}) \qquad \forall i \in \text{G}, \forall t, s = 0 \qquad (4.8)$$

$$P_{its} \leq P_{it}^{\text{dch,max}} u_{it} - P_{it}^{\text{ch,min}} v_{it} \qquad \forall i \in \text{S}, \forall t, \forall s \qquad (4.9)$$

$$P_{its} \geq P_{it}^{\text{dch,min}} u_{it} - P_{it}^{\text{ch,max}} v_{it} \qquad \forall i \in \text{S}, \forall t, \forall s \qquad (4.10)$$

$$C_{its} = C_{i(t-1)s} - P_{its} u_{it} \tau / \eta_i - P_{its} v_{it} \tau \qquad \forall i \in \text{S}, \forall t, \forall s \qquad (4.11)$$

$$C_i^{\min} \leq C_{its} \leq C_i^{\max} \qquad \forall i \in \text{S}, \forall t, \forall s \qquad (4.12)$$

$$T_i^{\text{ch}} \geq MC_i(u_{it} - u_{i(t-1)}) \qquad \forall i \in \text{S}, \forall t, s = 0 \qquad (4.13)$$

$$T_i^{\text{dch}} \geq MD_i(v_{it} - v_{i(t-1)}) \qquad \forall i \in \text{S}, \forall t, s = 0 \qquad (4.14)$$

$$u_{its} + v_{its} \leq 1 \qquad \forall i \in \text{S}, \forall t, s = 0 \qquad (4.15)$$

$$D_{ts}^{PM} \leq LS_{ts}(1 - U_{ts}) \qquad \forall t, \forall s \qquad (4.16)$$

$$-P^{G,\max}(1 - U_{ts}) \leq D_{ts}^{PM} \leq P^{G,\max}(1 - U_{ts}) \quad \forall t, \forall s \qquad (4.17)$$

The power balance equation (4.2) prevents frequency and voltage fluctuations. This equation comprises the generated power by local DGs, stored power in the DES, the power exchange with the utility grid, and the local demand. The PMG load demand is added to the power balance equation to maintain the supply-demand balance when the two microgrids exchanging power in the islanded operation mode. Parameter λ represents the local power exchange price, which is calculated based on the hourly unused capacity of the CMG. In other words, the CMG would sell its excess generation to the PMG during islanded mode with the marginal price of its last used DG.

Constraint (4.3) indicates the line capacity limit for the power exchange with the utility grid. The capacity limit in this constraint is further multiplied by a binary islanding indicator to impose a value of zero during the islanded operation. Generated power by

each dispatchable DG is constrained by the maximum and minimum capacity limits, and further subject to commitment state (4.4). Ramp up and down rate limits for the dispatchable DGs is satisfied in (4.5)-(4.6), respectively. Minimum up and down time limits of the dispatchable DGs are constrained in (4.7)-(4.8), respectively. A dispatchable DG could be further subject to fuel and emission constraints, which are neglected here. The DES constraints are represented in (4.9)-(4.15). Maximum and minimum limits for the DES charging/discharging are constrained in (4.9)-(4.10). Constraint (4.11) represents the available stored energy in the DES, in which is calculated based on the charging/discharging of power and the storage efficiency. The DES is further restricted by minimum and maximum capacity limits (4.12), and minimum successive operating time limit for both charging/discharging (4.13)-(4.14). Finally, (4.15) ensures only one operating mode (either charging/discharging) at each time period.

The power to be sold to the PMG is limited by the PMG's unmet power need, here identified a load curtailment on the PMG side, i.e., *LS*, and multiplied by a binary islanding indicator to ensure that it is only applicable in the islanded operation mode (4.16). Constraint (4.17) is added to ensure that the received PMG load demand is limited by the maximum and minimum tie-line capacity limits.

4.2.2 Provisional Microgrid Problem Formulation

The objective of the PMG optimal scheduling problem is to minimize the total operation cost in the grid-connected mode, and to decrease the amount of load curtailment during the islanded mode, as in (4.18):

$$\min \sum_t \sum_s \rho_t P_{ts}^{M,2} + \sum_t \sum_s \lambda_{ts} P_{ts}^{G} + \sum_t \sum_s \upsilon_t LS_{ts} \tag{4.18}$$

The first term in the objective represents the power exchange with the utility grid, which could be either revenue/cost depending on the flow direction, while the second term represents the cost of the power exchange with the CMG during the operation in the islanded mode. It is assumed that the PMG has adjustable loads (loads that can be curtailed/deferred); therefore the last term in the objective is added, which is multiplied by the VOLL, to calculate the load curtailment cost. The generation of nondispatchable DGs is forecasted based on the characteristics of that particular DG and the historical data, and hence considered as negative loads with zero cost in the problem formulation. The PMG optimal scheduling problem is subject to the following operational constraints:

$$P_{ts}^{M,2} + P_{ts}^{G} + LS_{ts} = \sum_{d} D_{dts} \qquad \forall t, \forall s \tag{4.19}$$

$$-P^{M,\max} U_{ts} \le P_{ts}^{M,2} \le P^{M,\max} U_{ts} \qquad \forall t, \forall s \tag{4.20}$$

$$-P^{G,\max}(1-U_{ts}) \le P_{ts}^{G} \le P^{G,\max}(1-U_{ts}) \quad \forall t, \forall s \tag{4.21}$$

$$D_{dt}^{\min} z_{dt} \le D_{dts} \le D_{dt}^{\max} z_{dt} \qquad \forall d \in \mathrm{D_A}, \forall t, \forall s \tag{4.22}$$

$$\sum_{t \in [\alpha_d, \beta_d]} D_{dts} = E_d \qquad \forall d \in \mathrm{D_A}, \forall s \tag{4.23}$$

$$T_d^{\mathrm{on}} \ge MU_d (z_{dt} - z_{d(t-1)}) \qquad \forall d \in \mathrm{D_A}, \forall t, s = 0 \tag{4.24}$$

The power balance equation (4.19) ensures the supply-demand balance among the power exchange with the utility grid, the power exchange with the CMG, and the PMG local demand. Load curtailment is also added to the power balance equation to achieve a feasible solution in the islanded mode and in case of insufficient generation. Constraint (4.20) is the line capacity limit for the line connecting the PMG to the utility grid, which is further multiplied by a binary islanding indicator to impose a value of zero when the

PMG operates in the islanded mode. Power exchange with the CMG is subject to the tie-line capacity limit (4.21), and further multiplied by a binary islanding indicator to ensure that it is only applicable in the islanded mode. Maximum and minimum rated power limits for the adjustable loads are restricted in (4.22). Adjustable loads total required energy to accomplish the operating cycle is satisfied in (4.23), where α_d and β_d indicate the user-defined start and end operating times, respectively. Certain loads are subject to minimum successive operating time when switched on as in (4.24).

4.3 Numerical Simulations

A CMG comprising four dispatchable DGs, one DES (with 90% efficiency), and two nondispatchable DGs is utilized to analyze and investigate the proposed communicative optimal scheduling model, with characteristics borrowed from [26]. A PMG with three nondispatchable DGs and five adjustable loads is further considered. The characteristics of the PMG nondispatchable DGs, adjustable loads, the PMG hourly fixed loads, and the hourly forecasted market prices are also borrowed from [26]. The line capacity limit for the lines that connect each of the microgrids to the utility grid is assumed to be 10 MW. A total of 25 scenarios are considered; scenario zero denotes the grid-connected mode and scenarios 1-24 imply the islanded mode. The power exchange between the microgrids would only be during the islanded operation, through a tie-line with a capacity limit of 4 MW. The proposed problems are modeled and solved using CPLEX 11.0 [76]. To investigate the mutual benefits that can be achieved by exchanging the power during the islanded operation, two case of independent and integrated scheduling are examined.

Case 1: Independent Scheduling: The power exchange between the microgrids is eliminated during both operation modes, i.e. grid-connected and islanded modes, in this case. The CMG total operation cost is calculated as $8,423.54, while the PMG total operation cost is calculated as $2,637.36. The CMG unused capacity and the PMG load curtailment are shown in Figures 4.3 and 4.4, respectively (mentioned as before interaction). The average PMG load curtailment in this case is 1.92 MWh. The commitment states for the dispatchable DGs and DES in CMG are illustrated in Table 4.3.

Case 2: Integrated Scheduling: In this case, the power exchange between the microgrids during the islanded operation is considered, where the price bids are sent from the CMG to the PMG and the unmet power need is sent from the PMG to the CMG iteratively until the optimal solution is found. The hourly price bids and the optimal local power exchange for the first iteration are shown in Tables 4.1 and 4.2, respectively. It should be noted that the local power exchange among the microgrids would be exactly the same for both microgrids; however, it appears in the PMG as an import and in the CMG as an export. The CMG total operation cost is calculated as $5,809.15, where the cost reduction occurs due to selling part of the unused capacity to the PMG. Figure 4.3 illustrates the reduction of the CMG unused capacity in this case (mentioned as after interaction), which is as high as 42.6%. The PMG total operation cost in this case is calculated as $5,509.87. Although the PMG total operation cost is increased, the PMG load curtailment is dropped to an hourly average of 0.12 MWh. Figure 4.4 shows the PMG hourly load curtailments (mentioned as after interaction), with a reduction of 93.75%. The load curtailment reduction indicates a significant improvement on the PMG

reliability levels. The commitment results of the CMG dispatchable DGs and the DES are illustrated in Table 4.3, where shaded values imply changes from Case 1 due to the power exchange with the integrated PMG. Figure 4.5 shows the average local power exchange price and the CMG unused capacity over iterations.

Table 4.1 Local Power Exchange Price

Time (h)	1	2	3	4	5	6	7	8
Price ($/MWh)	61.3	61.3	61.3	65.6	39.1	39.1	39.1	39.1
Time (h)	9	10	11	12	13	14	15	16
Price ($/MWh)	39.1	61.3	61.3	65.6	65.6	65.6	65.6	65.6
Time (h)	17	18	19	20	21	22	23	24
Price ($/MWh)	65.6	65.6	65.6	65.6	65.6	65.6	65.6	65.6

Table 4.2 Power Exchange Among Integrated Microgrids

Scenario	1	2	3	4	5	6	7	8
P^G/D^{PM} (MW)	3.66	3.82	3.81	3.72	1.36	0.68	1.48	1.29
Scenario	9	10	11	12	13	14	15	16
P^G/D^{PM} (MW)	1.47	1.91	2.1	0.55	0.53	0.19	1.15	0.83
Scenario	17	18	19	20	21	22	23	24
P^G/D^{PM} (MW)	1.32	1.08	1.55	1.43	2.5	3.18	3.9	3.82

Table 4.3 DER Schedule

	Hour (1-24)																							
G1	1	1	1	1	1	1	1	1	1	1	1	1	1	1	1	1	1	1	1	1	1	1	1	1
G2	1	1	1	1	1	1	1	1	1	1	1	1	1	1	1	1	1	1	1	1	1	1	1	1
G3	0	0	0	0	0	0	0	0	0	0	0	1	1	1	1	1	1	1	1	1	1	1	0	0
G4	0	0	0	0	0	0	0	0	0	0	0	1	1	1	1	1	1	1	1	1	1	1	0	0
DES	-1	-1	-1	-1	-1	-1	-1	1	1	1	1	1	0	0	0	1	1	1	1	1	0	0	0	0

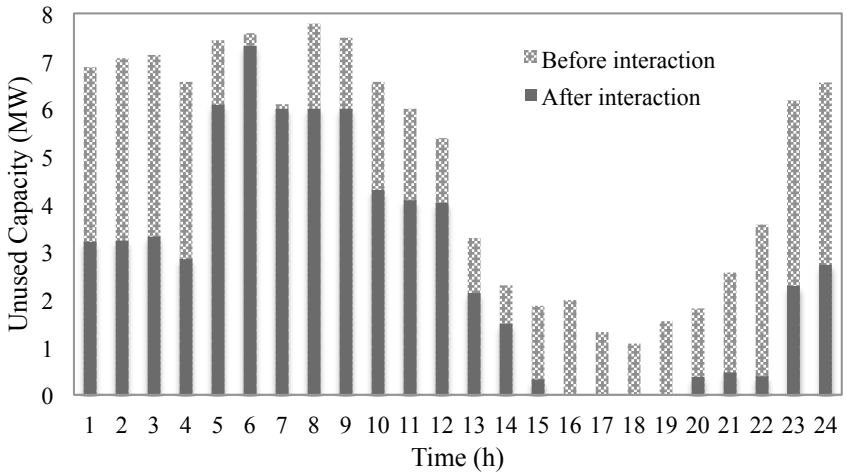

Figure 4.3 CMG unused capacity in the islanded operation modes.

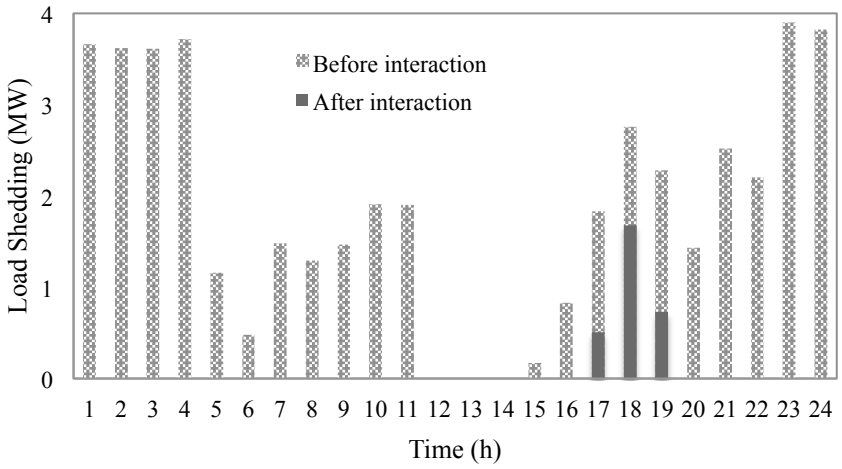

Figure 4.4 PMG load curtailments in the islanded operation modes.

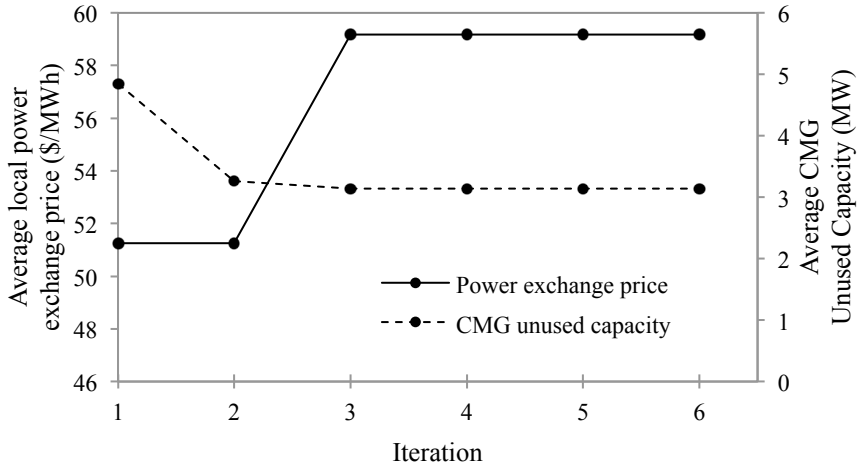

Figure 4.5 Average local power exchange price and the CMG unused capacity.

4.4 Discussion

An optimal scheduling model based on communications between a PMG and a CMG is proposed in this chapter. The objective is to enable power exchange between these two microgrids due to the mutual associated economic and reliability benefits. The local power exchange is optimally determined based on:

- The PMG unmet power in the islanded operation.

- The hourly price bids that are offered by the CMG based on the unused capacity.

The two problems are solved iteratively until the optimal solution for both problems is achieved. The impact of the power exchange on the integrated microgrids illustrates that the unused capacity in the CMG and the load curtailments in the PMG are reduced, and the total operation cost of the integrated system is minimized, advocating the viability of the model.

Chapter Five: Privacy-Preserving Optimal Scheduling of Integrated Microgrids

The prior work on integrated microgrids neglects some important practical factors such as privacy preservation, islanding, and a guarantee on solution optimality. This chapter builds on existing work on integrated microgrids operation and proposes a model with following contributions [77]:

- A privacy-preserving model for the optimal scheduling problem of integrated microgrids is proposed to ensure least possible data sharing between the microgrids.
- The proposed model maximizes the system-level reliability while minimizing individual microgrids and system aggregated operation cost.
- The proposed model is based on a high resolution scheduling, which takes into account intra-hour and inter-hour time periods to capture the variability and volatility of the renewable generation and loads.
- The grid-connected and islanded operation modes of the integrated microgrids are coordinated through an iterative method which is capable of managing the intricate dependencies between these two modes.

A Lagrange Relaxation (LR) method is applied to decompose the integrated problem to a set of smaller and individual scheduling problems for each microgrid. To achieve this, the inter-microgrids power transfer is penalized with a proper penalty coefficient and accordingly the problem is decomposed [78]-[81]. The mutual power

exchange of integrated microgrids is checked after each Lagrangian iteration until equality is obtained.

5.1 Integrated Microgrids Framework

Each microgrid within the integrated framework has clearly defined electrical boundaries and is operated by its associated master controller, while having the capability to operate in both grid-connected and islanded modes [7], [17]. If operated independently of other microgrids, each microgrid would supply local loads using local resources and power purchase from utility grid during the grid-connected mode (i.e., economic operation), while trying to minimize load curtailments once switched to the islanded mode (i.e., reliable operation) [6], [10]-[11]. In integrated microgrids, however, each microgrid has an additional source to leverage during the grid-connected and islanded modes, i.e., the power exchanged with the connected microgrids. In this case, if a microgrid has any surplus generation during the grid-connected mode, it can sell this generation to connected microgrids and accordingly increase its economic benefits and reduce its operation cost. Moreover, if a microgrid has unused capacity during the islanded mode, it can provide required generation for connected microgrids [28], [36]. This transactive strategy would enhance economic benefits for the microgrid that sells energy and improve reliability for the microgrid that purchases energy.

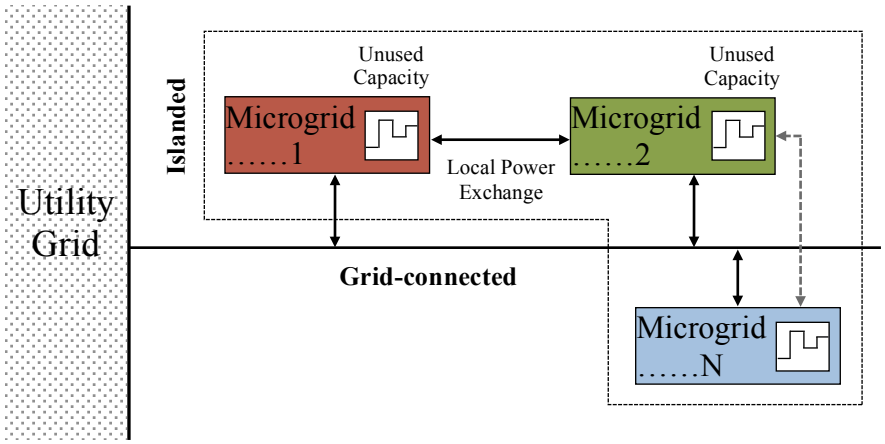

Figure 5.1 Integrated microgrids connected to the same upstream substation.

Figure 5.1 depicts possible interactions of a microgrid within the integrated microgrids framework, with the utility grid and other connected microgrids. Each microgrid has multiple options to supply local loads, e.g., from the utility grid or from other connected microgrids. Integrated microgrids operate simultaneously in the islanded mode in response to utility grid failures and/or voltage fluctuations, where it is assumed that the connection between the microgrids is maintained during islanding.

The proposed integrated microgrids framework attempts to minimize both the system aggregated operation cost (that consists of the operation cost of each individual microgrid) and the operation cost of each microgrid simultaneously. Generally, each microgrid is locally controlled by its own master controller and the system operator does not have any information on microgrids operations. In order to minimize system aggregated operation cost, the operation cost of each microgrid needs to be locally minimized while considering proper coordination between integrated microgrids. To this end, a LR method is proposed in this paper to address the multi-level coordination challenge by "relaxing" or temporarily ignoring the coupling constraints. The LR

decomposition procedure generates a separable problem by integrating some coupling constraints into the objective function, through "penalty factors" which are functions of the constraint violation [79]-[81]. These penalty factors, referred to as Lagrangian multipliers, are determined iteratively.

In addition, a multiple time-scale operation framework is developed in this work, comprising an hourly grid-connected operation and sub-hourly islanded operation. Short-time periods are employed to more accurately capture rapid changes in load and renewable generation as well as short islanding durations [11], [82]. The selection of a proper time period for scheduling represents a tradeoff between computational accuracy and efficiency. It is worth to mention that in order to characterize the microgrid islanding capability, a T-τ islanding criterion as proposed in [6] is applied, in which T and τ represent the total number of hours in scheduling horizon and the number of consecutive hours which the microgrid can operate in islanded mode, respectively. It should be mentioned that in terms of privacy, the proposed optimal scheduling model protects the microgrids' privacy by sharing minimum possible data among microgrids, which only includes the price signal of the local power exchange.

5.2 Integrated Microgrids Problem Formulation

To determine the optimal schedule of all integrated microgrids, the overall system aggregated problem (also called integrated grid problem) is first modeled, and further decomposed to obtain proper optimal scheduling problems for each individual microgrid as well as the price signals that will be used for coordinating the power exchange among the integrated microgrids.

5.2.1 Integrated Grid Problem

The aggregated operation cost of the integrated system is minimized, which is represented by the following objective function:

$$\min \tau \sum_{m\in \mathrm{M}} \sum_{t\in \mathrm{T_T}} \sum_{k\in \mathrm{T_K}} \sum_{s\in \mathrm{N}} \psi_s \Big(\sum_{i\in \mathrm{G}} F_{mi}(P_{mi,tks}) + \rho_{m,tk} P^{M}_{m,tks} + \sum_{n\in \mathrm{M}, n\neq m} \lambda_{mn,tk} P^{G}_{mn,tks} + \upsilon_{m,tk} LS_{m,tks} \Big) \tag{5.1}$$

This objective function represents four distinct terms including the generation cost of all dispatchable DGs, the cost of power exchange with the utility grid, the cost of power exchange with integrated microgrids, and the cost of unserved energy in the islanded operation. The indices m, i, t, k, and s represent the microgrids, the DERs, inter-hour time periods, intra-hour time periods, and the scenarios, respectively. Index n is further added for the connected microgrids. It should also be mentioned that the inter-hour time intervals and the intra-hour time intervals belong to sets {1, 2, 3, ... T} and {1, 2, 3, ... K}, respectively [11]. The dispatchable DGs' generation cost is represented as a single-step price value c_{mi} times the amount of generation of that individual dispatchable unit $P_{mi,tks}$, which can be extended to consider multiple price steps. The cost of power exchange with the utility grid is calculated as the market price $\rho_{m,tk}$ times the amount of exchanged power $P^{M}_{m,tks}$. This term could be positive (representing cost) or negative (representing benefit) for each microgrid, based on the flow direction (i.e., power import or export). The third term represents the cost of the power exchange with integrated microgrids, which is calculated as the local power exchange price $\lambda_{mn,tk}$ times the amount of the power exchange $P^{G}_{mn,tks}$ with integrated microgrids. This term could be either a cost or a benefit depending on the flow direction. It should be noted that this term is

always zero, as every power exchange is counted twice, once with a positive sign (from microgrid m to microgrid n) and once with a negative sign (from microgrid n to microgrid m). This term is included in the objective for the purpose of decomposition that is discussed later. The last term in the objective represents the cost of the unserved energy, i.e., the cost of the load curtailment, which only occurs during the islanded mode. This term is determined as the VOLL $\upsilon_{m,tk}$ times the amount of curtailed load $LS_{m,tks}$ in each microgrid m. This term is added to the objective function to account for system reliability.

The grid-connected and islanded operation modes are differentiated in the objective function and later in the constraints, using scenario s, where s=0 denotes the grid-connected mode and $s \geq 1$ denotes the islanded mode [26], [28]. The objective is subject to operational constraints, as follows:

$$P_{mi}^{\min} I_{mi,t} \leq P_{mi,tks} \leq P_{mi}^{\max} I_{mi,t} \qquad \forall m, \forall i, \forall t, \forall k, \forall s \tag{5.2}$$

$$\sum_{i \in \mathrm{A}} P_{mi,tks} + P_{m,tks}^{M} + \sum_{n \in \mathrm{M}, n \neq m} P_{mn,tks}^{G} + LS_{m,tks} = D_{m,tks} \qquad \forall m, \forall t, \forall k, \forall s \tag{5.3}$$

$$-P_{m}^{M,\max} U_{ts} \leq P_{m,tks}^{M} \leq P_{m}^{M,\max} U_{ts} \qquad \forall m, \forall t, \forall k, \forall s \tag{5.4}$$

$$-P_{mn}^{G,\max} \leq P_{mn,tks}^{G} \leq P_{mn}^{G,\max} \qquad \forall m, \forall n, \forall t, \forall k, \forall s \tag{5.5}$$

$$P_{mn,tks}^{G} + P_{nm,tks}^{G} = 0 \qquad \forall m, \forall n, \forall t, \forall k, \forall s \tag{5.6}$$

The dispatchable unit generation is subject to capacity and commitment limits, which are imposed using lower/upper generation values and the commitment state of the unit, as presented in (5.2). The power balance equation (5.3) ensures that the sum of

power generated by local DERs, exchanged with the utility grid, and exchanged with the integrated microgrids matches the local load. The load curtailment variable is further added to the load balance equation to ensure a feasible solution during islanded operation. Microgrids' power exchange with the utility grid is limited by the flow limits of the associated connecting line, as presented in (5.4), which will be further imposed to zero during the islanded operation using a binary islanding indicator. Each microgrid's power exchange with integrated microgrids is limited by the limits of the associated connecting line, as presented in (5.5). Finally, constraint (5.6) denotes that the summation of the local power exchange between any two connected microgrids is zero, i.e., it ensures that the amount of power offered by microgrid m/n is entirely provided to microgrid n/m, since they are equal in value but opposite in sign. Of course the power losses in the lines connecting the integrated microgrids are assumed to be negligible due to their proximity.

It is deduced from the proposed system aggregated model that the only coupling constraint among integrated microgrids is the power exchange among microgrids, represented in (5.6). In other words, if this term could be eliminated, the problem could be decomposed into m individual optimal scheduling problems, each associated with one microgrid. This can be achieved by penalizing the constraint (5.6) and adding it to the objective function.

5.2.2 Individual Microgrid Problem

Constraint (5.6) is penalized in the objective function using a Lagrangian multiplier μ. Accordingly, the proposed model is decomposed to m individual problems, one for each microgrid. This is possible due to the summation over m in the objective function and the fact that constraints are defined for each microgrid without any coupling

to other microgrids. The microgrid optimal scheduling problem is therefore modeled as follows:

$$\min \tau \sum_{t\in \mathrm{T_T}} \sum_{k\in \mathrm{T_K}} \sum_{s\in \mathrm{N}} \psi_s \Big(\sum_{i\in \mathrm{G}} F_{mi}(P_{mi,tks}) + \rho_{m,tk} P^M_{m,tks} + \sum_{n\in \mathrm{M}, n\neq m} (\lambda_{mn,tks} + \mu_{mn,tks}) P^G_{mn,tks} + \upsilon_{m,tk} LS_{m,tks} \Big) \tag{5.7}$$

$$\sum_{i\in \mathrm{A}} P_{mi,tks} + P^M_{m,tks} + \sum_{n\in \mathrm{M}, n\neq m} P^G_{mn,tks} + LS_{m,tks} = D_{m,tks} \qquad \forall t, \forall k, \forall s \tag{5.8}$$

$$-P^{M,\max}_m U_{ts} \le P^M_{m,tks} \le P^{M,\max}_m U_{ts} \qquad \forall t, \forall k, \forall s \tag{5.9}$$

$$-P^{G,\max}_{mn} \le P^G_{mn,tks} \le P^{G,\max}_{mn} \qquad \forall n, \forall t, \forall k, \forall s \tag{5.10}$$

The objective is to minimize the operation cost (5.7), consisting of the local generation cost, the cost of power exchange with the utility grid, the cost of power exchange with integrated microgrids, and the cost of unserved energy. Constraints include the power balance equation (5.8), utility grid power exchange and islanding limit (5.9), and integrated microgrids power exchange (5.10). The microgrid optimal scheduling problem is further subject to operational constraints for each component within each microgrid *m*, including dispatchable generators (5.11)-(5.15), DES (5.16)-(5.22), and adjustable loads (5.23)-(5.25).

$$P^{\min}_{mi} I_{mi,t} \le P_{mi,tks} \le P^{\max}_{mi} I_{mi,t} \qquad \forall i \in \mathrm{G}, \forall t, \forall k, \forall s \tag{5.11}$$

$$P_{mi,tks} - P_{mi,t(k-1)s} \le UR_i \qquad \forall i \in \mathrm{G}, \forall t, k \neq 1, \forall s \tag{5.12a}$$

$$P_{mi,t1s} - P_{mi,(t-1)Ks} \le UR_i \qquad \forall i \in \mathrm{G}, \forall t, \forall s \tag{5.12b}$$

$$P_{mi,t(k-1)s} - P_{mi,tks} \le DR_i \qquad \forall i \in \mathrm{G}, \forall t, k \neq 1, \forall s \tag{5.13a}$$

$$P_{mi,(t-1)Ks} - P_{mi,t1s} \le DR_i \qquad \forall i \in \mathrm{G}, \forall t, \forall s \tag{5.13b}$$

$$T_{mi}^{\mathrm{on}} \ge UT_{mi}(I_{mi,t} - I_{mi,(t-1)}) \qquad \forall i \in \mathrm{G}, \forall t, s = 0 \tag{5.14}$$

$$T_{mi}^{\mathrm{off}} \ge DT_{mi}(I_{mi,(t-1)} - I_{m,it}) \qquad \forall i \in \mathrm{G}, \forall t, s = 0 \tag{5.15}$$

$$P_{mi,tks} \ge P_{mi,tk}^{\mathrm{dch,min}} u_{mi,t} - P_{mi,tk}^{\mathrm{ch,max}} v_{mi,t} \qquad \forall i \in \mathrm{S}, \forall t, \forall k, \forall s \tag{5.16}$$

$$P_{mi,tks} \ge P_{mi,tk}^{\mathrm{dch,min}} u_{mi,t} - P_{mi,tk}^{\mathrm{ch,max}} v_{mi,t} \qquad \forall i \in \mathrm{S}, \forall t, \forall k, \forall s \tag{5.17}$$

$$C_{mi,tks} = C_{mi,t(k-1)s} - P_{mi,tks} u_{mi,t} \tau / \eta_i - P_{mi,tks} v_{mi,t} \tau \qquad \forall i \in \mathrm{S}, \forall t, k \ne 1, \forall s \tag{5.18a}$$

$$C_{mi,t1s} = C_{mi,(t-1)Ks} - P_{mi,t1s} u_{mi,t} \tau / \eta_i - P_{mi,t1s} v_{mi,t} \tau \qquad \forall i \in \mathrm{S}, \forall t, \forall s \tag{5.18b}$$

$$C_{mi}^{\min} \le C_{mi,tks} \le C_{mi}^{\max} \qquad \forall i \in \mathrm{S}, \forall t, \forall k, \forall s \tag{5.19}$$

$$T_{mi}^{\mathrm{ch}} \ge MC_{mi}(u_{mi,t} - u_{mi,(t-1)}) \qquad \forall i \in \mathrm{S}, \forall t, s = 0 \tag{5.20}$$

$$T_{mi}^{\mathrm{dch}} \ge MD_{mi}(v_{mi,t} - v_{mi,(t-1)}) \qquad \forall i \in \mathrm{S}, \forall t, s = 0 \tag{5.21}$$

$$u_{mi,ts} + v_{mi,ts} \le 1 \qquad \forall i \in \mathrm{S}, \forall t, s = 0 \tag{5.22}$$

$$D_{md,tk}^{\min} z_{md,t} \le D_{md,tks} \le D_{md,tk}^{\max} z_{md,t} \qquad \forall d \in \mathrm{D_A}, \forall t, \forall k, \forall s \tag{5.23}$$

$$\sum_{[\alpha_d, \beta_d]} D_{md,tks} = E_{md} \qquad \forall d \in \mathrm{D_A}, \forall s \tag{5.24}$$

$$T_{md}^{\mathrm{on}} \ge MU_{md}(z_{md,t} - z_{md,(t-1)}) \qquad \forall d \in \mathrm{D_A}, \forall t, s = 0 \tag{5.25}$$

The generation of the dispatchable DGs in each microgrid *m* is constrained by the maximum and minimum generation capacity limits (5.11), and further multiplied by a binary variable to indicate the commitment state of that individual DG. Ramping up and down for each DG are satisfied by (5.12) and (5.13), respectively. Equations (5.12a) and

(5.13a) represent the ramping constraints for intra-hour time intervals, while (5.12b) and (5.13b) represent the ramping constraints for inter-hour time intervals. Each dispatchable DG is subject to a minimum ON time once it is switched on, which is constrained in (5.14), and further subject to a minimum OFF time once it is shut down, which is satisfied by (5.15). Constraints (5.16)-(5.22) are provided to optimally manage the operation of the DES. The DES is subject to maximum and minimum charging and discharging limits, which are constrained by (5.16)-(5.17), and further multiplied by binary variables $u_{mi,t}$ and $v_{mi,t}$ to indicate its operation status, i.e., either charging or discharging. The stored energy in the DES is calculated in (5.18a) and (5.18b), respectively, for intra-hour and inter-hour time intervals, based on the available stored energy, amount of charged and discharged energy, and DES efficiency. The time period of charging and discharging is considered to be $\tau=(1/K)h$, where K is the number of intra-hour periods and h represents a time period of one hour. The stored energy in the DES is limited by the DES capacity as in (5.19). The DES is subject to minimum successive operating time limits for both charging and discharging, which are constrained by (5.20)-(5.21), respectively. Constraint (5.22) is provided to guarantee one operating mode at the scheduling time, i.e., either charging or discharging. Finally, (5.23)-(5.25) are provided to manage the operation of the installed adjustable loads in each microgrid *m*. Adjustable loads are restricted by maximum and minimum rated power limits, which are constrained by (5.23). The total required energy to accomplish the operating cycle for certain adjustable loads is satisfied by (5.24). In addition, some adjustable loads are subject to minimum successive operating time once they are switched on, which is satisfied by (5.25). It should be noted that hourly commitment is still considered for DERs in the

proposed model. However, the proposed model is generic and a higher resolutions could be considered for DERs' commitment without loss of generality.

5.2.3 Coordination through Price Signal Update

The proposed optimal microgrids scheduling problem can be solved by the master controller of each microgrid. The coordination among integrated microgrids is carried out via price updates.

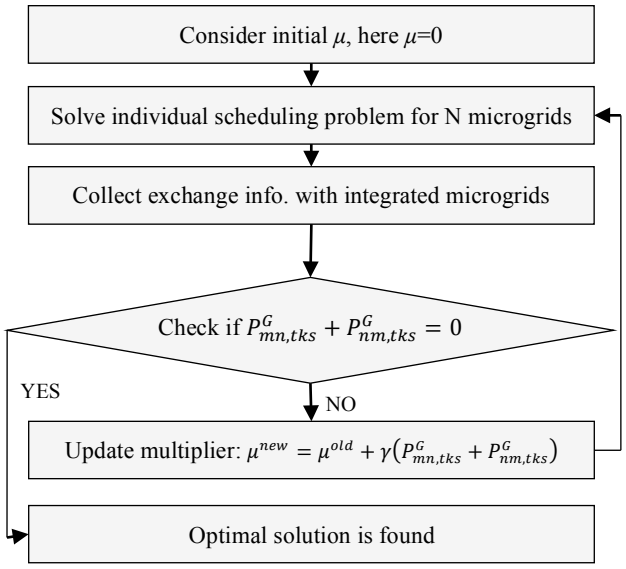

Figure 5.2 Flowchart of the proposed iteration procedure.

Based on the obtained objective, the price of purchasing power from microgrid n is λ_{mn}+μ_{mn}, where λ_{mn} is a constant original price and μ_{mn} is the added Lagrangian multiplier. The same price is used for microgrid *n* that sells energy to microgrid *m*. To control the power exchange between two microgrids, the Lagrangian multiplier between these two needs to be controlled. Figure 5.2 depicts the flowchart of the coordination among integrated microgrids. Initially the Lagrangian multiplier is assumed to be zero to solve the microgrid optimal scheduling problem. After obtaining all the scheduling

solutions, the penalized constraint (5.26) is checked to examine if the solution is feasible. If not, the Lagrangian multiplier is updated using (5.27), where γ is a constant positive number.

$$P^{G}_{mn,tks} + P^{G}_{nm,tks} = 0 \qquad \forall m, \forall n, \forall t, \forall k, \forall s \qquad (5.26)$$

$$\mu^{new} = \mu^{old} + \gamma(P^{G}_{mn,tks} + P^{G}_{nm,tks}) \qquad \forall m, \forall n, \forall t, \forall k, \forall s \qquad (5.27)$$

Based on (5.27), if the summation $P^{G}_{mn,tks} + P^{G}_{nm,tks}$ is positive, the exchange needs to be reduced, which will be done by increasing μ and making the power exchange with integrated microgrids less attractive (a larger μ in the objective results in a smaller $P^{G}_{mn,tks}$). Similarly, if the summation $P^{G}_{mn,tks} + P^{G}_{nm,tks}$ is negative, the exchange needs to be increased by decreasing μ, hence making the power exchange with integrated microgrids more attractive. The iterative price update and scheduling process will continue until it converges, i.e., (5.26) is satisfied for all microgrids and connections.

5.3 Numerical Simulations

An integrated microgrids test system with two microgrids is utilized to evaluate the performance and effectiveness of the proposed model. Microgrid A comprises four dispatchable units, two nondispatchable units, and one DES with 95% efficiency. Microgrid B comprises five dispatchable units, two nondispatchable units, and five adjustable loads. Microgrids characteristics (including loads consumption) are summarized in Tables 5.1 and 5.2. Hourly forecasted market prices, borrowed from [6], are listed in Table 5.3. The power exchange with the utility grid is limited by the connecting line capacity limit, which is assumed for both microgrids to be 10 MW. The local power exchange among the integrated microgrids is further subject to a line

capacity limit of 4 MW. It is worth mentioning that six intra-hour time intervals, i.e., K equal to 6, are considered in simulations. In other words, a ten-minute resolution in a 24-hour scheduling horizon is considered in this section. A total of 145 scenarios are considered in this study, where scenario 0 denotes the grid-connected operation and scenarios 1-144 represent the islanded operation. Each islanding scenario denotes the islanding operation in a specific ten-minute time interval, i.e., a T-1 islanding criterion. The problem is modeled and solved using CPLEX 11.0 [76]. Five cases are examined to investigate the power exchange merits among the integrated microgrids.

Table 5.1 Microgrid A Characteristics

Dispatchable Units								
Unit	Cost Coefficient ($/MWh)		Min.-Max. Capacity (MW)		Min. Up/Down Time (h)		Ramp Up/ Down Rate (MW/h)	
G1	27.7		1 – 5		3		2.5	
G2	39.1		1 - 5		3		2.5	
G3	61.3		0.8 - 3		1		3	
G4	65.6		0.8 - 3		1		3	
Aggregated Generation of Nondispatchable Units								
Time (h)	1	2	3	4	5	6	7	8
Power (MW)	0	0	0	0	0.63	0.80	0.62	0.71
Time (h)	9	10	11	12	13	14	15	16
Power (MW)	0.68	0.35	0.62	1.11	1.21	1.57	1.23	1.28
Time (h)	17	18	19	20	21	22	23	24
Power (MW)	1.05	0.82	0.71	0.92	0.57	0.60	0	0
DES								
Storage	Capacity (MWh)		Min.-Max. Charging/Discharging Power (MW)				Min. Charging/Discharging Time (h)	
DES1	10		0.4 – 2				5	
Hourly Fixed Load								
Time (h)	1	2	3	4	5	6	7	8
Load (MW)	9.00	8.80	8.73	9.31	9.06	9.08	10.43	11.27
Time (h)	9	10	11	12	13	14	15	16
Load (MW)	11.54	12.14	12.45	12.50	14.35	15.74	15.83	16.18
Time (h)	17	18	19	20	21	22	23	24
Load (MW)	16.63	16.64	16.04	15.99	14.43	13.43	10.12	9.74

Table 5.2 Microgrid B Characteristics

Dispatchable Units								
Unit	Cost Coefficient ($/MWh)		Min.-Max. Capacity (MW)		Min. Up/Down Time (h)		Ramp Up/ Down Rate (MW/h)	
G1	26.8		1 – 6		3		3	
G2	35.5		1 – 6		3		3	
G3	64.1		0.8 – 3		1		3	
G4	72.3		0.8 – 3		1		3	
G5	85.6		1 – 3		1		3	
Aggregated Generation of Nondispatchable Units								
Time (h)	1	2	3	4	5	6	7	8
Power (MW)	0	0	0	0	0.71	0.92	0.79	0.83
Time (h)	9	10	11	12	13	14	15	16
Power (MW)	0.79	0.47	0.74	1.31	1.47	1.69	1.31	1.36
Time (h)	17	18	19	20	21	22	23	24
Power (MW)	1.23	1.02	0.89	1.13	0.63	0.72	0	0
Adjustable Loads (S: Shiftable, C: Curtailable)								
Load	Type	Min.-Max. Capacity (MW)		Required Energy (MWh)		Required Start-End Time (h)		Min Up Time (h)
L1	S	0 – 0.4		1.6		11 – 15		1
L2	S	0 – 0.4		1.6		15 – 19		1
L3	S	0.02 – 0.8		2.4		16 – 18		1
L4	S	0.02 – 0.8		2.4		14 – 22		1
L5	C	1.8 – 2		47		1 – 24		24
Hourly Fixed Load								
Time (h)	1	2	3	4	5	6	7	8
Load (MW)	17.05	16.60	15.62	17.35	18.07	19.12	18.51	17.31
Time (h)	9	10	11	12	13	14	15	16
Load (MW)	16.49	18.16	18.43	20.46	21.33	22.69	23.91	24.21
Time (h)	17	18	19	20	21	22	23	24
Load (MW)	24.76	24.59	22.11	21.93	19.62	17.39	17.09	16.69

Table 5.3 Hourly Market Price

Time (h)	1	2	3	4	5	6	7	8
Price ($/MWh)	15.03	10.97	13.51	15.36	18.51	21.80	17.30	22.83
Time (h)	9	10	11	12	13	14	15	16
Price ($/MWh)	21.84	27.09	37.06	68.95	65.79	66.57	65.44	79.79
Time (h)	17	18	19	20	21	22	23	24
Price ($/MWh)	115.45	110.28	96.05	90.53	77.38	70.95	59.42	56.68

Case 1: Independent Scheduling: In this case each of the microgrids are autonomously scheduled (no power exchange) during both operation modes, i.e., in the grid-connected and islanded modes. As shown in Table 5.9, the total operation costs for microgrids A and B are $8,908 and $21,570, respectively. Figure 5.3 depicts the exchanged power of Microgrid A and Microgrid B with the utility grid during the grid-

connected mode. It is observed from Figure 5.3 and Table 5.3 that, both microgrids import power in low price hours and export or decrease their import in high price hours to minimize their operation costs. In the islanded mode, the optimal scheduling of the installed DES in Microgrid A supports avoiding the undesired load shedding in this microgrid; the average load curtailment in Microgrid B equals to 1.01 MWh, ranging from 0.66 MW to 5.17 MW in peak load hours (between hours 13 and 20). The total daily load curtailment in Microgrid B is 24.27 MWh, and Figure 5.4 illustrates the hourly load curtailment in Microgrid B during the islanded operation.

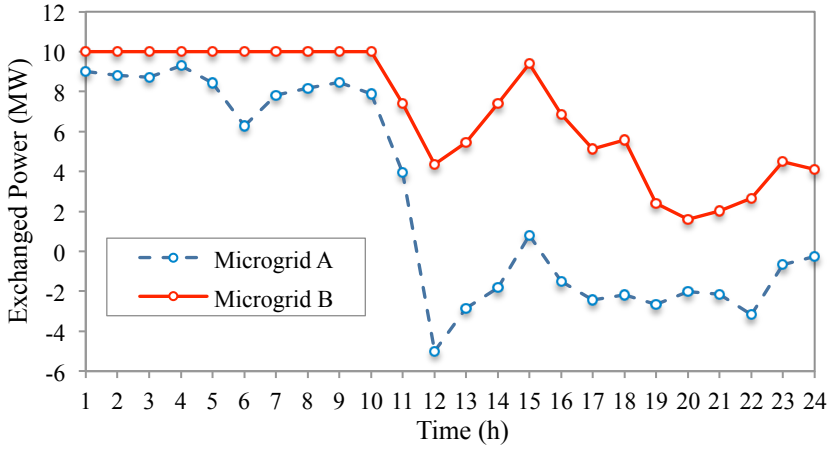

Figure 5.3 Power exchange with the utility grid during grid-connected mode in Case 1.

Case 2: Integrated Scheduling: In this case the power is exchanged among the integrated microgrids during the islanded operation. It should be mentioned that the objective is to minimize the integrated microgrids' operation cost and the load curtailment, which would result in increasing the operation cost in some microgrids to improve their reliability. The total operation cost of microgrid A is calculated as $6,743.80, which implies a reduction of -24.25% compared to Case 1, due to selling power to Microgrid B and leveraging the unused capacity. On the other hand, although

the total operation cost of Microgrid B is increased to $23,543.93, its average load curtailment is reduced to 0.29 MWh, i.e., a reduction of -70.87% compared to Case 1, which implies significant improvement of reliability. Table 5.9 summarizes the total operation costs of two microgrids and total curtailed loads in Microgrid B, for both cases. Figure 5.4 compares the hourly load curtailment in Microgrid B during the islanded operation in Cases 1 and 2. As Figure 5.4 depicts, the load curtailment of Microgrid B in Case 2, allowing interaction between microgrids, is reduced to three hours in a day, compared to eight hours in Case 1. Moreover, this reliability improvement represents a saving of $172,000 in terms of outages (assuming a relatively small VOLL of $10/kWh [83]). Commitment states of the dispatchable units and the DES for both microgrids, in Case 2, are listed in Tables 5.4 and 5.5, respectively, where bold values imply changes from Case 1. It is observed that the commitment status of the DES in Microgrid A and G5 in Microgrid B are changed from Case 1 to Case 2, to achieve the least-cost reliability-constrained schedule for both microgrids.

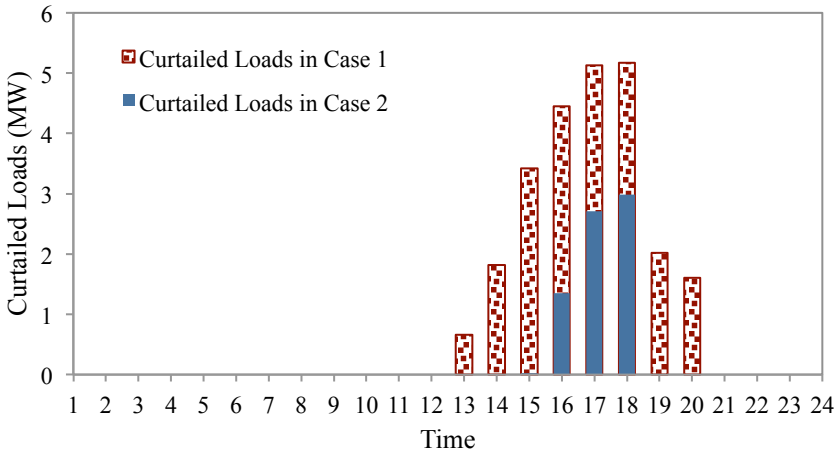

Figure 5.4 Microgrid B load curtailment during the islanded operation.

Table 5.4 Dispatchable Units and DES Schedule for Microgrid A

	Hour (1-24)																							
G1	1	1	1	1	1	1	1	1	1	1	1	1	1	1	1	1	1	1	1	1	1	1	1	1
G2	1	1	1	1	1	1	1	1	1	1	1	1	1	1	1	1	1	1	1	1	1	1	1	1
G3	0	0	0	0	0	0	0	0	0	0	0	1	1	1	1	1	1	1	1	1	1	1	1	0
G4	0	0	0	0	0	0	0	0	0	0	0	1	1	1	1	1	1	1	1	1	1	1	0	0
DES	-1	-1	-1	-1	-1	0	0	1	1	1	1	1	0	0	**1**	1	1	1	1	1	0	0	0	0

Table 5.5 Dispatchable Units and DES Schedule for Microgrid B

	Hour (1-24)																							
G1	1	1	1	1	1	1	1	1	1	1	1	1	1	1	1	1	1	1	1	1	1	1	1	1
G2	1	1	1	1	1	1	1	1	1	1	1	1	1	1	1	1	1	1	1	1	1	1	1	1
G3	1	1	1	1	1	1	1	1	1	1	1	1	1	1	1	1	1	1	1	1	1	1	1	1
G4	1	1	1	1	1	1	1	1	1	1	1	1	1	1	1	1	1	1	1	1	1	1	1	1
G5	1	**0**	0	1	**0**	1	1	**0**	0	1	1	1	1	1	1	1	1	1	1	1	1	1	**0**	1

The hourly power exchange between the two microgrids is shown in Table 5.6. As the table shows, the hourly exchanged power among the integrated microgrids varies between 0.4 MW and 3.4 MW, based on the available capacity in the microgrids while taking into account the supply-demand balance for the entire system.

Table 5.6 Power Exchange Among Integrated Microgrids (Case 2)

Time (h)	1	2	3	4	5	6	7	8
$P^{A\text{-}B}$ (MW)	0	- 0.4	0	0	- 1.16	0	0	- 0.28
$P^{B\text{-}A}$ (MW)	0	0.4	0	0	1.16	0	0	0.28
Time (h)	9	10	11	12	13	14	15	16
$P^{A\text{-}B}$ (MW)	0	0	0	0	- 0.66	- 1.82	- 3.4	- 3.1
$P^{B\text{-}A}$ (MW)	0	0	0	0	0.66	1.82	3.4	3.1
Time (h)	17	18	19	20	21	22	23	24
$P^{A\text{-}B}$ (MW)	- 2.42	- 2.18	- 2.02	- 1.6	0	0	- 0.89	0
$P^{B\text{-}A}$ (MW)	2.42	2.18	2.02	1.6	0	0	0.89	0

Figure 5.5 shows the exchanged power of both microgrids with the utility grid during the grid-connected mode in Case 2. It is observed that the exchanged power in Case 2 is almost the same as Case 1, with slight changes in three hours. These insignificant changes are due to revised schedules of DES and DGs. The two microgrids are connected to the same bus, accordingly same price, at the utility side in grid-connected mode. It should be noted that the exchanged power between microgrids is zero

during the grid-connected mode, as the optimal scheduling enforces them to exchange power with the utility grid instead of with the other microgrid. To clarify this issue, assume that there is adequate line capacity between each microgrid and the utility grid, Microgrid A has surplus generation, and Microgrid B has deficient power. In case the utility price is higher than the local power exchange price, Microgrid B would be interested in purchasing power from Microgrid A; however, Microgrid A would sell its surplus generation to the utility grid as it would result in higher profit. The same is true when the utility price is lower than the local power exchange price; where Microgrid B in this case prefers to import its power need from the utility grid rather than Microgrid A, as it is cheaper and would further minimizes its operation cost.

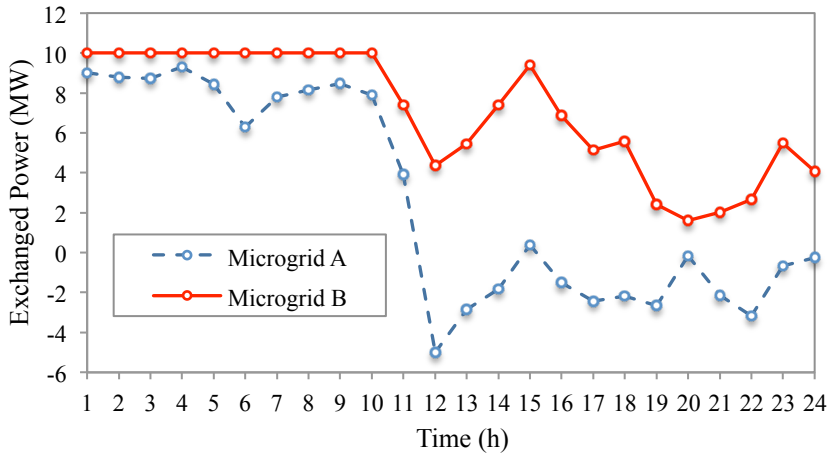

Figure 5.5 Power exchange with the utility grid during grid-connected mode in Case 2.

Figure 5.6 shows the sensitivity of load curtailment in Microgrid B and total operation cost of both microgrids with respect to the maximum line capacity between microgrids. Results show that Microgrid A operation cost decreases by increasing the line capacity limit, while Microgrid B operation cost increases by increasing the line capacity limit. The increase in Microgrid B operation cost is due to the increased power import

from Microgrid A to alleviate the load curtailment (which is decreased by increasing the limit of the line) and to enhance the local reliability.

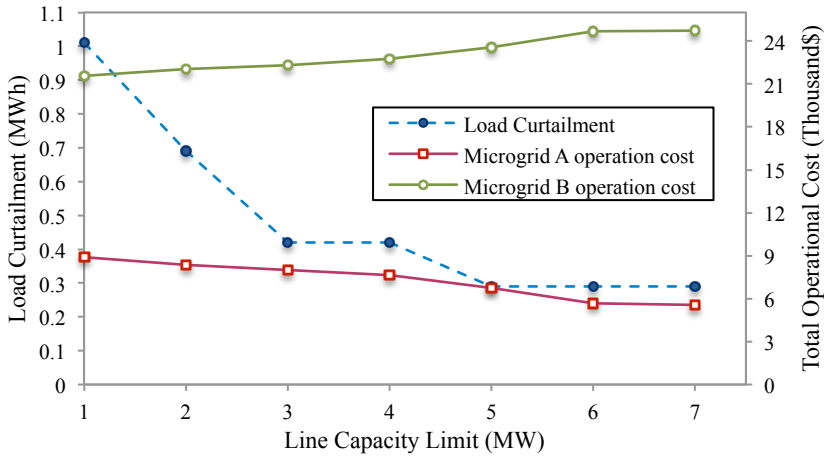

Figure 5.6 Sensitivity analysis of load curtailment and microgrids operation cost with respect to line capacity limit.

Case 3: Both Microgrids have Deficient Generation: In this case, the fixed load in Microgrid A is increased by 35% to investigate its impact on the power exchange scheduling among the integrated microgrids when both microgrids have deficient generation. In this case, the power is exchanged among the integrated microgrids in only two hours (i.e., 8 and 21). The exported power from Microgrid A to Microgrid B in hour 8 is 0.28 MW, while the exported power from Microgrid B to Microgrid A in hour 21 is 0.19 MW, which are illustrated in Table 5.7. Power exchange between the microgrids, while both have deficient generation, minimizes the individual operation cost along with the system aggregated operation cost. Nevertheless, in this case, both microgrids encounter load curtailments, which are shown in Figure 5.7. Microgrid A operation cost increases to $15,642.58, i.e., increased by 75.7% compared with the base case, due to the increase in the local demand. On the other side, even though Microgrid B encounters load

curtailment equals to the base case, it saves $86.5 in terms of the operation cost compared to the base case. Table 5.9 shows the integrated microgrids operation cost. This study indicates that the power exchange scheduling among the integrated microgrids relies on the unused capacity in each microgrid in the integrated system, and further on the generation cost of the dispatchable DGs in all microgrids to minimize the individual operation cost and the aggregated system operation cost.

Table 5.7 Power Exchange Among Integrated Microgrids (Case 3)

Time (h)	1	2	3	4	5	6	7	8
$P^{A\text{-}B}$ (MW)	0	0	0	0	0	0	0	- 0.28
$P^{B\text{-}A}$ (MW)	0	0	0	0	0	0	0	0.28
Time (h)	9	10	11	12	13	14	15	16
$P^{A\text{-}B}$ (MW)	0	0	0	0	0	0	0	0
$P^{B\text{-}A}$ (MW)	0	0	0	0	0	0	0	0
Time (h)	17	18	19	20	21	22	23	24
$P^{A\text{-}B}$ (MW)	0	0	0	0	0.19	0	0	0
$P^{B\text{-}A}$ (MW)	0	0	0	0	-0.19	0	0	0

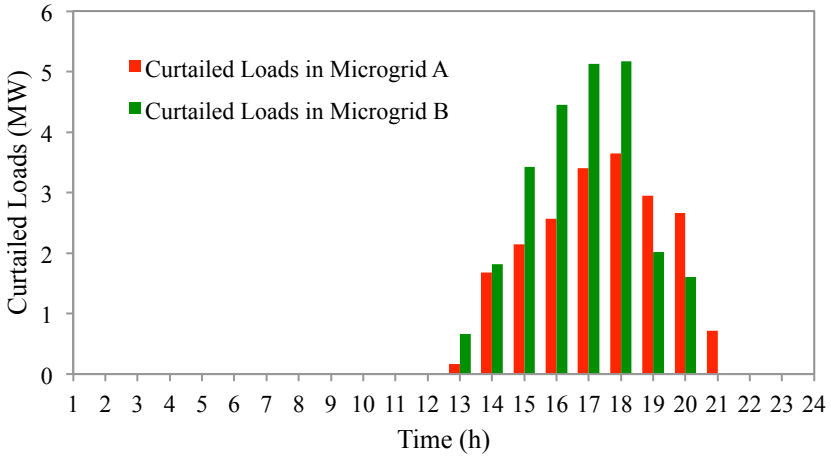

Figure 5.7 Microgrids load curtailments during the islanded operation in Case 3.

Case 4: Both Microgrids have Surplus Generation: In this case, the fixed load in Microgrid B is decreased by 35% to investigate its impact on the power exchange scheduling among the integrated microgrids when both microgrids have surplus

generation. Even though both microgrids have surplus generation, the power is exchanged among the integrated microgrids in four hours (i.e., 2, 5, 6, and 15) to minimize the entire system operation cost, which is illustrated in Table 5.8. Microgrid A's operation cost is $8,894.68, while Microgrid B's operation cost is $10,663.02, which are shown in Table 5.9. The load curtailments in this case for both microgrids are zero due to the surplus in the generation.

Table 5.8 Power Exchange Among Integrated Microgrids (Case 4)

Time (h)	1	2	3	4	5	6	7	8
$P^{A\text{-}B}$ (MW)	0	-0.59	0	0	-0.835	-1.308	0	0
$P^{B\text{-}A}$ (MW)	0	0.59	0	0	0.835	1.308	0	0
Time (h)	9	10	11	12	13	14	15	16
$P^{A\text{-}B}$ (MW)	0	0	0	0	0	0	-1.051	0
$P^{B\text{-}A}$ (MW)	0	0	0	0	0	0	1.051	0
Time (h)	17	18	19	20	21	22	23	24
$P^{A\text{-}B}$ (MW)	0	0	0	0	0	0	0	0
$P^{B\text{-}A}$ (MW)	0	0	0	0	0	0	0	0

Table 5.9 Total Operation Cost and Curtailed Load

Case No.	Microgrid A Operation Cost	Microgrid B Operation Cost	System Total Operation Cost	Curtailed Load in Microgrid A	Curtailed Load in Microgrid B
Case 1	$8,903.04	$21,570.62	$30,473.66	-	24.27 MWh
Case 2	$6,743.80 (-24.25%)	$23,543.93 (9.15%)	$30,287.73 (-0.61%)	-	7.07 MWh (-70.87%)
Case 3	$15,642.58	$21,484.12	$37,126.7	19.92 MWh	24.27 MWh
Case 4	$8,894.68	$10,663.02	$19,557.7	-	-
Case 5	$6,740.15	$23,533.92	$30,274.07	-	7.03 MWh

The obtained results show that all decisions are based on the microgrids operation cost, not on the surplus or deficit in generation. However, it should be noted that the proposed optimal scheduling model motivates the power exchange between the integrated microgrids, when one of the microgrids can offer power with a lower cost compared to the generation cost of the already installed DERs at the other microgrid. This would positively impact the economic benefits for both microgrids. In other words, the proposed

optimal scheduling model is generic and could be applied to integrated microgrids under any operational settings.

Case 5: High Resolution: In this case, the optimal scheduling problems for Case 2 is solved again but with considering 10 min intra-hour time periods (sub-hourly) to investigate the high resolution capability of the proposed model. The differences in the power exchange scheduling of the integrated microgrids in this case compared with the lower resolution in Case 2 is depicted in Figure 5.8. Slight differences can be seen between the two cases, which is due to the capability to capture the variability and volatility of loads and renewable generations in Case 5. Total curtailed load in Microgrid B, in this case, is 7.03 MWh, which is reduced by 0.57% compared with Case 2 as illustrated in Figure 5.9. It is seen that the load curtailment in this case is almost similar to Case 2, however with a higher resolution. The integrated microgrids operation cost considering the high resolution are shown in Table 5.9, where the system aggregated operation cost is reduced by 0.045% compared to Case 2.

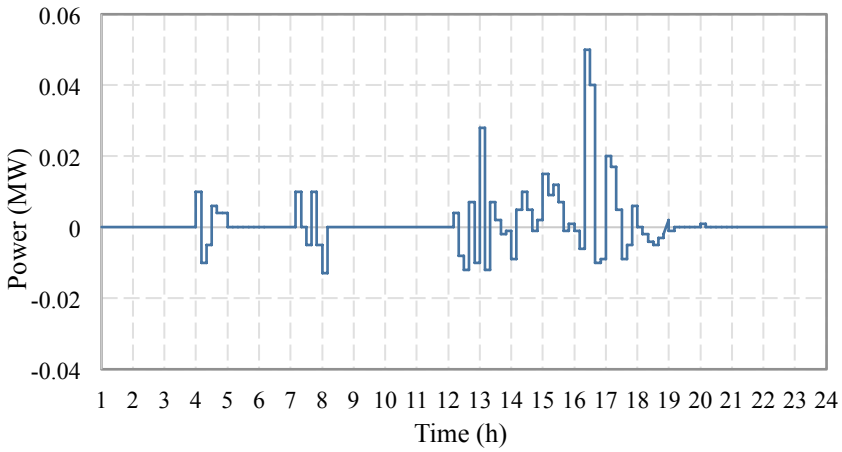

Figure 5.8 The difference of the power exchange among the integrated microgrids between the high resolution and the low resolution cases.

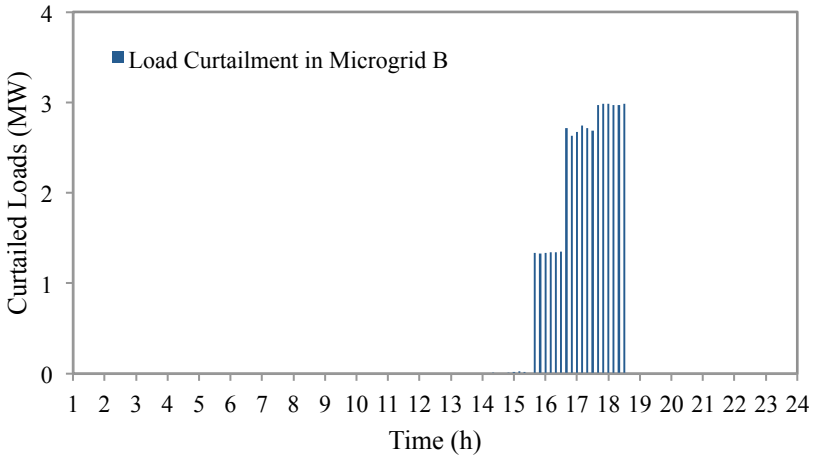

Figure 5.9 Microgrid B load curtailment with a higher resolution.

It should be noted that the microgrids' privacy is highly protected while performing these numerical simulations and the only information that is exchanged is the local power exchange prices signals, iteratively. Furthermore, it is worth to mention that the proposed model is generic and could be applied to various time period, multiple microgrids, and smaller intra-hour time periods.

5.4 Discussion

Microgrids can be utilized in an integrated fashion in order to leverage their available/unused capacity for supporting other connected microgrids that lack adequate power. This chapter develops an optimal scheduling model of integrated microgrids, which utilized the LR method to find an optimal solution while minimizing data sharing among microgrids. The presented LR model determines the least-cost schedule of all microgrids' loads and DERs and provides the optimal scheduling for all integrated microgrids. Moreover, the proposed model could ensure that the amount of load shedding for all integrated microgrids is minimized, thereby increasing the system reliability. In addition, the privacy concerns are taken into account in the proposed optimal scheduling

model of integrated microgrids, while ensuring that all microgrids could reach their associated least-cost schedule without sharing any private data with other microgrids. A high resolution optimal scheduling for the integrated microgrids systems is further presented, taking into account intra-hour and inter-hour time periods, to capture the variability and volatility of the renewable generation and loads. Numerical simulations on a test system show a reduction in the total operation cost and improvement in system reliability of integrated microgrids based on the proposed model, advocating on its acceptable performance and practical merits.

Chapter Six: Integrated Microgrids in the Holonic Distribution Grids

The smart grid's continuous evolution requires rethinking the current structure of distribution grids, as that is a key element in achieving smart grid objectives. An innovative idea in restructuring the distribution grids is to move towards a holonic architecture. Holonic distribution grids are highly flexible and structurally controllable grids that can promote the connectivity among the grid entities, such as prosumers and microgrids, to realize the highest local and global benefits. This chapter investigates and discusses the holonic distribution grids and their importance in the future power systems, and further examines how the spinning reserve in microgrids can impact the connections among the integrated players in holonic distribution grids [75], [84].

6.1 Holonic Distribution Grids - Definition and Significance

The penetration of the DERs is continuously growing in distribution networks [67], [74]. However, current distribution networks may not be able to adequately handle the new dynamics offered by the DERs, especially in case of high penetrations, which necessitate the transition into more dynamic and adaptive distribution networks. The concept of a holonic distribution grid is proposed to address such challenges and to create an intelligent environment for the next generation of smart grids. Holonic structure is based on a dynamic hierarchy concept of holons, where each holon represents a self-contained and autonomous system (e.g., a microgrid or a prosumer with decision-making capability). Nonetheless, each holon in holonic distribution grids can contain or can be

contained by other holons in the system, where this topology adapts for the benefit of the individual systems and the aggregated system of systems [67]-[68], [74]. Connected holons in the system can create an aggregated holon called a super-holon. The provided topology by the holonic distribution grids can therefore be recognized as a hybrid between the centralized and distributed approaches, where the self-contained subsystems can be adapted within the holonic system autonomously and managed by a supervisory controller. Figure 6.1 shows a holonic distribution grid structure.

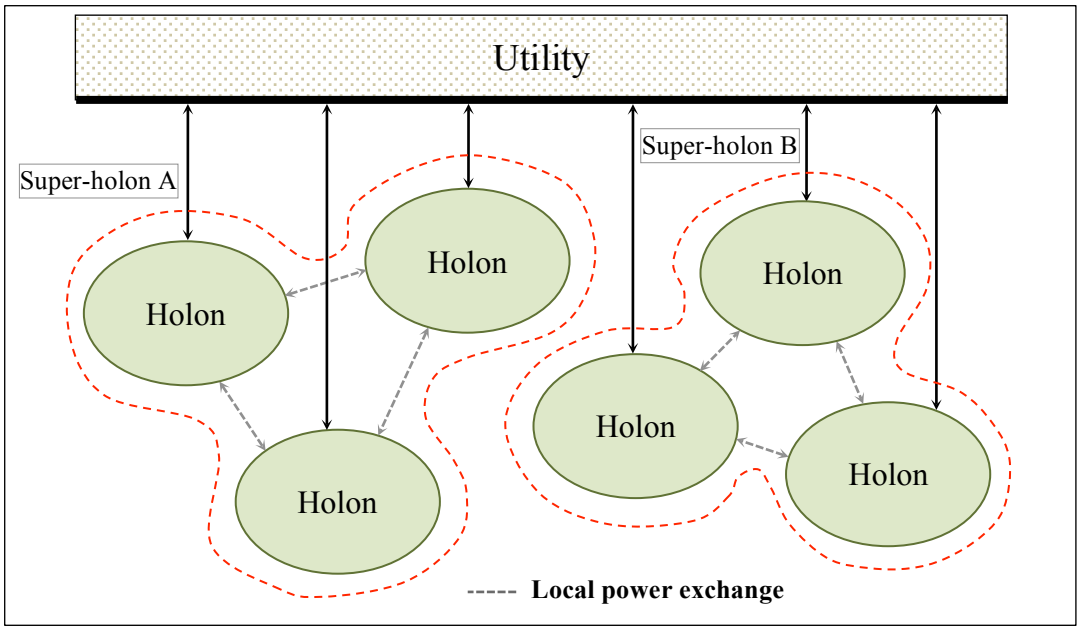

Figure 6.1 A holonic distribution grid structure.

The holons in the holonic distribution grid can be dynamically reorganized or reconfigured to adapt themselves in an active environment. In addition, the holons can interact through cooperation and competition to create an intelligent setting that promotes local and global benefits [67], [75]. Hence, the holonic distribution grids would optimally identify the optimal connection or reconfiguration of the integrated microgrids that can enhance the individual and the entire system objectives.

6.2 Optimal Scheduling of Integrated Microgrids in Holonic Distribution Grids

This section proposes an optimal scheduling model for managing integrated microgrids in a holonic distribution grid [75]. The proposed model is capable of determining the optimal connections among the integrated microgrids during the islanded operation mode, while minimizing individual operation cost and improving the system-wide reliability, taking into account the dynamic operation of the dispatchable DGs, DES units, and the adjustable loads.

6.2.1 Model Outline

The proposed optimal scheduling of the integrated microgrids in the holonic distribution grid minimizes the aggregated system operation cost and maximizes the overall reliability by identifying proper connections among the integrated microgrids. Figure 6.2 shows the holonic scheme and illustrates the initial possible connections among the integrated microgrids. In this study, provisional microgrids are selected over prosumers, which are typically elevated prosumers, as described in [24]-[26]. The reason behind this selection is the holons requirement in being capable of making optimal decisions (i.e., the capability of being connected or disconnected to other holons) by the presence of local controllers, which exist in provisional microgrids but not necessary in prosumers.

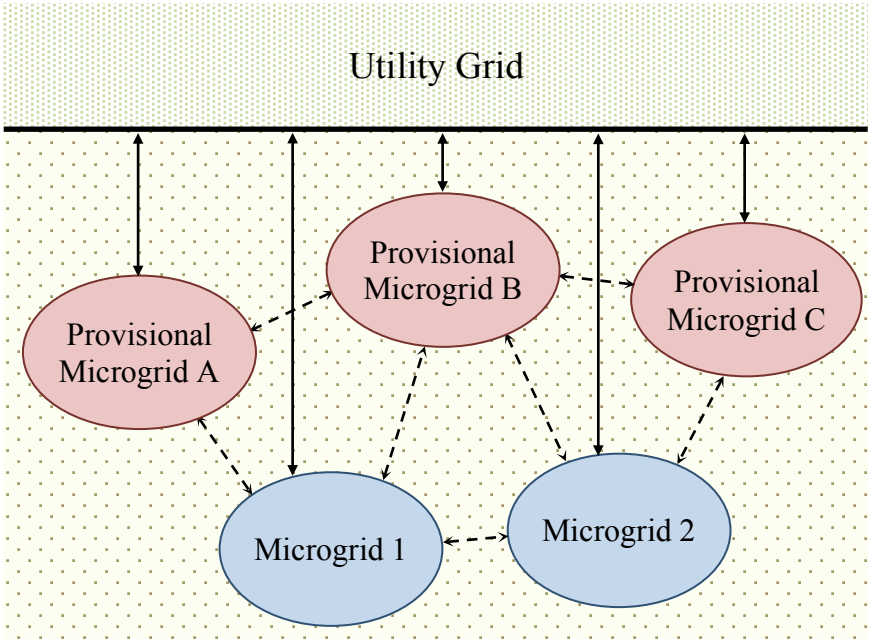

Figure 6.2 Integrated microgrids in a holonic distribution grid.

In the grid-connected mode, each microgrid optimally schedules its generation and load resources, power exchange with the utility grid, and the local power exchange with the integrated microgrids in order to maintain the supply-demand balance while minimizing its operation cost. In the islanded operation mode, all microgrids in the holonic distribution grid are disconnected from the utility grid and rely on local DERs generation as well as the power exchange with connected microgrids. In case of insufficient power (in any microgrid in the holonic distribution grid), part of the local load would be curtailed based on the need and loads criticality.

The proposed optimal scheduling model is capable of determining the optimal connections (i.e., a network reconfiguration) among the integrated microgrids in each emergency incident, i.e., in cases of islanding operation. As holonic distribution grids enable connections among the participated holons, optimally defining connections among

holons would increase the anticipated economic benefits and significantly improves the entire system reliability, as each holon (microgrid) would find the optimal paths for exporting/importing its surplus/deficient generation. In addition, it could positively impact the environment by boosting the utilization of the renewable energy resources, due to enabling local power exchanges. This feature provided by the proposed model offers basic needs for obtaining intelligent networks. Nonetheless, it should be noted that even though connections among the integrated microgrids are supposed to be sustained during the grid-connected operation, each microgrid in the holonic distribution grid prefers to import/export power with the utility grid rather than other connected microgrids, which returns to the fact that (assuming adequate line capacity limits between each microgrid and utility): (i) when the market prices are higher than the prices of the power exchange with other microgrids, microgrids with surplus generation prefer to sell power to the utility grid to increase their economic benefits; (ii) when the market prices are lower than the prices of the power exchange with other microgrids, microgrids with deficient generation prefer to import power from the utility grid, which results in minimizing their operation cost. By these considerations, there would be no power exchange between the microgrids during the grid-connected operation, as it would result in decreasing the individual economic benefit.

6.2.2 Problem Formulation

The objective of the integrated microgrids optimal scheduling problem (in the holonic distribution grid) is to minimize the system-aggregated operation cost, as proposed in (6.1):

$$\min \sum_{m\in \mathrm{M}} \sum_{t\in \mathrm{T}} \sum_{s\in \mathrm{N}} \Big(\sum_{i\in \mathrm{G}} F_{mi}(P_{mits}) + \rho_{mt} P^{M}_{mts} + \sum_{n\in \mathrm{M}, n\neq m} \lambda_{mnt} P^{G}_{mnts} + \upsilon_{mt} LS_{mts} \Big) \tag{6.1}$$

The grid-connected and islanded operations are differentiated using scenarios index s, where s=0 represents the grid-connected operation and $s\geq 1$ represents the islanded operation. The first term in the objective shows the aggregated cost of dispatchable DGs, where it is calculated as the amount of generation multiplied by the marginal generation cost of that dispatchable unit. Nondispatchable DGs generations are forecasted values calculated based on the historical data and the individual unit characteristics. Therefore, they are treated as constant values in the problem formulation (i.e., negative loads). The second term in the objective represents the cost of power exchange with the utility grid. It should be noted that this term could be positive/negative, representing cost/revenue, depending on the power flow direction. The third term denotes the power exchange with the connected microgrids, which also could be positive/negative depending of the power flow direction. The last tem in the objective represents the value of the unserved energy, which occurs only during the islanded operation. This term is calculated as the amount of the curtailed load multiplied by the associated VOLL, and further indicates the system reliability. This objective is subject to the following constraints.

$$\sum_{i\in \mathrm{A}} P_{mits} + P^{M}_{mts} + \sum_{n\in \mathrm{M}, n\neq m} P^{G}_{mnts} + LS_{mts} = D_{mts} \qquad \forall m, \forall t, \forall s \tag{6.2}$$

$$-P^{M,\max}_{m} U_{ts} \leq P^{M}_{mts} \leq P^{M,\max}_{m} U_{ts} \qquad \forall m, \forall t, \forall s \tag{6.3}$$

The power balance equation is crucial for maintaining the supply-demand balance and preventing the undesired voltage/frequency variation, which is satisfied by (6.2). The

power balance equation involves the aggregated generation of dispatchable and nondispatchable DGs, stored energy in DES units, power exchange with the utility grid, local power exchange with the connected microgrids, and the total load demand with an opposite sign, where the summation of all together must equal zero. The load curtailment is added to the power balance equation to achieve a feasible solution once the system is operated in the islanded mode. Power exchange with the utility grid is subject to the line capacity limit (6.3), which is further restricted by an islanding indicator, i.e. the binary indicator U, which imposes the power exchange with the utility to be zero once the system switches to the islanded mode.

Dispatchable DGs are subject to constraints (6.4)-(6.8).

$$P_{mi}^{\min} I_{mit} \le P_{mits} \le P_{mi}^{\max} I_{mit} \qquad \forall m, \forall i \in \mathrm{G}, \forall t, \forall s \qquad (6.4)$$

$$P_{mits} - P_{mi(t-1)s} \le UR_{mi} \qquad \forall m, \forall i \in \mathrm{G}, \forall t, \forall s \qquad (6.5)$$

$$P_{mi(t-1)s} - P_{mits} \le DR_{i} \qquad \forall m, \forall i \in \mathrm{G}, \forall t, \forall s \qquad (6.6)$$

$$T_{mi}^{\mathrm{on}} \ge UT_{mi}(I_{mit} - I_{mi(t-1)}) \qquad \forall m, \forall i \in \mathrm{G}, \forall t, s = 0 \qquad (6.7)$$

$$T_{mi}^{\mathrm{off}} \ge DT_{mi}(I_{mi(t-1)} - I_{mit}) \qquad \forall m, \forall i \in \mathrm{G}, \forall t, s = 0 \qquad (6.8)$$

Generated power by dispatchable DGs is restricted by maximum and minimum generation limits, which is represented in (6.4). Ramping up and down limits of the dispatchable DGs are satisfied in (6.5) and (6.6), respectively. Certain dispatchable DGs are subject to minimum successive up/down time limits once switched ON/OFF, which are satisfied by (6.7) and (6.8), respectively.

DES units are subject to the following constraints (6.9)-(6.15):

$$P_{mits} \le P_{mit}^{\mathrm{dch,max}} u_{mit} - P_{mit}^{\mathrm{ch,min}} v_{mit} \qquad \forall m, \forall i \in \mathrm{S}, \forall t, \forall s \tag{6.9}$$

$$P_{mits} \ge P_{mit}^{\mathrm{dch,min}} u_{mit} - P_{mit}^{\mathrm{ch,max}} v_{mit} \qquad \forall m, \forall i \in \mathrm{S}, \forall t, \forall s \tag{6.10}$$

$$C_{mits} = C_{mi(t-1)s} - \frac{P_{mits} u_{mit} \tau}{\eta_i} - P_{mits} v_{mit} \tau \quad \forall m, \forall i \in \mathrm{S}, \forall t, \forall s \tag{6.11}$$

$$C_{mi}^{\min} \le C_{mits} \le C_{mi}^{\max} \qquad \forall m, \forall i \in \mathrm{S}, \forall t, \forall s \tag{6.12}$$

$$T_{mi}^{ch} \ge MC_{mi}(u_{mit} - u_{mi(t-1)}) \qquad \forall m, \forall i \in \mathrm{S}, \forall t, s = 0 \tag{6.13}$$

$$T_{mi}^{\mathrm{dch}} \ge MD_{mi}(v_{mit} - v_{mi(t-1)}) \qquad \forall m, \forall i \in \mathrm{S}, \forall t, s = 0 \tag{6.14}$$

$$u_{mits} + v_{mits} \le 1 \qquad \forall m, \forall i \in \mathrm{S}, \forall t, s = 0 \tag{6.15}$$

Charging and discharging of the DES units are restricted by maximum and minimum rated power limits, which are represented in (6.9)-(610). Constraint (6.11) computes the stored/available energy in the DES based on the amount of charging and discharging power and the storage efficiency. Constraint (6.12) ensures that the stored energy in the DES does not exceed the associated capacity limit. Minimum charging and discharging successive time limits are represented in (6.13) and (6.14), respectively. Constraint (6.15) ensures that only one operating mode is valid, i.e., either charging or discharging, at each time period.

Managing adjustable loads operation requires following developed constraints (6.16)-(6.18):

$$D_{mdt}^{\min} z_{mdt} \le D_{mdts} \le D_{mdt}^{\max} z_{mdt} \qquad \forall m, \forall d \in \mathrm{D_A}, \forall t, \forall s \tag{6.16}$$

$$\sum_{[\alpha_d, \beta_d]} D_{mdts} = E_{md} \qquad \forall m, \forall d \in \mathrm{D_A}, \forall s \tag{6.17}$$

$$T_{md}^{\text{on}} \geq MU_{md}(z_{mdt} - z_{md(t-1)}) \qquad \forall m, \forall d \in \mathrm{D_A}, \forall t, s = 0 \tag{6.18}$$

Constraint (6.16) implies the maximum and minimum rated power limits for each adjustable load, while constraint (6.17) signifies the required energy to accomplish the operating cycle once each individual adjustable load is switched ON, which is further subject to start/end operating times. Certain adjustable loads are subject to minimum operating time when switched ON, which is satisfied in (6.18).

Achieving the most possible local and global benefits in the holonic distribution grids requires identifying the optimal connections/reorganization among the integrated microgrids in the system. Accordingly, the following constraints (6.19)-(6.21) are developed to manage the power exchange among the integrated microgrids by determining the optimal connections.

$$-P_{mn}^{G,\max} w_{mnts} \leq P_{mnts}^{G} \leq P_{mn}^{G,\max} w_{mnts} \qquad \forall m, \forall n, \forall t, \forall s \tag{6.19}$$

$$P_{mnts}^{G} + P_{nmts}^{G} = 0 \qquad \forall m, \forall n, \forall t, \forall s \tag{6.20}$$

$$\sum_{n \in \mathrm{M_C}} w_{mnts} \geq 1 \qquad \forall m \in \mathrm{M_P}, \forall t, \forall s \tag{6.21}$$

Local power exchange among the integrated microgrids is restricted by the tie-line capacity limits, and further multiplied by a binary connection indicator to indicate the connection status among the integrated microgrids, as represented in (6.19). Constraint (6.20) is added to ensure that the power offered by microgrid *m* is fully received by microgrid *n*, and vice versa. It should be noted that the power losses in the tie-lines are neglected. Provisional microgrids, as defined in [24]-[26], require that connection to at least one microgrid be maintained for the islanding purposes. Therefore, (6.21) is

developed which ensures that each provisional microgrid in the system is coupled to at least one microgrid in the holonic distribution grid.

6.2.3 Numerical Simulations

Two microgrids (named Microgrids 1 and 2) and three provisional microgrids (named Microgrids 3, 4, and 5) are utilized to investigate the proposed integrated microgrids optimal scheduling model in the holonic distribution grid. Figure 6.2 shows the initial connections among the integrated microgrids. Microgrids' characteristics are provided in Tables 6.1 – 6.5. Aggregated generation of nondispatchable units, hourly fixed load, and adjustable load data are shown in Tables 6.1 – 6.3, respectively. Dispatchable DGs and DES units' characteristics are shown in Tables 6.4 and 6.5, respectively. Local power exchange price for the power exchange among the integrated microgrids are assumed to be $100/MWh. Line capacity limits for all tie-lines between the integrated microgrids are limited by a maximum of 2 MW. Table 6.6 shows the hourly market price, borrowed from [26]. The proposed problem is solved for a 24-hour scheduling horizon using one-hour time intervals. In addition, a total of 25 operation scenarios are considered in this study (1 for grid-connected operation and 24 for islanded operation), where each islanding scenario indicates the islanded operation in a specific time interval during the scheduling horizon. The problems are modeled and solved using CPLEX 11.0 [76]. The following cases are studied.

Table 6.1 Aggregated Generation of Nondispatchable Units (MW)

Time (h)	1	2	3	4	5	6	7	8
Microgrid 1	0	0	0	0	0.63	0.8	0.62	0.71
Microgrid 2	0	0	0	0	0	0	0	0.02
Microgrid 3	0.95	1.05	1.19	1.86	1.57	0.91	0.48	0.84
Microgrid 4	1.09	0.96	1.11	1.54	1.49	2.07	2.02	2.13
Microgrid 5	1.13	0.95	0.92	1.26	1.17	0.97	0.81	0.84
Time (h)	9	10	11	12	13	14	15	16
Microgrid 1	0.68	0.35	0.62	1.11	1.21	1.57	1.23	1.28
Microgrid 2	0.08	0.26	0.48	0.74	0.92	0.99	0.97	0.91
Microgrid 3	0.64	1.92	1.96	1.89	1.79	3.27	3.21	3.12
Microgrid 4	2.47	2.81	2.13	2.57	2.21	2.0	2.13	1.71
Microgrid 5	1.43	1.69	1.72	1.71	1.68	1.31	1.41	1.31
Time (h)	17	18	19	20	21	22	23	24
Microgrid 1	1.05	0.82	0.71	0.92	0.57	0.6	0	0
Microgrid 2	0.83	0.72	0.45	0.12	0	0	0	0
Microgrid 3	3.38	3.35	2.11	2.25	1.18	0.99	1.06	0.91
Microgrid 4	1.6	1.31	1.03	1.51	1.23	1.01	1.88	1.64
Microgrid 5	1.15	1.09	1.34	1.47	1.24	1.51	0.93	0.89

Table 6.2 Hourly Fixed Load (MW)

Time (h)	1	2	3	4	5	6	7	8
Microgrid 1	8.73	8.54	8.47	9.03	8.79	8.81	10.12	10.93
Microgrid 2	6.20	6.19	6.07	5.91	4.43	4.79	5.09	4.75
Microgrid 3	1.09	1.12	1.83	1.95	1.61	1.86	2.57	2.95
Microgrid 4	1.29	1.16	1.34	1.79	1.99	2.11	2.84	2.99
Microgrid 5	1.17	1.51	1.82	1.29	1.19	1.74	1.84	1.85
Time (h)	9	10	11	12	13	14	15	16
Microgrid 1	11.19	11.78	12.08	12.13	13.92	15.27	15.36	15.69
Microgrid 2	4.93	5.69	4.91	5.79	6.92	7.81	8.09	8.08
Microgrid 3	2.87	1.98	2.05	3.97	3.99	3.37	4.41	5.39
Microgrid 4	2.93	2.89	2.81	2.98	2.71	2.65	2.82	1.73
Microgrid 5	1.47	1.72	1.74	2.81	3.49	3.24	3.11	2.64
Time (h)	17	18	19	20	21	22	23	24
Microgrid 1	16.13	16.14	15.56	15.51	14.0	13.03	9.82	9.45
Microgrid 2	7.07	6.41	5.46	5.27	6.01	6.43	7.15	7.12
Microgrid 3	3.42	3.39	3.26	2.28	3.46	3.14	1.16	1.14
Microgrid 4	1.85	1.91	2.33	2.01	2.71	2.62	2.91	1.64
Microgrid 5	2.06	2.01	2.31	2.41	2.06	1.51	1.33	1.36

Table 6.3 Adjustable Load (S: Shiftable, C: Curtailable)

System	Load	Type	Min.-Max. Capacity (MW)	Required Energy (MWh)	Required Start-End Time (h)	Min Up Time (h)
Microgrid 1	L1	S	0 – 0.4	1.6	11 – 15	1
	L2	S	0 – 0.4	1.6	15 – 19	1
	L3	S	0.02 – 0.8	2.4	16 – 18	1
	L4	S	0.02 – 0.8	2.4	14 – 22	1
	L5	C	1.8 – 2	47	1 – 24	24
Microgrid 2	L1	S	0 – 0.4	1.6	12 – 16	1
	L2	S	0.02 – 0.8	2.4	15 – 23	1
	L3	C	1.8 – 2	47	1 – 24	24

Microgrid 4	L1	S	0 – 0.4	1.6	4 – 6	1
	L2	S	0.02 – 0.8	2.4	10 – 13	1

Table 6.4 Dispatchable Units

System	Unit	Cost Coefficient ($/MWh)	Min.-Max. Capacity (MW)	Min. Up/Down Time (h)	Ramp Up/ Down Rate (MW/h)
Microgrid 1	G1	27.7	1 – 5	3	2.5
	G2	39.1	1 – 5	3	2.5
	G3	61.3	0.8 – 3	1	3
	G4	65.6	0.8 – 3	1	3
Microgrid 2	G1	30.9	1 – 2	4	1
	G2	45.7	0.5 – 2	4	2
	G3	73.5	0.5 – 1	2	1
	G4	78.4	1 – 3	3	1.5

Table 6.5 DES

System	Storage	Capacity (MWh)	Min.-Max. Charging/Discharging Power (MW)	Min. Charging/Discharging Time (h)
Microgrid 1	DES	10	0.4 – 2	5
Microgrid 2	DES	5	0.2 – 1	4

Table 6.6 Hourly Market Price ($/MWh)

Time (h)	1	2	3	4	5	6	7	8
Price	15.03	10.97	13.51	15.36	18.51	21.80	17.30	22.83
Time (h)	9	10	11	12	13	14	15	16
Price	21.84	27.09	37.06	68.95	65.79	66.57	65.44	79.79
Time (h)	17	18	19	20	21	22	23	24
Price	115.45	110.28	96.05	90.53	77.38	70.95	59.42	56.68

Case 1: Individual Scheduling: In this case, the optimal scheduling for each microgrid in the system is determined independently (no power exchange with other microgrids/provisional microgrids). The operation costs of the microgrids 1-5 are calculated as $11,744.87, $8,431.57, $1,196.96, $853.37, and $1,119.24, respectively, and shown in Table 6.7. In this case, microgrids 3, 4, and 5 encounter load curtailment due to deficiency in generation capacity, where the average load curtailments in these microgrids are 0.93 MW, 0.56 MW, and 0.71 MW, respectively. The average load curtailment is shown in Table 6.8. Microgrids 1 and 2 do not have any load curtailment

due to the existence of the dispatchable DGs and DES units, which are optimally scheduled to supply local loads. Figure 6.3 demonstrates the hourly load curtailment in microgrids 3, 4, and 5 during the islanded operation.

Case 2: Holonic Distribution Grid Scheduling: In this case, the power exchange among the integrated microgrids is enabled, where the optimal connections among the integrated microgrids during the islanded operation are identified by the proposed model. Enabling local power exchange highly impacts individual operation cost and improves the entire system reliability. Microgrids operation costs, in this case, are calculated as \$8,308.72 (-29.5%), \$7,139.79 (-15.32%), \$3,278.96 (+173.94%), \$2,161.37 (+153.27%), and \$2,620.24 (+134.11%), respectively, where the changes in the microgrids' operation costs are resulted from importing/exporting power from/to the other connected microgrids in the system. Table 6.7 illustrates the operation cost of all microgrids and shows the difference compared to Case 1. Although the operation costs in microgrids 3, 4, and 5 are increased, their individual reliability level is significantly improved. Microgrids 3, 4, and 5 average load curtailments are reduced to 0.065 MW (-93.03%), 0.015 MW (-97.39%), and 0.114 MW (-83.99%), respectively. Table 6.8 shows the average load curtailment and demonstrates the difference compared to Case 1. The hourly load curtailments are illustrated in Figure 6.3. Table 6.9 illustrates the binary results for the optimal connections among the integrated microgrids in the holonic distribution grid during each islanded operation scenario.

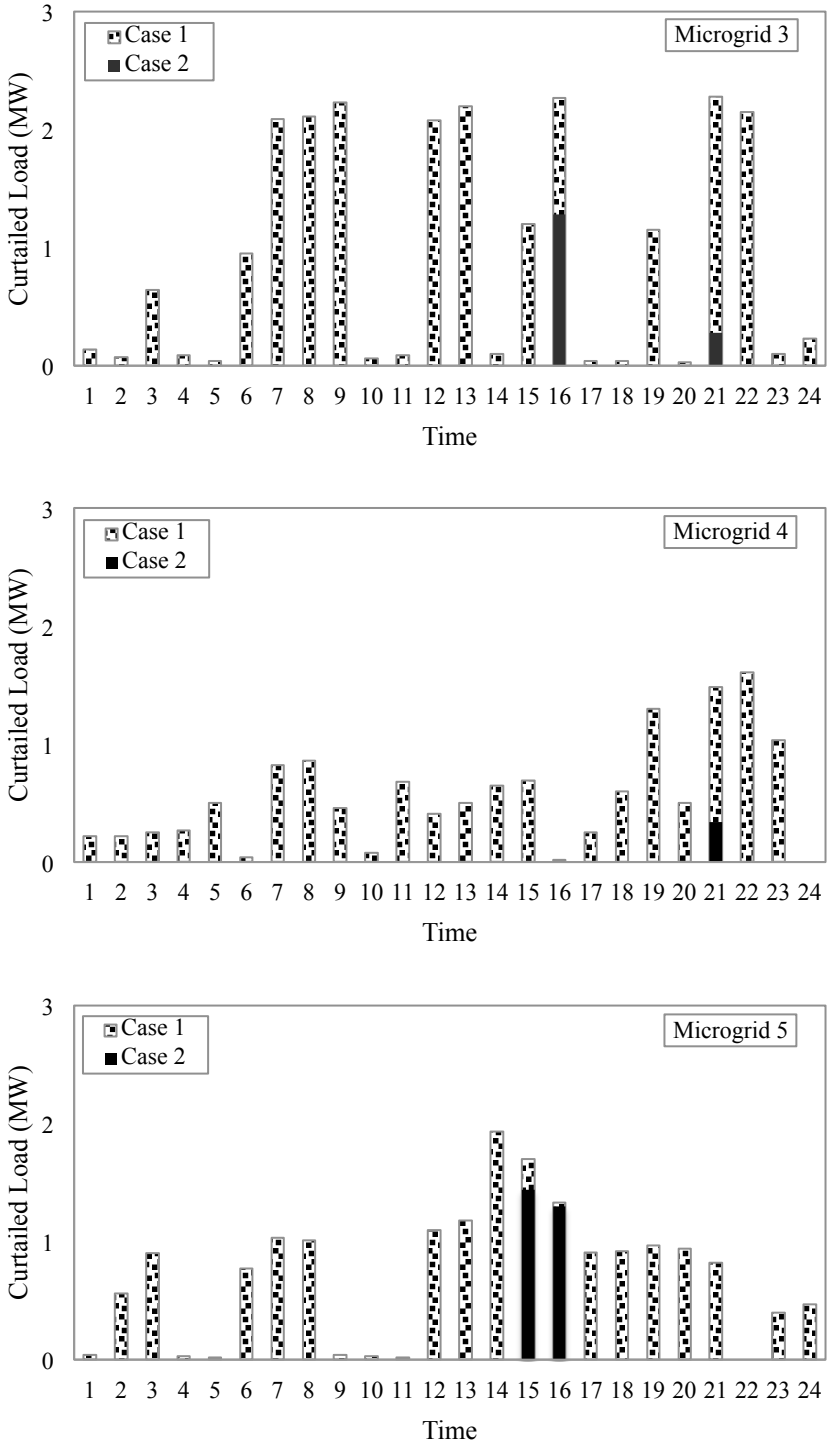

Figure 6.3 Curtailed load in microgrids 3, 4, and 5 during the islanded operation.

Table 6.7 Operation Cost

Case Number	Microgrid 1	Microgrid 2	Microgrid 3	Microgrid 4	Microgrid 5
Case 1	$11,744.87	$8,431.57	$1,196.96	$853.37	$1,119.24
Case 2	$8,308.72	$7,139.79	$3,278.96	$2,161.37	$2,620.24
Change	-29.25%	-15.32%	173.94%	153.27%	134.11%

Table 6.8 Average Load Curtailment

Case Number	Microgrid 1	Microgrid 2	Microgrid 3	Microgrid 4	Microgrid 5
Case 1	-	-	0.93 MW	0.56 MW	0.71 MW
Case 2	-	-	0.065 MW	0.015 MW	0.114 MW
Change	0%	0%	-93.03%	-97.39%	-83.99%

Table 6.9 Optimal Connection Among the Integrated Microgrids During all Islanded Operation Scenarios

Tie-Line	Islanded scenario (1-24)																							
1-2	1	1	1	0	0	0	0	0	0	0	0	0	1	1	0	0	0	0	0	0	0	0	0	
1-3	1	1	1	1	1	1	1	1	1	1	1	1	1	1	1	1	1	1	1	1	1	1	1	
1-4	1	1	1	1	1	0	1	1	1	1	1	1	1	1	1	0	1	1	1	1	1	1	1	
2-4	0	0	0	0	0	1	0	0	1	0	0	0	0	0	0	1	0	1	1	0	1	1	0	0
2-5	1	1	1	1	1	1	1	1	1	1	1	1	1	1	1	1	1	1	1	1	1	1	1	
3-4	0	0	0	0	0	0	1	1	1	0	0	1	1	0	0	0	0	0	0	0	0	1	0	0
4-5	0	0	0	0	0	0	0	0	0	0	0	1	1	0	0	0	0	0	0	0	0	0	1	1

In order to show the mechanism of Table 6.9, i.e., the obtained optimal network topology during each islanded operation, one of the islanding operation scenario (here scenario 20) is demonstrated in Figure 6.4. The obtained optimal connections among the integrated microgrids during this islanding scenario deliver the minimum system-aggregated operation cost and maximize the entire system reliability for all participated holons in the holonic distribution grid. These connections are made to support the microgrids' needs, either to increase profits or to improve the local reliability level. The obtained network topology is based on the initially assumed connections that mentioned in Figure 6.2. The amount of the power transfer among the integrated microgrids during this islanded operation scenario are 0.03 MW from microgrid 1 to 3, 0.5 MW from microgrid 1 to 4, and 0.94 MW from microgrid 2 to 5.

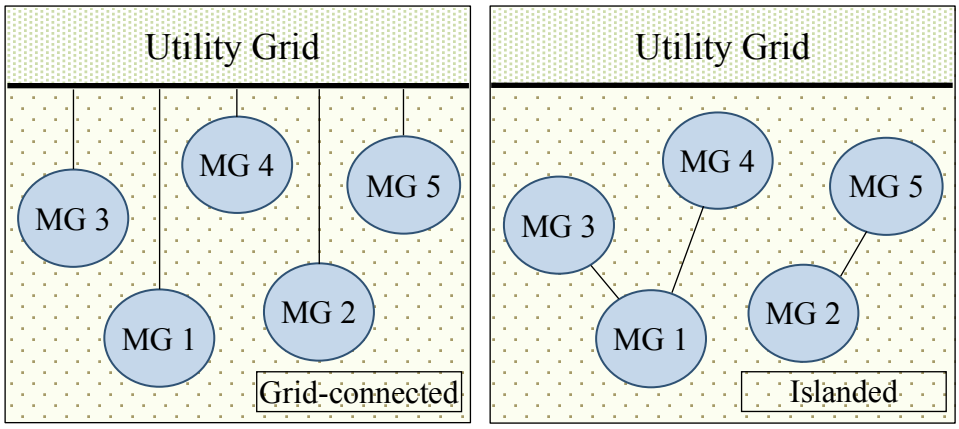

Figure 6.4 Optimal network topology during grid-connected mode and islanded operation scenario 20.

6.3 Spinning Reserve Based Topology Control in Holonic Distribution Grids

The spinning reserve capacity is a significant requirement to ensure power systems reliability without having to resort to undesirable supply-demand balance solutions such as load shedding. The spinning reserve is considered as an ancillary service that is capable of providing the system with an immediate supply of power once a credible contingency takes place [85]-[87]. It supports the withstanding of the system towards the uncertainty of the nondispatchable units' generation, the unforeseen increase in load, and the sudden outages. Therefore, preserving an appropriate amount of spinning reserve is fundamental in power systems operation. This section discusses the role of the spinning reserve in the holonic distribution grids [84]. In addition, it investigates the impact of the microgrids' spinning reserve on enabling the local power exchange, and hence its importance in improving the entire system reliability.

6.3.1 Spinning Reserve - A Key Element in Successful Implementation of Holonic Distribution Grids

The spinning reserve requirement is typically set as a base component plus a fraction of the high operating limit of the largest committed unit or a fraction of the load in bulk energy systems. The spinning reserve requirement is defined as follows:

$$sr_{it} = \min\left\{10MSR_i, P_i^{\max} - P_{it}\right\} \tag{6.22}$$

$$0 \le sr_{it} \le 10MSR_i I_{it} \tag{6.23}$$

where sr_{it} is the spinning reserve requirement, MSR_i is the 10-minute maximum sustained rate, and $P^{\max}$ and P_{it} are the maximum capacity and current generation of the on-line unit i, respectively, at a specific operating period t. The binary variable I represents the commitment state of dispatchable units in the holon. In a super-holon, the aggregated and net spinning reserves can be defined and calculated as follows:

$$SR_h = \sum_{i \in H_h} sr_i \tag{6.24}$$

$$PD_h = \sum_{i \in H_h} pd_i \tag{6.25}$$

$$SR_h^N = SR_h - PD_h \ge 0 \tag{6.26}$$

where SR and PD are the total spinning reserve and power deficiency in the super-holon, respectively, index h refers to the super-holon, and H is the set of holons. The superscript N indicates the net spinning reserve in a super-holon. Positive net spinning reserve in a super-holon indicates that the load shedding in that super-holon is zero, while a negative value shows that there is no adequate generation capacity to fully supply loads within the super-holon.

Increasing the spinning reserve requirement can significantly reduce the potential of load shedding. However, it would increase the system total cost due to the need for committing additional units. Therefore, the spinning reserve requirement is determined based on a tradeoff between the economics and the reliability objectives [85], [88]. Although the spinning reserve could help improve reliability, it could further offer additional intelligent paths to improve the economic benefits by exploiting those unused capacities.

6.3.2 Illustrative Study

A holonic distribution grid with five microgrids is used to demonstrate the impact of the microgrids' spinning reserve on enabling the local power exchange among the integrated players, and consequently enhancing the player-specific and system-wide reliability and economic benefits. These microgrids include two typical microgrids (named Microgrid 1 and Microgrid 2) and three provisional microgrids (named Provisional Microgrids 1, 2, and 3). Provisional microgrids are elevated prosumers, as described in [24]-[26]. The initial spinning reserve and unmet power in each holon (microgrid or provisional microgrid) in the holonic distribution grid are provided in Figure 6.5 for a given operating hour.

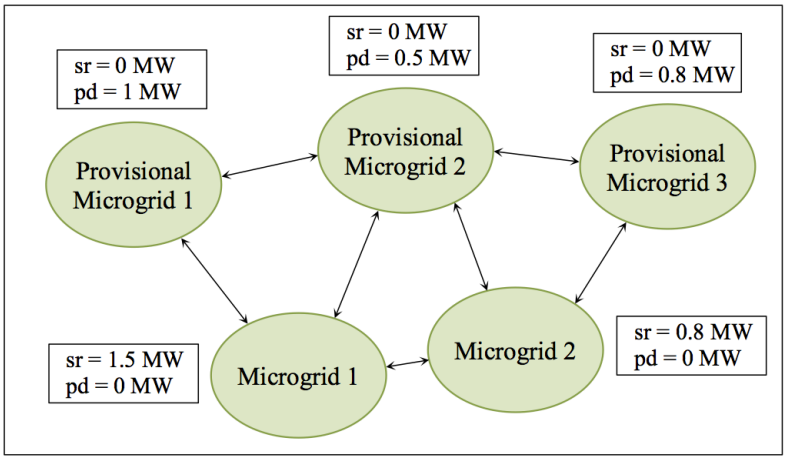

Figure 6.5 Spinning reserve and power deficient in each holons in the holonic distribution grid.

Those unused capacities provided by the microgrids' spinning reserve and the additional requirement of power in the provisional microgrids create a motivated environment for the power exchange among the players for mutual benefits. Since the investigated holonic distribution grid contains five holons, several rational combinations (i.e., super-holons) can be created within the holonic distribution grid. Figure 6.6 shows six different super-holons combinations and further shows the net spinning reserve of the super-holons once they are created. Even though several super-holon solutions can be generated in the holonic distribution grid, the optimal topology would be the one that best matches spinning reserve to deficient load, i.e., a minimum net spinning reserve solution. In the created six examples, in Figure 6.6(a), provisional microgrid 3 experiences a load curtailment of 0.8 MW; in Figure 6.6(b) either provisional microgrid 2 or 3 would experience a load curtailment of 0.3 MW; in Figure 6.6(c) none of the provisional microgrids would face load curtailment since the spinning reserve in these two super-holons are equal to their power deficiency; in Figure 6.6(d) provisional microgrid 1 experiences a load curtailment of 1 MW; in Figure 6.6(e) provisional microgrid 3

experiences a load curtailment of 0.8 MW; and in Figure 6.6(f) provisional microgrid 2 experiences a load curtailment of 0.5 MW.

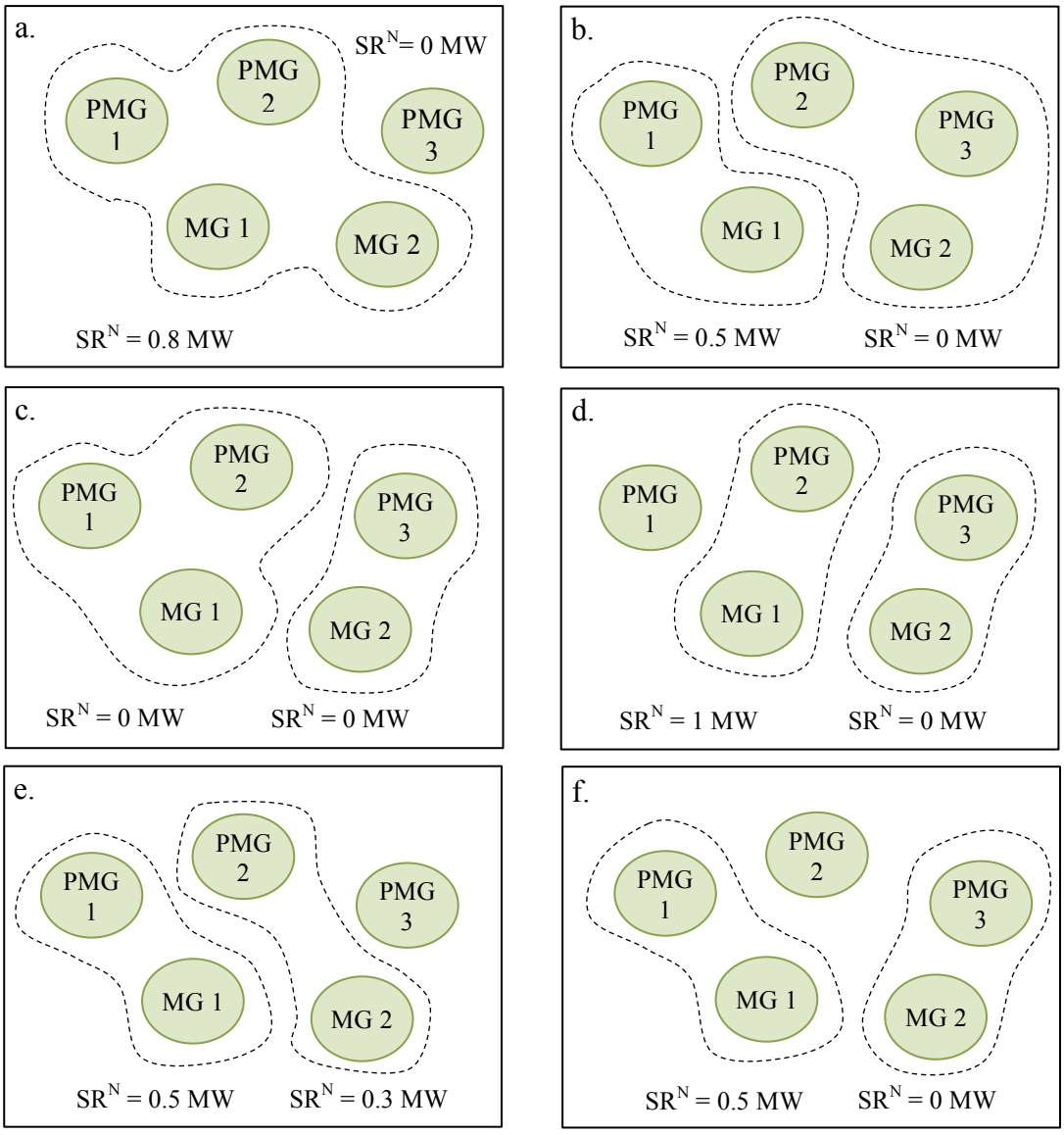

Figure 6.6 Different super-holons reconfigurations.

Based on the discussion and demonstrated figures, the combination in Figure 6.6(c) seems to be the most desirable solution as (1) microgrids can fully use their unused capacity and benefit from selling power to provisional microgrids in the islanded mode,

and (2) provisional microgrids can fully supply their local load through power exchange with microgrids in their super-holon, thus reducing load curtailment and increasing their reliability.

6.4 Discussion

Holonic distribution grids promote the systemic features of diversity, autonomy, and connectivity in the system, and further boost local and global objectives through identifying the optimal distribution network reconfiguration and proper connection of distribution players. This concept is investigated in this chapter, and the microgrids' spinning reserve impact on the local power exchange in holonic distribution grids is further discussed. An illustrative study is implemented to show the impact of identifying the optimal system reconfiguration and the microgrids' spinning reserve on enabling the optimal local power exchange, and therefore improving the entire system reliability and economic objectives. In addition, this chapter develops an optimal scheduling model for managing integrated microgrids in a holonic distribution grid that is capable of identifying the optimal connections among the integrated microgrids, enabling enhancement of individual microgrid and system-aggregated benefits.

The results and conclusions in this study can be used in a follow on research to develop an optimization problem that can determine the optimal system topology without the need for examining all possible combinations. The objective function of such optimization problem would be to minimize the aggregated net spinning reserve in super-holons within the distribution grid.

Chapter Seven: Conclusion and Future Directions

Integrating the microgrids is predicted to be an essential application and a key operational feature toward the envisioned smart grids. The integrated operation of microgrids can enhance the local power system reliability and resilience, promote the individual microgrids' economic benefits, and support further utilization of renewable energy resources. Therefore, determining the optimal schedule of the integrated microgrids during the grid-connected and islanded operation modes is crucial to achieving the most possible economic and environmental benefits.

In this dissertation, the optimal operation of the integrated microgrids was studied and investigated. The impact of elevating prosumers to provisional microgrids was examined by making proper connections to an adjacent microgrid, and efficient optimal scheduling models for the provisional microgrid and the coupled microgrids were developed. The microgrid's unused capacity during the islanded operation mode was further investigated to determine its equivalent price/quantity curve that will be used in offering the unused capacity to connected microgrids/loads during islanded operation. An optimal scheduling model based on communications between the integrated microgrids was proposed, where the power exchange between these integrated microgrids was enabled, motivated by associated economic and reliability benefits. The microgrids' privacy was taken into account by developing an optimal scheduling model of integrated microgrids, which utilized the Lagrange Relaxation method, to find the optimal solution

while minimizing data sharing among microgrids. In addition, the operation of the integrated microgrids in the holonic distribution grids was investigated, and an optimal scheduling model for managing the integrated microgrids in such distribution grids was developed, where the proposed model was capable of identifying the optimal connections among the integrated microgrids that enhances individual microgrid and system-aggregated benefits.

Investigating the impact of such systems, i.e., the integrated microgrids, from the utilities' perspective seems necessary to overcome challenges that might be caused by the emerging of those intelligent technologies. In addition, investigating the control aspects of the integrated systems seems crucial to prevent the undesired voltage and frequency fluctuations. Moreover, studying the power flow of the integrated microgrids in the holonic distribution grids is challenging which require further attention along with the optimal planning studies to achieve the sought smart grids.

REFERENCES

[1] Microgrid Exchange Group. (2011, Aug.). DOE *Microgrid Workshop Report* [Online]. Available: http://energy.gov/oe/downloads/ microgrid-workshop-report-august-2011.

[2] N. Hatziargyriou, H. Asano, M. R. Iravani, and C. Marnay, "Microgrids: An overview of ongoing research, development and demonstration projects," *IEEE Power Energy Mag.*, vol. 5, no. 4, pp. 78–94, Jul./Aug. 2007.

[3] B. Kroposki, R. Lasseter, T. Ise, S. Morozumi, S. Papathanassiou, and N. Hatziargyriou, "Making microgrids work," *IEEE Power Energy Mag.*, vol. 6, no. 3, pp. 40–53, May 2008.

[4] F. Katiraei and M. R. Iravani, "Power management strategies for a microgrid with multiple distributed generation units," *IEEE Trans. Power Syst.*, vol. 21, no. 4, pp. 1821–1831, Nov. 2006.

[5] I. Bae and J. Kim, "Reliability evaluation of customers in a microgrid," *IEEE Trans. Power Syst.*, vol. 23, no. 3, pp. 1416–1422, Aug. 2008.

[6] A. Khodaei, "Microgrid optimal scheduling with multi-period islanding constraints," *IEEE Trans. Power Syst.*, vol. 29, no. 3, pp. 1383–1392, May 2014.

[7] A. Khodaei and M. Shahidehpour, "Microgrid-based co-optimization of generation and transmission planning in power systems," *IEEE Trans. Power Syst.*, vol. 28, no. 2, pp. 1582–1590, May 2013.

[8] H. Kanchev, D. Lu, F. Colas, V. Lazarov, and B. Francois, "Energy management and operational planning of a microgrid with a PV-based active generator for smart grid applications" *IEEE Trans. on Industrial Elect.*, vol. 58, no. 10, pp. 4583-4592, Oct. 2011.

[9] P.M. Costa and M.A. Matos, "Assessing the contribution of microgrids to the reliability of distribution networks," *Electr. Power Syst. Res.*, vol. 79, no. 2, pp. 382–389 Feb. 2009.

[10] K. Balasubramaniam, P. Saraf, R. Hadidi, and E.B. Makram, "Energy management system for enhanced resiliency of microgrids during islanded operation," *Electr. Power Syst. Res.*, vol. 137, pp. 133-141 Aug. 2016.

[11] A. Majzoobi and A. Khodaei, "Application of microgrids in supporting distribution grid flexibility," *IEEE Trans. Power Syst.*, vol. PP, no. 99, pp. 1-1, 2016.

[12] S. Kennedy and M. Marden, “Reliability of islanded microgrids with stochastic generation and prioritized load,” in *Proc. IEEE Bucharest Powertech*, Romania, Bucharest, Jun. 2009, pp. 1–7.

[13] O. Hafez and K. Bhattacharya, “Optimal planning and design of a renewable energy based supply system for microgrids” *Renewable Energy*, Vol. 45, pp. 7-15, Sep. 2012.

[14] A. G. Tsikalakis and N. D. Hatziargyriou, “Centralized control for optimizing microgrids,” *IEEE Trans. Energy Convers.*, vol. 23, no. 1, pp. 241–248, Mar. 2008.

[15] C. Hou, X. Hu, and D. Hui, “Hierarchical control techniques applied in micro-grid,” in *Proc. IEEE Conf. Power Syst. Tech. (POWERCON)*, Hangzhou, China, Oct. 2010, pp. 1–5.

[16] M. Shahidehpour, “Role of smart microgrid in a perfect power system,” in *Proc. IEEE Power Energy Soc. Gen. Meeting*, Minneapolis, MN, USA, 2010.

[17] M. Shahidehpour and J. Clair, “A functional microgrid for enhancing reliability, sustainability, and energy efficiency,” *Elect. J.*, vol. 25, no. 8, pp. 21–28, Oct. 2012.

[18] A. Flueck and Z. Li, “Destination perfection,” *IEEE Power Energy Mag.*, vol. 6, no. 6, pp. 36–47, Nov./Dec. 2008.

[19] S. Bahramirad, W. Reder, and A. Khodaei, “Reliability-constrained optimal sizing of energy storage system in a microgrid,” *IEEE Trans. Smart Grid*, vol. 3, no. 4, pp. 2056–2062, Dec. 2012.

[20] A. Khodaei, “Resiliency-oriented microgrid optimal scheduling,” *IEEE Trans. Smart Grid*, vol. 5, no. 4, pp. 1584–1591, Jul. 2014.

[21] S. Bahramirad, A. Khodaei, J. Svachula, and J. R. Aguero, “Building resilient integrated grids: One neighborhood at a time,” *IEEE Electrif. Mag.*, vol. 3, no. 1, pp. 48–55, Mar. 2015.

[22] M. Sandoval and S. Grijalva, “Future grid business model innovation: A prosumer-based cost-benefit framework for valuation of distributed energy resources,” *IEEE PES Innov. Smart Grid Techn. Latin America (ISGT LATAM)*, Montevideo, Uruguay, 2015, pp. 450-455.

[23] A. Albaker and A. Khodaei, “Valuation of microgrid unused capacity in islanded operation,” in *Proc. IEEE North American Power Symposium (NAPS)*, Morgantown, WV, USA, 2017.

[24] A. Khodaei, "Provisional microgrids," *IEEE Trans. Smart Grid*, vol. 6, no. 3, pp. 1107-1115, May 2015.

[25] A. Khodaei, "Provisional microgrid planning," *IEEE Trans. Smart Grid*, vol. 8, no. 3, pp. 1096-1104, May 2017.

[26] A. Albaker and A. Khodaei, "Elevating prosumers to provisional microgrids," in *Proc. IEEE Power Energy Soc. Gen. Meeting*, Chicago, IL, USA, 2017.

[27] A. Albaker and A. Khodaei, "Design and operation of provisional microgrids," *CIGRE Grid of the Future Symposium*, Cleveland, OH, USA, 2017.

[28] A. Albaker and A. Khodaei, "Communicative scheduling of integrated microgrids," in *Proc. IEEE Power Energy Soc. T&D*, Denver, CO, USA, 2018.

[29] Z. Wang, B. Chen, J. Wang, and C. Chen, "Networked microgrids for self-healing power systems," *IEEE Trans. on Smart Grid*, vol. 7, no.1, Jan. 2016.

[30] A. G. Madureira, J. C. Pereira, N. J. Gil, J. A. P. Lopes, G. N. Korres, and N. D. Hatziargyriou, "Advanced control and management functionalities for multi-microgrids," *International Trans. on Electrical Energy Systems*, vol. 21, no. 2, pp. 1159–1177, Mar. 2011.

[31] J. Vasiljevska, J. A. P. Lopes, and M. A. Matos, "Evaluating the impacts of the multi-microgrid concept using multicriteria decision aid," *Electr. Power Syst. Res.*, vol. 91, pp. 44–51, Oct. 2012.

[32] L. Che, X. Zhang, M. Shahidehpour, A. Alabdulwahab, and A. Abusorrah, "Optimal interconnection planning of community microgrids with renewable energy sources," *IEEE Trans. on Smart Grid*, vol. 8, no. 3, May 2017.

[33] Md. Asaduz-Zaman and A. H. Chowdhury, "Optimum economic dispatch of interconnected microgrid with energy storage system," *Int. Conf. Electrical Engineering and Information Communication Technology (ICEEICT)*, Dhaka, Bangladesh, May 2015, pp. 1-6.

[34] W. Xi, Q. Xiaoyan, J. Runzhou, L. Dan, W. Gang, and L. Qian, "Economic operation of multi-microgrids containing energy storage system," *Int. Conf. Power System Technology (POWERCON)*, Chengdu, China, Oct. 2014, pp. 1712-1716.

[35] W. Saad, Z. Han, and H. V. Poor, "Coalitional game theory for cooperative micro-grid distribution networks," in *Proc. IEEE International Conference on Communication Workshops (ICC)*, Kyoto, Japan, Jun. 2011, pp. 1–5.

[36] G. S. Kasbekar and S. Sarkar, "Pricing games among interconnected microgrids," in *Proc. IEEE PES General Meeting*, Jul. 2012, pp. 1–8.

[37] K. Rahbar C. C. Chai, and R. Zhang, "Real-time energy management for cooperative microgrids with renewable energy integration," *IEEE International Conference on Smart Grid Communications (SmartGridComm)*, Venice, Italy, Nov. 2014.

[38] Y. Li, N. Liu, and J. Zhang, "Jointly optimization and distributed control for interconnected operation of autonomous microgrids," *IEEE Innovative Smart Grid Technologies - Asia (ISGT ASIA)*, Bangkok, Thailand, Nov. 2015.

[39] Y. Li, N. Liu, C. Wu, and J. Zhang, "Distributed optimization of generation scheduling of interconnected microgrids," *IEEE PES Asia-Pacific Power and Energy Engineering Conference (APPEEC)*, Brisbane, QLD, Australia, Nov. 2015.

[40] F. Xiao and Q. Ai, "New modeling framework considering economy, uncertainty, and security for estimating the dynamic interchange capability of multi-microgrids," *Electr. Power Syst. Res.*, vol. 152, pp. 237–248, Nov. 2017.

[41] D.I. Papaioannou, C.N. Papadimitriou, A.L. Dimeas, E.I. Zountouridou, G.C. Kiokes, and N.D. Hatziargyriou, "Optimization & sensitivity analysis of microgrids using HOMER software—a case study," *MedPower*, Athens, 2014, pp. 1–7.

[42] Z. Wang, B. Chen, J. Wang, M. Begovic, and C. Chen, "Coordinated energy management of networked microgrids in distribution systems," *IEEE Trans. Smart Grid*, vol. 6, no. 1, pp. 45-53, Jan. 2015.

[43] G.N. Korres, N.D. Hatziargyriou, and P.J. Katsikas, "State estimation in multi-microgrids," *Int. Trans. Electr. Energy Syst.*, vol. 21, no. 2, pp. 1178-1199, Mar. 2011.

[44] H. Dagdougui, L. Dessaint, and A. Ouammi, "Optimal power exchanges in an interconnected power microgrids based on model predictive control," *IEEE Power Energy Soc. Gen. Meeting*, National Harbor, MD, July 2014.

[45] M. E. Gamez Urias, E. N. Sanchez, and L. J. Ricalde, "Electrical microgrid optimization via a new recurrent neural network," *IEEE Systems Journal*, vol. 9, no.3, Sept. 2015.

[46] J. Vasiljevska, J. A. P. Lopes, and M. A. Matos, "Integrated micro-generation, load and energy storage control functionality under the multi micro-grid concept," *Electr. Power Syst. Res.*, vol. 95, pp. 292–301, Feb. 2013.

[47] S. Moayedi and A. Davoudi, "Distributed tertiary control of dc microgrid clusters," *IEEE Trans. on Power Electronics*, vol. 31, no. 2, April 2015.

[48] A. A. Mohamed, A. T. Elsayed, T. A. Youssef, and O. A. Mohammed, "Hierarchical control for DC microgrid clusters with high penetration of distributed energy resources," *Electr. Power Syst. Res.*, vol. 148, pp. 210–219, July 2017.

[49] S. A. Arefifar and Y. A. I. Mohamed, "Optimized multiple microgrid-based clustering of active distribution systems considering communication and control requirements," *IEEE Trans. on Industrial Electronics*, vol. 62, no. 2, Aug. 2014.

[50] M. He and M. Giesselmann, "Reliability-constrained self-organization and energy management towards a resilient microgrid cluster," *IEEE PES Innovative Smart Grid Technologies Conference (ISGT)*, Washington DC, Feb. 2015.

[51] Q. Shafiee, T. Dragicevic, F. Andrade, J. C. Vasquez, and J. M. Guerrero, "Distributed consensus-based control of multiple DC-microgrids clusters," *IEEE PES Innovative Smart Grid Technologies Conference (ISGT)*, 2015.

[52] R. H. Lasseter, "Smart distribution: Coupled microgrids," *Proceedings of the IEEE*, vol. 99, no. 6, pp. 1074–1082, June 2011.

[53] Q. Shafiee, T. Dragicevic, J. Vasquez, and J. M. Guerrero, "Modeling, stability analysis and active stabilization of multiple DC-microgrid clusters," *IEEE International Energy Conference (ENERGYCON)*, Cavtat, Croatia, May 2014.

[54] H. Lin, C. Liu, J. M. Guerrero, J. C. Vasquez, and T. Dragicevic, "Modular power architectures for microgrid clusters," *International Conference on Green Energy*, Sfax, Tunisia, Mar. 2014.

[55] A. Kargarian, B. Falahati, Y. Fu, and M. Baradar, "Multiobjective optimal power flow algorithm to enhance multi-microgrids performance incorporating IPFC," *Proc. IEEE PES General Meeting*, San Diego, CA, Jul. 2012, pp. 1–6.

[56] Z. Wang, B. Chen, J. Wang, and J. Kim, "Decentralized energy management system for networked microgrids in grid-connected and islanded modes," *IEEE Trans. Smart Grid*, vol. 7, no. 2, pp. 1097-1105, Jun. 2015.

[57] A.G. Anastasiadis, A.G. Tsikalakis, and N.D. Hatziargyriou, "Operational and environmental benefits due to significant penetration of microgrids and topology sensitivity," *Proc. IEEE PES General Meeting*, Providence, RI, Jul. 2010.

[58] P. Li, X. Guan, J. Wu, and D. Wang, "An integrated energy exchange scheduling and pricing strategy for multi-microgrid system," *IEEE Region 10 Conference (31194) TENCON*, Xi'an, China, Oct. 2013, pp. 1–5.

[59] H. Wang and J. Huang, "Incentivizing energy trading for interconnected microgrids," *IEEE Trans. Smart Grid*, (in press) http://doi.org/10.1109/TSG.2016.2614988.

[60] J. Lee, J. Guo, J.K. Choi, and M. Zukerman, “Distributed energy trading in microgrids: a game-theoretic model and its equilibrium analysis,” *IEEE Trans. Ind. Electron.*, vol. 62, no. 6, pp. 3524-3533, Jun. 2015.

[61] N. Nikmehr and S.N. Ravadanegh, “Optimal power dispatch of multi-microgrids at future smart distribution grids,” *IEEE Trans. Smart Grid*, vol. 6, no. 4, pp. 1648-1657, Jul. 2015.

[62] D.T. Nguyen and L.B. Le, “Optimal energy management for cooperative microgrids with renewable energy resources,” *IEEE International Conference on Smart Grid Communications (SmartGridComm)*, Vancouver, BC, Canada, 2013, pp. 678–683.

[63] H. Wang and J. Huang, “Bargaining-based energy trading market for interconnected microgrids,” *IEEE International Conference on Communications (ICC)*, London, UK, Jun. 2015, pp. 776–781.

[64] A.K. Marvasti, Y. Fu, S. DorMohammadi, and M. Rais-Rohani, “Optimal operation of active distribution grids: a system of systems framework,” *IEEE Trans. Smart Grid*, vol. 5, no. 3, pp. 1228-1237, May 2014.

[65] A. Pahwa, S. A. DeLoach, B. Natarajan, S. Das, A. R. Malekpour, S. S. Alam, and D. M. Case, "Goal-based holonic multiagent system for operation of power distribution systems," *IEEE Trans. on Smart Grid*, vol. 6, no. 5, pp. 2510-2518, Sep. 2015.

[66] E. Negeri, and N. Baken, “Architecting the smart grid as a holarchy,” *In Proc. of the 1st International Conference on Smart Grids and Green IT Systems*, Porto, Portugal, April 2012.

[67] S. Howell, Y. Rezgui, J. L. Hippolyte, B. Jayan, and H. Li, “Towards the next generation of smart grids: Semantic and holonic multi-agent management of distributed energy resources,” *Renewable and Sustainable Energy Reviews*, vol. 77, pp. 193-214, 2017.

[68] A. Ferreira, A. Ferreira, O. Cardin, and P. Leitão, “Extension of holonic paradigm to smart grids,” *IFAC-PapersOnLine*, vol. 48, no. 3, pp. 1099-1104, 2015.

[69] A. Koestler, “The ghost in the machine,” *Penguin Group*, New York, 1990.

[70] S. Frey, A. Diaconescu, D. Menga, and I. Demeure, “A holonic control architecture for a heterogeneous multi-objective smart micro-grid,” *IEEE In Self-Adaptive and Self-Organizing Systems (SASO)*, Sept. 2013.

[71] A. Pahwa, S. A. DeLoach, S. Das, B. Natarajan, X. Ou, D. Andresen, N. Schulz, and G. Singh, “Holonic multi-agent control of power distribution systems of the future,” *Grid of the Future Symposium (CIGRE)*, 2012.

[72] G. Florea, O. Chenaru, R. Dobrescu, and D. Popescu, "A fractal model for power smart grids," *IEEE 20th International Conference on Control Systems and Computer Science (CSCS)*, pp. 572-577, May 2015.

[73] F. Ounnar, A. Naamane, P. Pujo, and N. K. M'Sirdi, "Intelligent control of renewable holonic energy systems," *Energy Procedia*, vol. 42, pp. 465-472, 2013.

[74] E. Negeri, N. Baken, and M. Popov, "Holonic architecture of the smart grid," *Smart Grid and Renewable Energy*, vol. 4, no. 2, p.p 202, 2013.

[75] A. Albaker and A. Khodaei, "Optimal scheduling of integrated microgrids in holonic distribution grids," *in Proc. IEEE North American Power Symposium (NAPS)*, Fargo, ND, USA, 2018.

[76] ILOG CPLEX. (2009). ILOG CPLEX Homepage [Online]. Available: http://www.ilog.com

[77] A. Albaker, A. Majzoobi, G. Zhao, J. Zhang, and A. Khodaei, "Privacy-preserving optimal scheduling of integrated microgrids," *Electr. Power Syst. Res.*, vol. 163, pp.164-173, Oct. 2018.

[78] F. Zhuang and F.D. Galiana, "Towards a more rigorous and practical unit commitment by Lagrangian relaxation," *IEEE Trans. Power Syst.*, vol. 3, no. 2, pp. 763-773, May 1988.

[79] T. Li and M. Shahidehpour, "Price-based unit commitment: a case of Lagrangian relaxation versus mixed integer programming, " *IEEE Trans. Power Syst.*, vol. 20, no. 4, pp. 2015-2025, Nov. 2005.

[80] L. Lai, L. Xie, Q. Xia, H. Zhong, and C. Kang, "Decentralized multi-area economic dispatch via dynamic multiplier-based Lagrangian relaxation," *IEEE Trans. Power Syst.*, vol. 30, no. 6, pp. 3225-3233, Nov. 2015.

[81] C.P. Cheng, C.W. Liu, and C.C. Liu, "Unit commitment by Lagrangian relaxation and genetic algorithms," *IEEE Trans. Power Syst.*, vol. 15, no. 2, pp. 707-714, May 2000.

[82] A. Majzoobi and A. Khodaei, "Application of microgrids in providing ancillary services to the utility grid," *Energy*, vol. 123, pp. 555-563, Mar. 2017.

[83] Estimating the Value of Lost Load [Online]. Available: http://www.ercot.com/ content/gridinfo/resource/2015/mktanalysis/ERCOT_ValueofLostLoad_ LiteratureReviewandMacroeconomic.pdf.

[84] A. Albaker and A. Khodaei, "Spinning reserve based topology control in holonic distribution grids," *CIGRE Grid of the Future Symposium*, Reston, VA, USA, 2018.

[85] M. Q. Wang, and H. B. Gooi, "Spinning reserve estimation in microgrids," *IEEE Transmission & Distribution Conference & Exposition: Asia and Pacific*, pp.1-4, Oct. 2009.

[86] S. Lou, S. Lu, Y. Wu, and D. S. Kirschen, "Optimizing spinning reserve requirement of power system with carbon capture plants," *IEEE Trans. on Power Syst.*, vol. 30, no. 2, pp. 1056-1063, Mar. 2015.

[87] M. Amirahmadi and N. Boroomand, "Energy and spinning reserve markets scheduling considering interruptible load and demand-side reserve," *IEEE Power and Energy International Conference (PECon)*, pp. 384-389, Nov. 2016.

[88] C. Poomahapinyo and S. Chaitusaney, "Impact of renewable energy on spinning reserve based on economic dispatch," *IEEE Electrical Engineering/Electronics, Computer, Telecommunications and Information Technology Conference (ECTI-CON)*, pp. 357-360, June 2017.

APPENDIX

List of publication

- **A. Albaker** and A. Khodaei, "Elevating prosumers to provisional microgrids," *in Proc. IEEE Power Energy Soc. General Meeting*, Chicago, IL, USA, 2017.

- **A. Albaker** and A. Khodaei, "Valuation of microgrid unused capacity in islanded operation," *in Proc. IEEE North American Power Symposium (NAPS)*, Morgantown, WV, USA, 2017.

- **A. Albaker** and A. Khodaei, "Design and operation of provisional microgrids," *CIGRE Grid of the Future Symposium*, Cleveland, OH, USA, 2017.

- **A. Albaker** and A. Khodaei, "Communicative scheduling of integrated microgrids," *in Proc. IEEE Power Energy Soc. T&D*, Denver, CO, USA, 2018.

- **A. Albaker** and A. Khodaei, "Optimal scheduling of integrated microgrids in holonic distribution grids," *in Proc. IEEE North American Power Symposium (NAPS)*, Fargo, ND, USA, 2018.

- **A. Albaker** and A. Khodaei, "Spinning reserve based topology control in holonic distribution grids," *CIGRE Grid of the Future Symposium*, Reston, VA, USA, 2018.

- **A. Albaker**, A. Majzoobi, G. Zhao, J. Zhang, and A. Khodaei, "Privacy-preserving optimal scheduling of integrated microgrids," *Elsevier Electr. Power Syst. Res. (EPSR)*, vol. 163, pp.164-173, Oct. 2018.